THE UNIVERSITY OF WESTERN ONTARIO

and

COMMUNICATIONS RESEARCH CENTRE

FINAL REPORT

CRC Contract No. U6800-9-0696

THE SEARCH FOR A STATISTICAL APPROACH CAPABLE OF PREDICTING THE COUPLING STRENGTH FROM AN EXTERNAL ELECTROMAGNETIC FIELD TO ELECTRONIC EQUIPMENT

Prepared for:

Neil Simons, Ph.D. and Jasmin Roy, Ph.D.

Communication research Centre
3701 Carling Ave., Box 11490, Station H
Ottawa, Ontario, Canada, K2H 8S2

Prepared by:

Serguei Primak, Ph.D. and Joe LoVetri, Ph.D., P.Eng.

Department of Electrical and Computer Engineering
The University of Western Ontario
London, Ontario, Canada N6A 5B9

March 1999

Table of Contents

I. Introduction . . . 3
1.1 Objectives . . . 3
1.2 Background and overview of deterministic EMC analysis . . . 3
1.2.1 Electromagnetic topology . . . 3
1.2.2 Deterministic formulations and numerical modelling . . . 4
1.2.3 Motivation for a statistical formulation and solution to the EMC problem . . . 5
1.3 Summary of the report . . . 6

II. Literature Review . . . 10
2.1 Statistical description of electromagnetic fields inside a complex enclosures . . . 10
2.1.1 Lehman's fundamental publication [33] . . . 10
2.1.2 R. Holland and R. St. John group publications [34-39] . . . 12
2.1.3 D. Hill group publications [43-48] . . . 13
2.1.4 Other publications . . . 14
2.2 Experimental results of electromagnetic coupling . . . 17
2.3 Coupling of statistically described fields to transmission lines . . . 19
2.4 Statistical description of cross-talk in multiconductor transmission lines . . . 19

III. The Physics of Complex Enclosures . . . 21
3.1 Resonance of a one dimensional enclosure . . . 21
3.1.1 Solution based on transmission line equations . . . 21
3.1.2 Eigenmode expansion, Method A: expansion in terms of sines and cosines . . . 23
3.1.3 Eigenmode expansion, Method B: expansion in terms of exponentials . . . 27
3.1.4 Solution of the transcendental equations for small losses . . . 28
3.1.5 Eigenfunction expansion . . . 29
3.1.6 Morse approximation and the number of modes excited . . . 29
3.2 Numerical simulations of the one dimensional resonator . . . 31
3.2.1 Consistency of all solutions for the case of lossless walls . . . 31
3.2.2 Effects of losses on the field distribution inside 1-D resonator . . . 31
3.3 Summary of one dimensional resonators . . . 32
3.4 Fields inside a two dimensional enclosure . . . 38
3.4.1 The two dimensional model . . . 38
3.4.2 Solution in terms of standing waves . . . 38
3.4.3 The uniform-field approximation . . . 39
3.5 Numerical simulations of the two dimensional enclosure . . . 40
3.5.1 Equivalence between two methods . . . 40
3.6 Frequency Stirring . . . 42

3.7 Power balance . . . 43
3.8 Generic description of the Quality Factor of cavities . . . 44
3.8.1 Wall Losses . . . *44*
3.8.2 Absorption . . . *45*
3.8.3 Aperture leakage . . . *46*
3.8.4 Receiving antenna . . . *46*
3.9 Aperture excitation . . . 47

IV. Field Statistics for Lossy Cavities . . . 49
4.1 Motivation and Generic Model . . . 49
4.2 General form of the electromagnetic field intensity PDF . . . 50
4.2.1 Kluyver equation . . . *50*
4.2.2 Moments of the intensity . . . *51*
4.2.3 Two-parameter distributions . . . *55*
4.3 The K distribution as a model for the electromagnetic field inside enclosures . . . 56
4.3.1 PDF and CDF . . . *56*
4.3.2 Characteristic Function . . . *56*
4.3.3 Moments . . . *57*
4.3.4 Intensity distribution . . . *58*
4.3.5 Distribution of instantaneous values [32] . . . *60*
4.4 Other candidates . . . 62
4.4.1 The generalized Gamma distribution . . . *62*
4.4.2 The log-normal distribution . . . *62*
4.4.3 The Weibull distribution . . . *63*
4.4.4 Comparison of the statistical moments for various intensity distributions . . . *63*
4.5 Conclusions . . . 65

V. FDTD Simulation of a Computer Box . . . 66
5.1 Geometry of the problem . . . 66
5.2 Simulation results . . . 68
5.3 Conclusions . . . 68

VI. The Coupling of Statistical Fields to Transmission Lines . . . 72
6.1 Solution of the inhomogeneous transmission line equations . . . 73
6.2 Random field generation . . . 75
6.2.1 An exponentially correlated Markov chain . . . *75*
6.2.2 Program description . . . *78*
6.3 Numerical Results . . . 80
6.3.1 Default Input Parameters . . . *80*
6.3.2 Example of the generated report . . . *84*
6.4 Conclusions . . . 85

VII. Conclusions and Recommendations . . . 86
7.1 Overview and conclusions . . . 86
7.2 Recommendations for future work . . . 87

VIII. Appendix: Review of Some Basics on Statistics and Stochastic Processes . . . 89

8.1 Basic definitions 89
8.2 The Gaussian, uniform, Rayleigh, and Chi-square density functions 91
8.3 Functions of a random variable 93
8.3.1 The sum of two random variables *94*
8.3.2 Expected values: mean, moments, and variance *94*
8.4 Review of stochastic processes 96

IX. Additional Comments and Clarifications 98
9.1 Comments on Chapter III 98
9.1.1 Complex Q *98*
9.1.2 How small should be? *98*

X. References 100
10.1 Electromagnetic compatibility, electromagnetic topology, and bounds 100
10.2 Books on probability theory, stochastic processes, EM theory and integration 101
10.3 Statistical approach to EM coupling 102
10.4 Other related publications 104
10.5 Random field generation 106
10.6 UWO internal notes 107

I. Introduction

1.1 Objectives

The purpose of this research is to investigate statistical, *i.e.* non-deterministic, methods for modelling the electromagnetic interference and compatibility (EMI/EMC) in electronic systems. Although there exists an extensive amount of literature on deterministic electromagnetic modelling methods applied to the EMC problem, relatively little work has been done on the use of statistical techniques for characterizing the EMC in electronic systems. The first part of this research report consists of an in-depth critical literature review of the subject. In the second part, some of the statistical techniques which were found in the literature, as well as some newly proposed methods, are applied to the canonical system of a transmission line inside an enclosure with an external disturbing electromagnetic field. The goal of this second part is to determine the applicability and usefulness of these techniques to a typical EMC problem. Although the canonical problem chosen is relatively simple, both from a topological and geometric viewpoint, it allows for a thorough testing of the validity of the assumed premises and the utility of the proposed methods. Finally, conclusions and recommendations for future research are made.

1.2 Background and overview of deterministic EMC analysis

1.2.1 Electromagnetic topology

Electromagnetic topology methods have been used in the past to break up an electronic system into parts relevant to the EMI/EMC problem. The electromagnetic topology consists of a description of the electromagnetically distinct volumes and their associated surfaces. Electromagnetic interactions occur between volumes through the associated surfaces [1, 2]. Other than being "a good way to think about electromagnetic interactions" the topology concept does not lend itself to quantitative study of the EMC problem unless some quantitative information is loaded into the topology. A relatively successful technique, in the area of electromagnetic pulse (EMP) studies, has been the use of norms to bound the energy and waveforms in the topology [3, 4, 5, 6, 7].

An attempt to generalize and quantify (to some extent) the use of electromagnetic topology, by introducing *electromagnetic attributes,* was described in [8]. In this work, use was made of the so called *interaction sequence diagram* corresponding to a particular topology to keep track of the interaction paths

throughout the system. In [9], the problem was formulated using *fuzzy variables* to describe the attributes, and *fuzzy logic* operators were used to propagate the attributes throughout the topology. The major problem with this technique is the lack of a validated database of electromagnetic attributes which is sufficiently comprehensive to make it useful to the EMC engineer. A quantitative technique for acquiring fuzzy data for some canonical systems was introduced in [10].

1.2.2 Deterministic formulations and numerical modelling

A wide spectrum of deterministic formulations and corresponding numerical techniques to obtain solutions to the formulated problems exist for characterizing interactions such as the coupling of electromagnetic waves through apertures and onto cables and printed circuit boards (PCB's). Full-field formulations generally start with Maxwell's equations, or some derived potential equations in either an integral or a differential equation form, and then a numerical technique which is applicable to that form is used to solve for electromagnetic field quantities (or other derived variables such as voltage and current).

Quasi-static and quasi-TEM (transverse electromagnetic) formulations are approximate representations of some electromagnetic field problems which result in efficient numerical solutions. As an example, the coupling of electromagnetic plane waves into printed multiconductor transmission line (MTL) networks, where the geometry and the electrical parameters are known, was considered in [11]. The methods developed therein can be applied to general networks of MTL's with non-linear loads. When a multiconductor transmission line network exists inside an enclosure, the field distribution inside the enclosure is much more complex than a plane wave and, for most coupling problems, a full-field analysis would be required. That is, most of the plane wave coupling models which exist in the literature would not be applicable. Some experimental, as well as Finite Difference Time Domain (FDTD) and Transmission Line Matrix (TLM) modelling results for this more difficult coupling problem, have been published in [12]. The configuration which was considered in [12] consists of a circuit board inside a metallic enclosure in which a monopole antenna is also present. The monopole was excited by a transient current and the resulting voltages on the circuit were measured. The full-field numerical modelling and the experiments agreed quite well.

For realistic PCB's, containing hundreds of traces and nodes, numerical simulation of the problem would require enormous computational resources. At the same time "accurate" solutions, obtained from these types of numerical methods may not be necessary for EMI type problems. For many practical EMI applications only certain induced variables (maximum induced peak voltage, duration of peaks, induced energy *etc.*) are important. Moreover, the exact topology of the PCB in question may be unknown. One technique of coping with this type of uncertainty is the determination of bounds on the intensity of the field inside an enclosure. This approach was taken in the work reported in [13, 14, 15, 16, 17, 18, 19]. It should be noted that these investigations were <u>not</u> statistical in nature.

As can be seen, even the deterministic problem of determining voltages and currents induced on a PCB which is packaged in an enclosure is quite difficult to model. For more complicated systems, the numerical modelling becomes prohibitive. Some recent experimental and modelling research on the disruption of various state-of-the-art personal computers (PC's) which were exposed to microwave radiation in the frequency range of 1-4 GHz has been reported in [20]. The purpose in this work was to evaluate the high power microwave (HPM) threat in the context of electromagnetic terrorism--a subject of growing interest in the electromagnetic compatibility (EMC) community. Several PC's: 133, 200, and 300 MHz clock rates, were exposed to microwave energy in the controlled environment of an anechoic chamber. The energy was radiated using calibrated horn antennas and could be approximated as a plane wave at the location of the PC. Various modulations of the carrier frequency were used and the effects on the computers which were running a common spread-sheet software package, performing continuous disk/memory read-write operations, were noted. The effects varied from disk-access failure (requiring the operator to reboot the computer) to automatic power down (requiring the operator to disconnect the computer from the power mains before rebooting). One interesting result of these experiments was the relatively low electric field values which were capable of disrupting the PC; field values as low as 30 V/m caused disruption in some cases. Modelling the PC enclosure, using FDTD, revealed that the natural frequencies of the chassis resonances corresponded to the frequencies at which the disruptions occurred. Thus, in this case, numerical modelling of a simplified geometry representing the PC revealed the coupling mechanism which played the important part in the failure.

1.2.3 Motivation for a statistical formulation and solution to the EMC problem

Even if the assumption is made that a supercomputer and a state-of-the-art numerical technique were available, a deterministic solution to modelling the EMC in a complex system would be of little value because slight changes in the system configuration (for example, a slight rotation of the enclosure with respect to the incident wave, or a slight displacement of a cable in the system or a slight change in the frequency of the microwave or RF disturbing source) would change the resulting coupling. In contrast to a "deterministic" description when "local" properties of the fields are under consideration, statistical methods are based on the idea that we want to describe a physical quantity in "global" terms and thus small deviations of local behaviour would have little impact on the distribution parameters. Therefore a statistical characterization of the problem will allow for a better accounting of the uncertainties which are common in such systems. It seems a reasonable assumption that a statistical characterization of, say, the electromagnetic field intensity inside an equipment enclosure, would not be sensitive to slight changes in the system configuration. On the other hand, it is important to determine which system parameters will change, or affect, the statistical description of the electromagnetic interactions. It is these system parameters which will need to be determined for any particular system which is being analysed.

The subject of Electromagnetic Compatibility is fundamentally a sub-area in the study of the reliability of electronic systems. It is somewhat surprising, therefore, that a statistical treatment of electromagnetic interference is not common and that the methods of such a treatment have not been fully developed. The reason seems to be that there is a lack of understanding on how to apply statistical methods to such complicated problems. It can be argued that a statistical description of EMI in complicated systems will become much more common in the future and thus it is important to develop and validate the mathematical techniques which can be used to efficiently implement such a characterization.

1.3 Summary of the report

The remainder of this report consists of a review of existing literature on the subject of statistical electromagnetic fields as applicable to EMC as well as some original material which we have developed in this area. An appendix giving an introductory overview of some basic statistical concepts is included at the end of the report. The purpose of this appendix is to give the reader a brief review but it also serves the purpose of establishing the notation which will be used in this report. Some deviation from this notation will occur from time to time when results from the literature are directly reported.

Chapter II contains the literature review. It is broken up into the four main sub-areas which we have found the literature to be divided into. These are: a) the statistical description of fields inside *complex enclosure* and *reverberation chambers*; b) experimental results of electromagnetic coupling; c) the coupling of statistically described fields into transmission lines; and d) the statistical characterization of cross-talk in multiconductor transmission lines. Generally, it was found that a relatively substantial amount of work has been done on trying to characterize the statistical distributions which govern the electromagnetic field in various circumstances. An attempt has been made to put physical understanding at the basis of the chosen distributions but we feel that the task has not been accomplished. It seems that different conditions require different distributions and the transition from one to the other is not smooth. We address this problem by the introduction of the K distribution in Chapter IV. Other work which is reviewed in this chapter includes experimental studies on large systems such as the EMPTAC test airframe and the Celestron 8 satellite. This data is important in that it gives one the opportunity to compare theory with experiment. The final two topics which are reviewed are the coupling to transmission lines as well as the cross-talk problem. It was found that almost all the theoretical work dealing with transmission lines has been based on simple quasi-TEM models of the lines.

Chapter III gives a detailed account of the physics of resonant enclosures. The concepts of *Quality Factor, Q,* and *modes of resonance* are introduced in this chapter. The concept of electromagnetic resonance is fundamental in our study of the fields inside enclosures and in this chapter we attempt to bring the reader up to speed on the relevant physics and mathematics applicable to the subject. The simplest way to proceed, the way which is chosen, is with simple one dimensional and two dimensional examples of

resonance. We find that, even with these simple examples, once lossy boundaries are included, the deterministic mathematical description of the fields becomes quite difficult. In the one dimensional lossless resonator example, we first obtain an analytic solution based on the transmission line equations. Although useful, this form of solution does not give much insight into the resonances which are inherent in the problem. We go on to formulate the eignefunction expansion of the problem and in this form the resonant frequencies are clearly identifiable: they are the frequencies at which singularities exist in the solution. Once losses are introduced in the walls of the one dimensional resonator, a numerical technique must be used to determine the eigenvalues. We make an approximation, for the case of low losses, by performing a small parameter expansion of the eigenvalues (the normalized wall impedance being the small parameter with which the expansion is made). A second approximation, which we call the *Morse Approximation*, is introduced. This approximation consists of modifying the propagation constant of the waves inside the enclosure and keeping the eigenvalues the same as those of the lossless resonator. The modification requires a knowledge of the Q of the enclosure. Numerical examples are considered to exemplify the differences in the field solutions predicted by these various methods. It is shown that the main differences show up near the boundaries of the enclosure. It was found that the number of modes excited which carry significant energy is very low and this may be a concern since many of the statistical techniques which have been reported in the literature require that a large number of modes be present for the techniques to be valid.

The Green function for the two dimensional resonator is considered next. It is shown how *frequency stirring* can be used to obtain a relatively uniform field intensity throughout the cavity. This is done by averaging the field intensity at an arbitrary point inside the cavity over a desired bandwidth. This average value is then compared to other points inside the cavity. It is found that as the frequency bandwidth is increased, the average value becomes more uniform as a function of position. Uniform field intensifies are desirable in such things as reverberation chambers which are used for electromagnetic compatibility measurements.

Chapter III ends with a description of the *power balance method* for describing leaky/lossy enclosures. In this technique, the average field inside an enclosure is approximated by the knowledge of some relatively generic parameters. For instance, the Q of a cavity can be approximated by a knowledge of its volume, surface area, the conductivity of the walls, and the losses due to apertures existing in the walls. Once the Q is estimated, an approximation for the average field intensity inside the cavity can be obtained, under steady-state conditions, by a knowledge of the power input into the cavity (*i.e.* via sources external or internal to the cavity). Once the average field intensity is known, if the shape of the distribution is also known, then one parameter of the PDF for the field can be determined. The main importance of this method is the relatively few and generic attributes which need to be known about the enclosure; this makes the method applicable to many systems of interest.

In Chapter IV, we investigate some alternate more general distributions and propose a new class of distributions for describing the field inside enclosures. This new class, the *K* distributions, is well known in the statistics literature but has never been applied to the electromagnetic compatibility problem before. Basically these distributions are defined by the Bessel function of order ν, and are denoted as $K_\nu(x)$. It coincides with the Chi-square distribution for $\nu = \infty$ and it also contains the Lehman distribution for $\nu = 3$. A smooth transition between these two classes can be achieved by varying the parameter ν. From another point of view, it is shown that the moments of the intensity of the random field described by a *K* distribution are always bounded by those of log-normal (upper bound) and those of the Chi-square and generalized Gamma distribution (lower bound). The fact that the K distributions are two-parameter distributions gives an additional degree of freedom for modelling purposes. Yet another useful property is the invariance of a *K* distributed random field under a linear transformation. This may be extremely useful when the effect of the external coupling into transmission lines is considered in more detail.

In Chapters V and VI we apply the finite difference technique to two problems which are of great interest: a) the coupling of randomly oriented plane waves into enclosures with an aperture (Chapter V); and b) the coupling of statistically described fields to a single transmission line (Chapter VI). In the first problem the randomness is incorporated in the angle of incidence and polarization of the impinging plane wave. Full-wave finite difference time domain (FDTD) simulations are used to obtain data. The applicability of the method to derive the appropriate statistics of the electromagnetic field inside enclosures is proven. Using a simple example of a computer box with its front cover removed, we show that the *K* distribution provides a better fit to the numerical data than the Chi-square distribution at least for a cavity whose size is larger than the wavelength of the incident field. However more work is required to investigate the case when the frequency of the excitation is close to the cut-off frequency of the box. It is also shown that even a "weak randomization" (*i.e.* averaging over only a few incident angles) of the incident field allows one to obtain results close to those predicted by statistical theory. Contrary to commonly made assumptions about the phase distribution inside an enclosure, the data in these simulations show that the phase distribution is not uniform but rather can be modelled as a mixture of Tikhonov distributions.

In the second problem, the coupling field is described by its distribution and correlation length. The UWO FDTD program was used to perform the calculations in the enclosure problem. A novel computer program (which we call "STEM" for STatistical ElectroMagnetics) was written in the MATLAB environment for performing the calculations of the transmission line problem. In this code the quasi-TEM (transverse electromagnetic) approximation is made to model the transmission line and the coupling is represented as distributed voltages and currents along the line. These distributed sources are randomly generated according to a user specified distribution and correlation length. The Monte Carlo technique is used to generate the corresponding probability density functions for the voltages at the resistive

terminations of the line. In this way the effects of different correlation lengths and different assumed field distributions on the termination voltages can be studied. It is shown that deviations of the coupling field statistics from Chi-square lead to similar deviations in the statistics of the induced voltages and currents at the ends of the transmission line but this effect disappears when the length of the transmission line approaches several wavelengths. Furthermore, on one hand, we see that a completely decorrelated excitation along the line results in an almost Chi-square behaviour of the terminal voltages and currents even for relatively short (less then 0.25λ) transmission lines. On the other hand, highly correlated non-Chi-square external fields result in highly irregular terminal voltage behaviour, *i.e.* deviations from the Chi-square statistics is significant even for relatively long transmission lines.

We conclude, in Chapter VII, by overviewing what has been accomplished in this report and by making recommendations for future research. A complete set of references, segregated into subject areas, is included in Chapter VIII. An addendum report, consisting of the INSPEC literature search which was performed for this research, is also available.

II. Literature Review

In this chapter, a review of the existing literature on statistical methods of characterizing electromagnetic compatibility problems is made. As was discussed in the introduction, the main reason for investigating statistical modelling techniques is that it is unreasonable to expect to perform a detailed electromagnetic field analysis of a large electronic system, complete with circuit boards, cables and electronics using a computational electromagnetics method. Modelling approximations must be made and these lead to uncertainty in the applicability of the results to the actual problem. It is surprising to find that it has taken so long, with respect to the development of EMC mathematical models, for researchers to investigate, develop and emphasize the need for statistical techniques. This review is divided into four parts: a) the statistical description of fields inside *complex enclosures* and *reverberation chambers*; b) experimental results of electromagnetic coupling; c) the coupling of statistically described fields into transmission lines; and d) the statistical characterization of cross-talk in multiconductor transmission lines.

2.1 Statistical description of electromagnetic fields inside a complex enclosures

2.1.1 Lehman's fundamental publication [33]

Lehman's work [33], inspired by [58], is an attempt to describe the general statistics of the electromagnetic field inside an arbitrarily shaped, lossy, and electrically large cavity excited by an internal source. The goal was to derive an applicable distribution which does not depend on the particular cavity's shape and size. The following assumptions were made with regard to the cavity: a) the complex cavity assumption; b) the large number of modes assumption; and c) that all the modes excited have equal energy. Lehman defines a complex cavity as one in which the coherent contributions from the wall reflections are minimal. That is, at any point inside the cavity, the total electric field (or magnetic field) can be well approximated as the summation of a large number of non-coherent contributions.

In [33], Lehman derives a novel, but approximate, form for the expansion of an arbitrary field inside an arbitrary enclosure. Various conclusions were drawn about the statistical properties inside a complex cavity. With the assumption of a large number of modes, the amplitude of each component of the field is shown to be distributed according to a normal (*i.e.* Gaussian) distribution. This automatically implies the fact that the *magnitude* of a component of the total electric field in a complex cavity obeys the Rayleigh

distribution and the square of a component of the time averaged total electric field is distributed according to a Chi-square distribution with two degrees of freedom (*i.e.* an exponential distribution). Yet another consequence of the overmoded cavity assumption defines the correlation properties of the field inside the enclosure. Expressions for the spatial $K_s(r_1, r_2;\omega)$, and temporal, $K_T(t_1, t_2;r_1, r_2)$, correlation functions are given in [33].

One of the most fundamental conclusions obtained in this paper is the fact that the probability density function and the correlation functions are independent of the shape of the cavity as long as it satisfies the definition of a complex cavity, *i.e.* the theory states that for a given set of cavities with the same volume, V, and quality factor, Q, the statistics will be the same. A number of other publications exist on this subject of relating Q and V to the cavity statistics and these are considered below. It is also shown in [33] that volume averages can be replaced by the ensemble averages[1]. This is important for the case of stirred-mode chambers since with this fact one need only average the field at one point over stirrer positions and this will be equivalent to averaging the fields over the volume of the chamber. The theory also predicts the possibility of "statistical homogenization" of the fields inside an enclosure using frequency and phase stirring. This is based on the fact that the quality factor Q of any realistic enclosure is a slowly varying function of the frequency.

Although the theory in [33] is promising, some discrepancies between theoretical and experimental results, or so called "outliers" (values higher than those predicted by an exponential distribution), were reported in experimental tests. The possible cause of this, in mode-stirred chambers, was speculated on. One possible explanation for the existence of these differences may be the small number of excited modes (*i.e.* not enough for a valid application of the theory). A number of additional unsolved problems in the theory are also discussed. In fact, there is no precise definition of what a "complex cavity" means. It is not possible *a priori* to validate the complexity of a cavity for every cavity of interest. The only practical way to proceed is to assume the complexity of the cavity based on experience with various other cavities and then to use experimental data to justify the assumption. One possible way to validate this assumption would be to numerically determine the mode shapes of cavities with complex shapes. This would not be a particularly difficult computation since the walls of the cavity can be assumed to be perfectly conducting. Other authors of the same research group have considered an overmoded cavity as just an electrically large cavity, that is, assuming that its characteristic dimension is larger than $(6 \rightarrow 10)\ \lambda$ [34-41] and assuming also that the cavity has a high Q. The "ideal" results depend on the cavity not having a frequency-dependent Q and on all parts of the cavity being equally shielded (*i.e.* no sub-enclosures within the enclosure, no regions with closely spaced walls which could act like a waveguide below cutoff, and no observations made at points significantly illuminated by direct radiation from the driving source) [39]. The

1. A phenomena similar, or inverse, to ergodicity [24].

case of evanescent waves was not considered at all; this makes the applicability of the theory to smaller systems questionable. In fact, the case of small enclosures will be an area of future study.

The source of *outliers* in mode-stirred chamber experiments has not been established. Since the mode-stirred chamber is essentially a rectangular enclosure with a mechanical stirrer to introduce complexity, it is not difficult to envision that the complexity assumption is not satisfied for some orientation of the stirrer. The coherent contribution from these outlier modes would dominate the measured response and the derived distributions would not be valid for this case[1]. One of the major difficulties, from our perspective, is the fact that the theoretically predicted Chi-square distribution is a one parameter distribution; that is, its variance is defined by its mean, and *vice versa*. However, this condition is not satisfied in practice. One suggestion has been to use a *log-normal* distribution (which is a two-parameter distribution) to obtain a better agreement with experiments. However, it has been known for a long time that this distribution is not accurate in describing the tails.

2.1.2 R. Holland and R. St. John group publications [34-39]

A number of publications have made an attempt to use the results described above in some practical applications. The following is a short description of these works. Various authors have considered the statistical distribution of the electromagnetic field or power flux in a reverberation chamber. The frequency of excitation or sensor (*i.e.* receiver) position are chosen as independent random variables, *i.e.* stirring can be achieved either by frequency modulation or by randomizing the geometry. It was concluded in [34-35] that a normal distribution of a field component (Chi-square for power flux) does not fit a number of experimentally and numerically obtained data. Thus an attempt to modify the results of the original papers [33, 34, 38] was undertaken. This resulted in, what has come to be known as, the Lehman distribution with so-called trends, considered in [33-38].

The main idea behind the Lehman derivation, is that the power flux density z_1 is still represented by the Chi-square distribution with two degrees of freedom, but now it is modulated by another random variable z_2 to incorporate the fact that the external illumination may come from three different spatial directions and every one of them has two possible polarizations. Thus, z_2 may be thought of as a Chi-square distribution with six degrees of freedom. Their product produces the Lehman distribution.

Four different models, based on Chi-square, Lehman, log-normal and a mixture of the log-normal and the Chi-square distributions are used to approximate the real statistics in a complex cavity. The manuscript

1. A similar phenomena can be observed in communication channels. In fact, if there is no Line Of Site (LOS) from the transmitting to the receiving antenna, the field distribution is due to a large number of small diffusion components, carrying approximately the same amount of energy which are randomly and uniformly shifted in phase. This creates a Gaussian distribution of the field and thus a Rayleigh distribution of its magnitude. If an LOS is present, it will dominate the diffusion components and the distribution of magnitudes appears to be a Rician distribution [30].

of [36] mostly concentrates on attempts to obtain the distribution of field components, given that the distribution of the power flux density is assumed to be the Lehman distribution.

Most of the material, produced by the Lehman-Holland-St. John group, and scattered through a number of conference publications, is concentrated in [36] and, in an up-coming book [39]. The main contribution of [36] is the development of an algorithm which models cable-drive fields simultaneously having a Chi-square power flux intensity distribution and the physically mandated local autocorrelation function at a spatial point as frequency is swept or at a fixed frequency as the power flux sensor is moved around to map the cavity response. It is proposed that this algorithm could later be used in a circuit analysis code to analyse a circuit representing part of an enclosed system's wiring.

The paper treats the deviation of real cavity statistics from the theoretically ideal Chi-square distribution of power flux density as an effect of "trends" - relatively slow varying modulations due to violation of ideal assumptions in the Lehman original paper [33]. In addition to the Lehman original six degree of freedom illumination [40], they deal with frequency dependent cavity Q's, cable attenuations, *etc.* Numerical techniques, allowing one to "demodulate" these trends are described.

The most recent publications deal with numerical, [62, 64-67, 69], and experimental, [43, 44, 47, 60, 61, 68, 70], verification of fields applied to equipment under test in a reverberation chamber. The Method of Moments (MoM) is used to predict the induced currents in a monopolar antenna [38-41]. The MoM produces a linear predictor equation and thus it makes it easy to calculate the statistics of the current, once a Gaussian distribution of electric and magnetic field is assumed. In fact, any linear transformations will result in a Gaussian process again, but possibly with a different correlation function. A Gaussian distribution is defined by its first two moments, thus only two quantities need be measured in practice to validate the results. Similar work was reported in [42] where the so-called Maximum-to-Mean ratio was experimentally compared against theoretical results.

2.1.3 D. Hill group publications [43-48]

In this group of papers, the reported research is on stirred-mode chambers. In this application, it is important to create a statistically uniform electromagnetic field inside a chamber. This is usually achieved by mechanical stirring, however frequency stirring can also be used.

The first paper published by the authors, [43], considered the coupling of an electromagnetic field into a coaxial air line through a small aperture. An analytical (and deterministic) model was developed and then experimental results, conducted in a reverberation chamber, were compared against this theory. The random nature of the field which was to be measured, prompted the consideration of the excitation of an arbitrary antenna by a random field. To achieve this goal the authors represented the incident field a sum of partial plane waves over all real angles. The following assumptions were made about the statistical

properties of the field:

- Two partial plane waves corresponding to different incident angles are independent;
- The energy of these partial waves are equal

These are the same assumptions which were made in Lehman's paper [33]. The integral expression was then derived for the average energy coupled into the antenna. Later, the spatial correlation function, coinciding with those in [33], was introduced in a short letter [46].

The next paper, [45], addresses problems in the mathematical modelling of the shielding effectiveness of electrically large enclosures which contain apertures and interior loading. Some mathematical expressions for the enclosure's Q were developed. These equations take into account wall losses, absorption and aperture leakage. An important contribution is that these formulas are generic, *i.e.* they are independent of the specific aperture dimensions, shape of the enclosure, *etc.* We describe these results in detail in Chapter III.

Investigations related to the creating of a statistically uniform electromagnetic field using frequency stirring were reported in [44]. A two dimensional geometry of a rectangular cavity, excited by a line source was considered. The exact solution was found first for the case of perfectly electric conducting (PEC) boundaries. Then, this solution was modified using the analytic continuation of the real wavevector, k, into the complex plane, *i.e.* $k_c = k(1 - j/2Q)$, where Q is the cavity quality factor. A further development was again based on the assumption that the statistical properties of the field are spatially uniform throughout the cavity. It was also assumed that the line source radiates the same field in a lossy enclosure as in a free space environment. These are equivalent to the assumption that the cavity itself is electrically large and that the source is located far from the walls. Expressions for Q in terms of lossy wall parameters are then developed [44, 48]. With these expressions in hand, the author considers frequency stirring of the chamber. An expression for the mode density as a function of the Q, the excitation frequency, and the chambers dimensions was found. It was then assumed that the excitation itself is wideband and thus excites more modes than just a single frequency excitation. This contributes to ameliorating the field uniformity (*i.e.* the more modes which are excited simultaneously the better the field uniformity). Multiple source as well as phase stirring were also considered. However it was mentioned that to achieve better results some mechanical stirring is still necessary.

2.1.4 Other publications

One of the pioneering works on statistical modelling of mode-stirred chambers is [69]. Here it is stated (as has been stated in [33] and other publications) that in order to get a statistically uniform field, the chamber has to be electrically large, overmoded, and observations should be made far from the walls. It is stated that the number of modes is approximately equal to $n = abc/\lambda^3$ where a, b and c are the room

dimensions and λ is the wavelength.

Six components are needed to describe both $\boldsymbol{E}$ and $\boldsymbol{H}$ fields at every point. Each of these components is assumed to be the sum of a large number of random variables (mode amplitudes) and thus should be normally distributed. It is also argued that these six components have to have a zero mean if there is not a significant direct-path signal from the antenna in the chamber to the measurement point. This may be achieved by placing an antenna close to and pointing into a corner of the chamber. This model leads to a Chi-square distribution with six degrees of freedom - a very slight generalization of the statistics used by the Lehman group. However, if a probe responds only to one component, then the statistics will be reduced to the Chi-square distribution with two degrees of freedom.

The paper also describes how the PDF can be used to build an optimal estimator of the distribution parameters - something totally neglected by other researchers. An example is developed for the case of the Chi-square distribution with two degrees of freedom. These estimates are later used to calculate a chamber's quality factor Q.

Similar investigations as to those of the statistics of an electromagnetic field inside enclosures can be found in more classical papers which deal with the wave propagation in a random medium. Many authors came to the conclusion that the magnitude of the electromagnetic field in this case is also distributed according to the Rayleigh law. A systematic derivation can be done on the basis of a perturbative diagrammatic technique [81-82]. This technique is based on the solution of the wave equation, for a scalar field component, with a random wave number:

$$\{\nabla^2 + k_0^2[1 + \mu(\boldsymbol{r})]\}E(\boldsymbol{r}, \omega) = 0 \tag{1}$$

supplemented with a proper source. In the diagrammatic approach one computes moments of the intensity $I = |E(\boldsymbol{r}, \omega)|^2$ and then constructs the PDF of the distribution $p_i(I)$. As in the Price or Lehman papers, a large number of approximately equal eigenmodes provide the necessary conditions for such statistics.

It was pointed out in [81], that the Rayleigh distribution applies to the case of a monochromatic wave propagating in an open system. A different type of problem arises if one considers the wave equation (1) in a closed geometry without sources. In this case one inquires about the statistical properties of a single eigenstate $E_\alpha(\boldsymbol{r})$ [1], *i.e.* about the distribution $p_i(I)$ of the quantity $I = |E_\alpha(\boldsymbol{r})|^2$. It was shown in [81, 86] that the main part of the distribution is described by the Porter-Thomas (PT) statistics:

$$p_{PT}(I) = \sqrt{\frac{V}{2\pi I}}\exp\left[-\frac{IV}{2}\right] \tag{2}$$

1. This is another limiting case. It seems to be a reasonable assumption that real situation in a leaky cavity can be described by some intermediate case.

where V is the volume of the cavity and $m_{PTl} = 1/V$. It is easy to see that the Porter-Thomas statistics is a particular case of the Gamma distribution (see Chapter IV for a more detailed description of this family). The following idea was suggested in [81]: let us assume that the cavity is weakly coupled to the environment (for example, through a small aperture). Then, by placing a monochromatic source inside the cavity [86] and tuning its frequency, ω, to a resonance, one will generate in the cavity an intensity pattern $I(\boldsymbol{r})$ which closely follows the pattern of $|E_\alpha(\boldsymbol{r})|^2$ of the eigenstate α with frequency $\omega_\alpha \approx \omega$. Thus, the intensity distribution will be given by the Porter-Thomas statistics (2). On the other hand, for a sufficiently strong coupling, in an open system, the distribution should obey the Chi-square statistics. The main result of [81] consists in the construction of the interpolating distribution between these two distributions.

In the same paper, the following differences between an open and a closed system were considered, using a simple picture of the addition of many random waves. In an open system, a field component $E(\boldsymbol{r}, t)$ can be viewed as the sum of a large number N of *travelling waves* arriving at a point $\boldsymbol{r}$ from various wave processes:

$$E(\boldsymbol{r}, t) = \frac{1}{\sqrt{N}} \sum_{n=1}^{N} \cos(\theta_n + \boldsymbol{k}_n \cdot \boldsymbol{r} - \omega t) \tag{3}$$

where the phases θ_n are completely random and all the amplitudes have been taken to be equal (one could assume random independent amplitudes without any change in the results). The wave vectors $\boldsymbol{k}_n$ are uniformly distributed on a d-dimensional sphere ($d = 2, 3$) of radius k_0. The instantaneous local field intensity is defined as $E(\boldsymbol{r}, t)^2$. The measured quantity is, however, the intensity averaged over one period, that is

$$I = \frac{2\pi}{\omega} \int_0^{\omega/2\pi} E(\boldsymbol{r}, t)^2 dt = \frac{1}{2N} \sum_{n,m}^{N} \cos[\theta_n - \theta_m + (\boldsymbol{k}_n - \boldsymbol{k}_m) \cdot \boldsymbol{r}] \tag{4}$$

The same expression can be obtained if the complex form of (3), that is

$$E(\boldsymbol{r}, t) = \frac{1}{\sqrt{N}} \sum_{n=1}^{N} e^{j(\theta_n + k_n \cdot r - \omega t)}, \tag{5}$$

is assumed and the intensity is defined as $|E(\boldsymbol{r})|^2$. In the limit, as $N \to \infty$, the distribution of the real and the imaginary parts of $E(\boldsymbol{r})$ become Gaussian, thus leading to a Chi-square distribution [33]. Let us note that travelling waves can be created in closed cavities by means of space, frequency or phase stirring [44] (as well as absorption by walls).

In a closed (*i.e.* resonant) system the field is viewed as a sum of many *standing waves*:

$$E(\boldsymbol{r}, t) = \frac{1}{\sqrt{N}} \sum_{n=1}^{N} \cos(\theta_n + \boldsymbol{k}_n \cdot \boldsymbol{r}) \cos\omega t \tag{6}$$

or, after time averaging of the intensity $I = |E(\boldsymbol{r}, t)|^2$

$$I = \frac{\omega}{2\pi} \int_0^{2\pi/\omega} |E(\boldsymbol{r}, t)|^2 dt = \frac{1}{4N} \sum_{m,n=1}^{N} \cos[\theta_n - \theta_m + (\boldsymbol{k}_n - \boldsymbol{k}_m) \cdot \boldsymbol{r}] \cos[\theta_n + \theta_m + (\boldsymbol{k}_n + \boldsymbol{k}_m) \cdot \boldsymbol{r}] \tag{7}$$

Let us emphasize here that θ_n is fixed and deterministic for the case of standing waves. In the limiting case as $N \rightarrow \infty$, the Porter-Thomas statistics (2) for the intensity I can be derived [81]. Detailed investigation of the statistics of the mixture of travelling and standing waves will be conducted during the next stage of this research.

Thus, two different extreme cases - standing waves or travelling waves only - will lead to two different results. In one case it is the well known Chi-square distribution [33], in the other is the Porter-Thomas statistics, widely used in the physics community but rarely used in the electrical engineering community. This gives yet another explanation of what should be understood by the term "overmoded" cavity [33]. An "overmoded" cavity is one in which no standing waves exist, or in other words where the standing wave ratio SWR is very low. This is achieved when the cavity has a lot of leakage or when it is well stirred.

This approach looks competitive with that which we are considering throughout this current report. It is partially implemented in our StEm Tool (see Chapter VI for details). However we propose to investigate this subject in depth during the next stages of this research.

2.2 Experimental results of electromagnetic coupling

In [34-36], some measurements were conducted in order to validate some of the models we have mentioned. In particular, the EMPTAC 720 (EMP Test AirCraft facility) shell[1] was externally illuminated by an elliptically polarized antenna and the frequency was swept from 0.1 to 1 GHz. The estimated mean and variance values of the induced currents on an internal cable were then used to generate a model distribution and this was compared against measured data. A numerical transmission-line model of the tested cable was created: length 20 m, characteristic impedance about 30 Ω, standoff $h = 5$ cm, per unit length inductance $L = 1\ \mu H/m$, and the capacitance was chosen to provide a propagation velocity equal to the speed of light. The cable was divided into 200 segments and excited by 1000 different frequencies which were exponentially stepped between 100 MHz and 1 GHz. The phase quadrature magnetic driving fields on each segment of cable were randomly chosen according to a Gaussian model [36].

1. Essentially, EMPTAC is a gutted 720 airframe. The electromagnetic energy is leaking inside EMPTAC through existing deliberate and inadvertent apertures and antenna feed cables [35].

Some data, related to the power-flux distribution in the Celestron 8 satellite are discussed. The applicability of the Lehman distribution is considered with respect to this data [34-36].

An externally illuminated, leaky, resonant-waveguide was used to test the Lehman statistics in [34-36]. The enclosure contained cables and the currents at their terminals were measured. The frequency was swept from 0.3 to 3.0 GHz to obtain the necessary stirring.

Experiments with a $1.2 \times 1.2 \times 7.3\ m^3$ sheet-metal walled chamber illuminated from one end were reported in [35]. The electric field was swept from *300 MHz* to *3 GHz* and was measured using an ACD-4D sensor connected to an HP8753 network analyser through an amplifier. The cavity was illuminated by a log-periodic antenna and driven by a network analyser. The currents were generated on the shield of a 1.2 m long coaxial cable which was placed in a variety of orientations in the illuminated enclosure and was terminated directly to the conducting walls of the chamber. The currents were measured through a Fisger PNF-65 probe. The placement of the current probe was in the centre of the cable. The electric-field probe was moved around within the volume for the four sets of data (usually between one and two meters from the cable). The orientation of the illuminating antenna was also changed.

An experimental study of the coupling of an electromagnetic field into a shielded cable through an aperture was reported in [43]. Measurements of the shielding effectiveness were conducted in a reverberation chamber over the frequency range of 1 to 18 GHz. The parameters of the apertures and coaxial air line were: line radius b = 3.5 mm, aperture location z_0 = 10.7 cm, aperture radius a = 1 mm, and characteristic impedance Z_c = 50 Ω. A second air line was also constructed with a larger aperture of a = 1.5 mm.

A rectangular cavity having size $1.75 \times 0.629 \times 0.514$ m, made of an aluminium alloy (FAA cavity) was built to validate the results obtained in [60]. Glass containers of salt water was used to introduce absorption losses. A circular aperture of radius r = 1.5 cm and three salt-water spheres of radius r_s = 6.6 cm were used in the experiments. Double-ridged horns were used for the transmitting and receiving signals in the range of 1 to 18 GHz. The measured Q was compared against the theoretical results.

A 4.57×3.05 m "two-dimensional" cavity with a line source and a quality factor $Q = 10^5$ was considered in [47]. The effect of the bandwidth of the excitation on the uniformness of the field inside the cavity was investigated. It was shown that the uniformity is improved if the source has a larger bandwidth. Also it was reported that frequency stirring improves uniformity at points close to the walls of the cavity.

A $10 \times 20 \times 8$ ft. mode-stirring chamber was investigated in [44]. Point measurements were made at ten locations and three frequencies: 4, 6, and 8 GHz. The square-law probe voltage was expected to be

exponentially distributed. A number of outliers were reported and their nature was not identified.

2.3 Coupling of statistically described fields to transmission lines

There are a few different ways of how a statistical description can be introduced into the problem of an external electromagnetic field coupling to a transmission line. First of all, one can assume that a plane wave of unknown polarization and direction of arrival hits a deterministically described transmission line. In this case, a Monte-Carlo simulation is easy to implement - each trial is nothing but a deterministic problem. This approach has been used in order to estimate the impact of an external field on power lines and is described in a number of papers [50, 52-57].

Another approach is to treat the excitation as deterministically known but treat the transmission line parameters as random variables. This approach is well suited for investigating the coupling of electromagnetic waves produced by a single known source (usually modelled as a plane, cylindrical or spherical wave) into PCB's whose parameters are random due to manufacturing tolerances. The uncertainties in such parameters are relatively small and this allows one to treat the problem in the frame of small perturbation theory. A number of papers can be found on this subject [50, 51, 52].

The most relevant formulation to EMC is, however, the case where the external field itself is considered as a random field[1]. This allows one to incorporate uncertainties in the receptor location, incident field parameters, and most important, allows one to approximate the effect of an enclosure of unknown geometry. The simplest model immediately follows from the Lehman theory. However, due to the discrepancies between predictions and measurements, this model cannot be universally accepted. Only a token number of papers are known which consider more sophisticated models. Most of them have appeared during the last few years in conference publications. [37, 65-68].

2.4 Statistical description of cross-talk in multiconductor transmission lines

An experimental study of cross-talk in twisted-pair communication cables was undertaken in [52]. This study revealed that a simple Gaussian probability density function model for pair-to-pair cross-talk, where the Gaussian PDF must be truncated to fit experimental measurements is not desirable since in practical repeater design applications it is the extreme tail region, below 0.1 percent, which is important. It was shown, using measured crosstalk data from 619 cables, that the gamma distribution is a more satisfactory approximation than the conventionally accepted normal distribution for modelling multi-pair crosstalk behaviour (using a decibel scale).

A strict analytical approach to evaluating the coupling between wires in a three conductor transmission line was undertaken in [51]. The distances between the wires and the ground plane were assumed to be

1. Here the term "random field" refers to a random function of three spatial variables

uniformly distributed within finite regions and the corresponding distribution of the coupling was computed using calculated distributions of the per-unit-length inductance and capacitance. The probability density function which was obtained confirms the fact that experimental data produces PDF's having relatively longer tails than a simple Gaussian PDF. A direct generalization of this method to the case of four or more wires is quite difficult; however, some attempts to build a suitable approximation were undertaken in [63].

A number of statistical models have been deduced from direct Monte-Carlo simulations of cross-talk. For example, Monte-Carlo simulations wherein various PCB parameters were randomized were reported in [52]. The worse-case scenario, *i.e.* maximum possible over-voltage, was then found using these simulations. Similar work was conducted in the case of multi-wire communication cables [63, 39]. A detailed investigation and statistical characterization of the cross-talk in MTL bundles consisting of more than 100 conductors was undertaken in [63]. In this work analytical, numerical, and experimental results were reported.

All of these statistical investigations show that useful models of structures with uncertain parameters can be derived using both analytical techniques and brute force Monte-Carlo processing using numerical techniques or experimental data. Once available, such statistical models of the expected electromagnetic interference can be considered in the design and simulation of digital devices.

III. The Physics of Complex Enclosures

In this section we investigate the physics of electromagnetic fields existing in, what have come to be known as in the statistical EMC literature, complex enclosures. The term "complex" refers to an enclosure in which the boundaries do not define a simple geometric object such as a sphere or a rectangular parallelepiped (or box). Additionally, there exist electromagnetic losses in the complex enclosure which are due to one or more of the following physical features: lossy or non-perfectly conducting walls, apertures which allow energy to escape, and absorbing structures such as printed circuit boards and cables inside the enclosure. The complexity of the enclosure is a measure of how many of these features exist. A relatively generic theory of these enclosures has been developed by Hill *et al.* [45, 48, 69]. The main electromagnetic concepts which is used for that theory are the concepts of resonance, quality factor Q, and the number of spatial frequency modes which are excited. In order to get a good understanding of these electromagnetic concepts, we begin by investigating some analytic and quasi-analytic solutions to lossy one dimensional and two dimensional resonators: a terminated transmission line and a hollow waveguide with an infinite line-source excitation.

3.1 Resonance of a one dimensional enclosure

Consider a one dimensional resonator which is terminated by lossy walls. This is equivalent to a single transmission line which is terminated at each end with impedances (voltage along the line maps to the electric field and current along the line maps to the magnetic field). First, we will develop an exact analytical expression for the field inside this 1-D resonator by modelling it as a transmission line with a current source excitation somewhere along the line. This expression will be compared against the eigenfunction expansion, obtained for the lossless case and modified using Morse's method [21]. Limits of this approximation are investigated. An approximate expression for the eigenvalues of the mixed boundary problem are also found.

3.1.1 Solution based on transmission line equations

Consider the transmission line of length d, excited by a point harmonic source of current I_s, located at the point $z = z_0$, as shown in Fig. 1. This is equivalent to a one dimensional resonator. The walls of this resonator are lossy and can be modelled by termination impedances, Z_w, on the transmission line. The

characteristic impedance of the transmission line is assumed to be real $Z_0 = R_0$. In free space we have $Z_0 = \eta_0 = \sqrt{\mu_0/\varepsilon_0}$ and the velocity of propagation (or phase velocity) is $v_p = c = (\mu_0\varepsilon_0)^{-1/2}$. The normalized termination impedances, ξ_w, are defined as

$$\xi_w = Z_w/Z_0 = r_w + jx_w. \tag{8}$$

Assuming a time-harmonic source of angular frequency ω, the corresponding propagation constant is defined as [87]

$$\beta = \omega/v_p \tag{9}$$

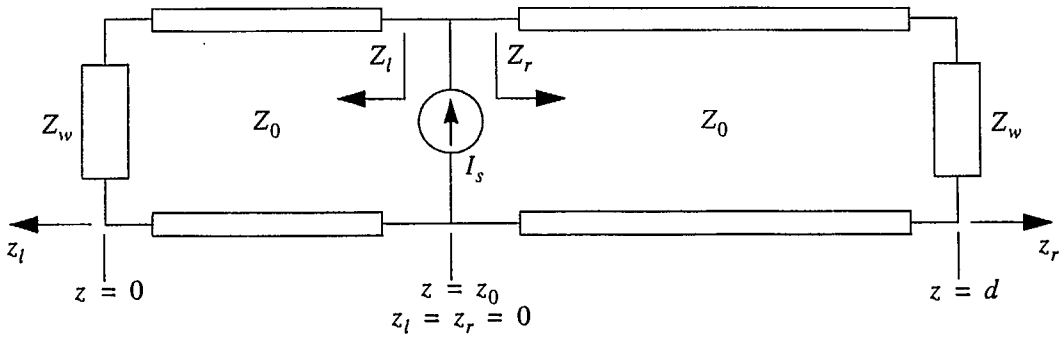

Figure 1. Geometry of the problem

Both load impedances can be transformed to the source point, at location $z = z_0$, according to the standard impedance transformation equation (see page 248 in [87]):

$$Z_l = Z_0 \frac{\xi_w \cos\beta z_0 + j\sin\beta z_0}{\cos\beta z_0 + j\xi_w \sin\beta z_0} \tag{10}$$

$$Z_r = Z_0 \frac{\xi_w \cos\beta(d - z_0) + j\sin\beta(d - z_0)}{\cos\beta(d - z_0) + j\xi_w \sin\beta(d - z_0)} \tag{11}$$

This allows us to find the corresponding driving currents, and thus, the voltage along the line as (see page 248 in [87])

$$E = I_s \frac{Z_r Z_l}{Z_r + Z_l},\ I_l = \frac{E}{Z_l},\ I_r = \frac{E}{Z_r} \tag{12}$$

$$\begin{aligned} V_l(z_l) &= E\cos\beta z_l - jI_l Z_0 \sin\beta z_l = E\cos\beta z_l - j\frac{E}{Z_l} Z_0 \sin\beta z_l \\ &= E\left[\cos\beta z_l - j\frac{\cos\beta z_0 + j\xi_w \sin\beta z_0}{\xi_w \cos\beta z_0 + j\sin\beta z_0}\sin\beta z_l\right] \\ &= E\left[\frac{\xi_w \cos\beta(z_l - z_0) - j\sin\beta(z_l - z_0)}{\xi_w \cos\beta z_0 + j\sin\beta z_0}\right] \end{aligned} \tag{13}$$

$$
\begin{aligned}
V_r(z_r) &= E\cos\beta z_r - jI_r Z_0 \sin\beta z_r = E\cos\beta z_r - j\frac{E}{Z_r}Z_0\sin\beta z_r \\
&= E\left[\cos\beta z_r - j\frac{\cos\beta(d-z_0)+j\xi_w\sin\beta(d-z_0)}{\xi_w\cos\beta(d-z_0)+j\sin\beta(d-z_0)}\sin\beta z_r\right] \\
&= E\left[\frac{\xi_w\cos\beta(d-z_r-z_0)+j\sin\beta(d-z_r-z_0)}{\xi_w\cos\beta(d-z_0)+j\sin\beta(d-z_0)}\right]
\end{aligned}
\tag{14}
$$

Defining the new variables, $z_l = -z + z_0$ and $z_r = z - z_0$, as in Fig. 1 allows us to re-write (13)-(14) as

$$
V_l(z_l) = E\left[\frac{\xi_w\cos\beta z + j\sin\beta z}{\xi_w\cos\beta z_0 + j\sin\beta z_0}\right],\ 0 \le z < z_0 \tag{15}
$$

$$
V_r(z_r) = E\left[\frac{\xi_w\cos\beta(d-z)+j\sin\beta(d-z)}{\xi_w\cos\beta(d-z_0)+j\sin\beta(d-z_0)}\right],\ z_0 < z \le d \tag{16}
$$

This form of the solution allows a fast and simple calculation of the electromagnetic field inside the one-dimensional cavity, however, it does not give a deep insight into the structure of the eigenmodes, which is of primary interest here.

3.1.2 Eigenmode expansion, Method A: expansion in terms of sines and cosines

We again use the transmission line analogy but now we obtain an eigenfunction expansion of the electromagnetic field (*i.e.* voltage) inside the one dimensional resonator. In the lossless case the eigenfunctions are either sines or cosines, depending on how the z-axis is chosen. The system of differential equations to be solved is

$$
\begin{aligned}
&\frac{d}{dz}V(z) + j\omega L I(z) = 0 \\
&\qquad\qquad\qquad\qquad\qquad\qquad , 0 < z < d \\
&\frac{d}{dz}I(z) + j\omega C V(z) = I_s\delta(z-z_0)
\end{aligned}
\tag{17}
$$

where L and C are the per unit length inductance and capacitance of the transmission line, the Dirac delta function term $I_s\delta(z-z_0)$ takes into account the current source located at $z = z_0$, $L = \mu_0$ and $C = \varepsilon_0$. From these, a second order differential equation for the voltage along the line can be derived as

$$
\frac{d^2}{dz^2}V(z) + \beta^2 V(z) = -j\omega L I_s\delta(z-z_0) \tag{18}
$$

where $\beta = \omega\sqrt{LC} = \omega/v_p$. For the lossless case the boundary conditions state that the voltage (*i.e.* the electric field) is zero at $z = 0$ and $z = d$. The solution in terms of an eigenfunction expansion for this lossless case is given in [23] as

$$V(z) = \frac{-j\omega 2LI_s}{d}\sum_{n=1}^{\infty}\frac{\sin\left(\frac{n\pi}{d}z_0\right)\sin\left(\frac{n\pi}{d}z\right)}{\beta^2-\left(\frac{n\pi}{d}\right)^2}. \tag{19}$$

Note that singularities in the solution exist at the resonance frequencies given by

$$f_{rn} = \frac{n}{2d\sqrt{LC}} = \frac{n}{2d\sqrt{\mu_0\varepsilon_0}}. \tag{20}$$

The solution becomes more difficult to obtain when the walls of the resonator are lossy. In order to simplify the equations, we introduce a new coordinate system defined as

$$u = z-a,\ a = d/2 \tag{21}$$

Thus the boundary conditions of the corresponding transmission line equations will be specified at $u = \pm a$. The eigenfunctions are obtained by solving for the homogeneous transmission line equations which are now given by

$$\begin{aligned}\frac{d}{du}V(u)+j\omega LI(u) &= 0\\ \frac{d}{du}I(u)+j\omega CV(u) &= 0\end{aligned},\ -a<u<a \tag{22}$$

It follows from (22) that

$$I(u) = \frac{-1}{j\omega L}\frac{d}{du}V(u). \tag{23}$$

At the terminations of the transmission line, the current and voltage are related by Ohm's law, that is

$$V(-a)+Z_wI(-a) = V(-a)-\frac{Z_w}{j\omega L}\frac{d}{du}V(u)\Big|_{u=-a} = 0 \tag{24}$$

$$V(a)-Z_wI(a) = V(a)+\frac{Z_w}{j\omega L}\frac{d}{du}V(u)\Big|_{u=a} = 0 \tag{25}$$

As before, it follows from the transmission line equations that both the voltage $V(u)$ and the current $I(u)$ obey the second order wave equation, that is

$$\frac{d^2}{du^2}V(u)+\beta^2V(u) = 0,\ \frac{d^2}{du^2}I(u)+\beta^2I(u) = 0 \tag{26}$$

The eigenfunctions of this equation are the sine and cosine functions

$$\Psi(u) = A\cos\gamma u + B\sin\gamma u \tag{27}$$

where the coefficients A, B and eigenvalue γ should be chosen to satisfy the boundary conditions (24) and (25) as well as represent a solution for the particular position of the exciting source. The final solution for the voltage or current along the line will be made up of an infinite summation of these eigenfunctions. The result will have the form of a series containing both cosines and sines:

$$V(u) = \sum_{n=0}^{\infty} A_n \cos\gamma_n u + B_n \sin\gamma_n u . \tag{28}$$

Taking the derivative of (27) with respect to u and calculating the values of $\Psi(u)$ and $\Psi'(u)$ at $u = \pm a$ one obtains

$$\Psi(-a) = A\cos\gamma a - B\sin\gamma a\,,\ \Psi'(u)\big|_{u=-a} = \gamma A\sin\gamma a + \gamma B\cos\gamma a \tag{29}$$

$$\Psi(a) = A\cos\gamma a + B\sin\gamma a\,,\ \Psi'(u)\big|_{u=a} = -\gamma A\sin\gamma a + \gamma B\cos\gamma a \tag{30}$$

Substitution of (29) and (30) into boundary conditions (24) and (25) one obtains

$$A\cos\gamma a - B\sin\gamma a - \frac{Z_w}{j\omega L}[\gamma A\sin\gamma a + \gamma B\cos\gamma a] = 0 \tag{31}$$

$$A\cos\gamma a + B\sin\gamma a + \frac{Z_w}{j\omega L}[-\gamma A\sin\gamma a + \gamma B\cos\gamma a] = 0 \tag{32}$$

and, after summing these two last equations, we get

$$2A\cos\gamma a - \frac{Z_w}{j\omega L}2\gamma A\sin\gamma a = 0 \tag{33}$$

On the other hand, after subtraction of the first from the second, we get

$$2B\sin\gamma a + \frac{Z_w}{j\omega L}2\gamma B\cos\gamma a = 0 . \tag{34}$$

These equations lead to the following two transcendental equations for the eigenvalues γ, which are independent on the magnitude of the coefficients A and β; these are

$$\gamma a\tan\gamma a = \frac{j\omega La}{Z_w}, \tag{35}$$

$$\gamma a\cot\gamma a = -\frac{j\omega La}{Z_w} . \tag{36}$$

It is worth noting that if $Z_w = 0$, then (35) and (36) reduce to

$$\tan\gamma a = \infty\,,\ \gamma_{2n+1} = \frac{\pi}{2a}(2n+1) = \frac{\pi}{d}(2n+1) \tag{37}$$

$$\tan\gamma a = 0\,,\ \gamma_{2n} = \frac{\pi}{2a}(2n) = \frac{\pi}{d}(2n) \tag{38}$$

which means that the eigenvalues are the familiar perfectly conducting parallel plate resonator eigenvalues [87]:

$$\gamma_m = \frac{\pi m}{d} . \tag{39}$$

For any transmission line with per unit length parameters $L = \mu$ and $C = \varepsilon$ we have

$$v_p = (LC)^{-1/2}, \quad Z_0 = \sqrt{L/C} \tag{40}$$

and therefore

$$L = Z_0/v_p \tag{41}$$

and (35) and (36) become

$$\gamma a \tan\gamma a = \frac{j\omega a}{v_p}\frac{Z_0}{Z_w} = \frac{j\beta a}{\xi_w} \tag{42}$$

$$\gamma a \cot\gamma a = -\frac{j\omega a}{v_p}\frac{Z_0}{Z_w} = -\frac{j\beta a}{\xi_w} \tag{43}$$

Equation (42) has infinitely many roots γ_n which are complex, in general. Let us assume that they have been calculated (*i.e.* by some numerical procedure) and let us calculate the ratio of the coefficients of the eigenfunctions:

$$\varepsilon_n = B_n/A_n \tag{44}$$

corresponding to each eigenvalue γ_n. This can be achieved by dividing boundary condition (31) by A_n and solving for ε_n to get

$$\varepsilon_n = \frac{\cos\gamma_n a - \dfrac{Z_w}{j\omega L}\gamma_n \sin\gamma a}{\sin\gamma_n a + \dfrac{Z_w}{j\omega L}\gamma_n \cos\gamma_n a} \tag{45}$$

From (35) we have $j\omega L/Z_w = \gamma_n \tan\gamma_n a$ which, after substitution into (45), gives

$$\varepsilon_n = \frac{B_n}{A_n} = \frac{\cos\gamma_n a - \dfrac{\sin\gamma a}{\tan\gamma_n a}}{\sin\gamma_n a + \dfrac{\cos\gamma_n a}{\tan\gamma_n a}} = 0 \Rightarrow B_n = 0 \tag{46}$$

This simple result is a consequence of a symmetry of the problem, that is, both boundaries have the same impedance. It allows us to choose only the cosine term for the eigenfunction, that is

$$\Psi_n(u) = \cos\gamma_n u. \tag{47}$$

Since in general, the eigenvalues, γ_n, are complex numbers, (47) represents a decaying cosine wave. Recalling that $u = z - d/2$, we finally obtain

$$\Psi_n(z) = \cos\gamma_n\left(z - \frac{d}{2}\right) \tag{48}$$

In the very same way eigenfunctions can be found corresponding to the eigenvalues found using (36).

3.1.3 Eigenmode expansion, Method B: expansion in terms of exponentials

In this case we are looking for the eigenfunctions in the form

$$\Psi(z) = Ae^{\mu z} + Be^{-\mu z}, \tag{49}$$

$$\Psi'(z) = \mu[Ae^{\mu z} - Be^{-\mu z}] \tag{50}$$

subject to the boundary conditions

$$\Psi(0) - \frac{Z_w}{j\omega L}\frac{d}{dz}\Psi(z)\Big|_{z=0} = 0 \tag{51}$$

$$\Psi(2a) + \frac{Z_w}{j\omega L}\frac{d}{dz}\Psi(z)\Big|_{z=2a} = 0. \tag{52}$$

From the first boundary condition, we obtain

$$A + B - \frac{Z_w}{j\omega L}\mu(A - B) = 0 \tag{53}$$

which can be rewritten as

$$\frac{Z_w}{j\omega L} = \frac{1}{\mu}\left[\frac{A+B}{A-B}\right] = \frac{1}{\mu}\left[\frac{1+B/A}{1-B/A}\right], \; A \neq 0 \tag{54}$$

The second boundary condition is used to find

$$Ae^{2\mu a} + Be^{-2\mu a} + \frac{1}{\mu}\left[\frac{A+B}{A-B}\right]\mu[Ae^{2\mu a} - Be^{-2\mu a}] = 0 \tag{55}$$

or, after some rearranging

$$A^2e^{2\mu a} = B^2e^{-2\mu a} \tag{56}$$

which, in turn is equivalent to

$$Ae^{\mu a} = \pm Be^{-\mu a} \tag{57}$$

and we have

$$B/A = \pm e^{2\mu a}. \tag{58}$$

Substituting this and (41) into (54) gives us the two equations

$$\mu a \tanh \mu a = -j\frac{\beta a}{\xi_w} \tag{59}$$

$$\mu a \coth \mu a = -j\frac{\beta a}{\xi_w} \tag{60}$$

These equations coincide with (42) and (43) if $\mu = j\gamma$. Finally, this last substitution gives

$$\gamma a \tan\gamma a = \frac{j\beta a}{\xi_w} \quad \Leftrightarrow \quad \cot\gamma a = -j\frac{\xi_w}{\beta a}(\gamma a) \tag{61}$$

$$\gamma a \cot\gamma a = -\frac{j\beta a}{\xi_w} \quad \Leftrightarrow \quad \tan\gamma a = j\frac{\xi_w}{\beta a}(\gamma a) \tag{62}$$

3.1.4 Solution of the transcendental equations for small losses

Let us assume that the wall losses are small and that the parameter ξ_w in equations (61)-(62) is much smaller then one, that is

$$|\xi_w| \ll 1 . \tag{63}$$

In this case, *i.e.* the case of high Q cavities, an approximate solution of the transcendental equations which give us the eigenvalues can be obtained using a small parameter expansion [88]. In this case, γ_n is represented as a series expansion with respect to small parameter $|\xi_w|$:

$$\gamma_n = \gamma_{0n} + |\xi_w|(\gamma_{nr}^{(1)} + j\gamma_{ni}^{(1)}) + |\xi_w|^2(\gamma_{nr}^{(2)} + j\gamma_{ni}^{(2)}) + \ldots, \; n = 1, 2, \ldots \tag{64}$$

where γ_{0n} are solutions corresponding to the case of $\xi_w = 0$, *i.e.* lossless case. We obtain

$$\gamma_{0n} a \cdot \tan\gamma_{0n} a = \infty \quad \Leftrightarrow \quad \cot\gamma_{0n} a = 0 \tag{65}$$

$$\gamma_{0n} a \cdot \cot\gamma_{0n} a = \infty \quad \Leftrightarrow \quad \tan\gamma_{0n} a = 0 \tag{66}$$

and $\gamma_{nr}^{(k)}$, $\gamma_{ni}^{(k)}$ are real and imaginary components of k^{th} order correction term. Here we will confine ourselves with only the first order correction term, *i.e.* we will assume that

$$\gamma_n = \gamma_{0n} + |\xi_w|(\gamma_{nr}^{(1)} + j\gamma_{ni}^{(1)}) . \tag{67}$$

The exact form of the γ_{0n} is well known as

$$\gamma_{0n} = \frac{\pi(2n+1)}{2a}, \; n = 1, 2, \ldots \tag{68}$$

for equation (65) and as

$$\gamma_{0n} = \frac{\pi 2n}{2a}, \; n = 1, 2, \ldots \tag{69}$$

for equation (66). These two are equivalent to

$$\gamma_{0n} = \frac{\pi n}{2a} = \frac{\pi n}{d}, \; n = 1, 2, \ldots \tag{70}$$

The next step is to use a small argument approximation for $\tan x$ and $\cot x$, that is we will use

$$\tan[(\gamma_{0n} + |\xi_w|(\gamma_{nr}^{(1)} + j\gamma_{ni}^{(1)}))a] \approx \tan\gamma_{0n} a + a|\xi_w|(\gamma_{nr}^{(1)} + j\gamma_{ni}^{(1)}) = a|\xi_w|(\gamma_{nr}^{(1)} + j\gamma_{ni}^{(1)}) . \tag{71}$$

After substituting this into (62) the following approximate equation is obtained

$$\tan\gamma_n a \approx a|\xi_w|(\gamma_{nr}^{(1)} + j\gamma_{ni}^{(1)}) = \frac{j\xi_w}{\beta a}\gamma_n a \approx \frac{j\xi_w}{\beta a} a(\gamma_{0n} + |\xi_w|(\gamma_{nr}^{(1)} + j\gamma_{ni}^{(1)})) \approx \frac{j|\xi_w| e^{j\theta_\xi}}{\beta a}\gamma_{0n} a \tag{72}$$

where $\theta_\xi = \arg(\xi_w)$. This immediately produces

$$\gamma_{nr}^{(1)} + j\gamma_{ni}^{(1)} = \frac{je^{j\theta_\xi}}{\beta a}\gamma_{0n} \tag{73}$$

and thus

$$\gamma_n \approx \gamma_{0n} + |\xi_w|\frac{je^{j\theta_\xi}}{\beta a}\gamma_{0n} = \gamma_{0n}\left(1 + \frac{j\xi_w}{\beta a}\right) \tag{74}$$

and γ_{0n} is given by (68) or (69). A similar equation was obtained in [89].

3.1.5 Eigenfunction expansion

The next step is to find the coefficients A and B in eigenfunction expansion (49). To achieve this, equation (53) is rewritten as

$$A_n + B_n - \frac{\xi_w}{\beta}\gamma_n(A_n - B_n) = 0 \tag{75}$$

which gives

$$A_n = -B_n\frac{1 + \frac{\xi_w}{\beta}\gamma_n}{1 - \frac{\xi_w}{\beta}\gamma_n} \tag{76}$$

i.e. the eigenfunctions are

$$\Psi_n(z) = B_n\left[-\frac{1 + \frac{\xi_w}{\beta}\gamma_n}{1 - \frac{\xi_w}{\beta}\gamma_n}e^{j\gamma_n z} + e^{-j\gamma_n z}\right] = \frac{-2B_n}{1 - \frac{\xi_w}{\beta}\gamma_n}\left[j\sin\gamma_n z + \frac{\xi_w}{\beta}\gamma_n\cos\gamma_n z\right]. \tag{77}$$

Note that there are no singularities in this solution. The remaining coefficient is obtained by expanding the source in terms of the eigenfunctions. Note, that for the case of lossless boundaries, *i.e.* $\xi_w = 0$, we obtain $\Psi_n(0) = \Psi_n(2a) = 0$ as required.

3.1.6 Morse approximation and the number of modes excited

The general eigenmode expansion for the field inside a perfectly conducting one dimensional resonator is written as [23, page 871]

$$V(z) = \frac{2}{d}\sum_{n=1}^{\infty}\frac{\sin\left(\frac{\pi n z_0}{d}\right)\sin\left(\frac{\pi n z}{d}\right)}{\beta_c^2 - \left(\frac{\pi n}{d}\right)^2} \tag{78}$$

where for this lossless case, $\beta_c = \beta = \omega\sqrt{\mu_0\varepsilon_0}$ is the propagation constant and we have chosen the magnitude of the current source I_s in equation (19) such as to remove the coefficient in front of the

summation. The approximation which was suggested by Morse [21] is to use a modified propagation constant which, for the one dimensional resonator, is given by

$$\beta_c = \beta\left(1 - j\frac{1}{2Q}\right). \tag{79}$$

In other words, one may rearrange the denominator in (78) in such a way that the effect of losses will be incorporated as changes in β rather than changes in γ_n, given by (74). To do this, the quality factor Q must be chosen in such a way that

$$\beta_c^2 - \gamma_{0n}^2 = \beta^2 - \gamma_n^2 \tag{80}$$

or, using (74) and (79)

$$\beta^2\left(1 - j\frac{1}{2Q}\right)^2 - \gamma_{0n}^2 = \beta^2 - \gamma_{0n}^2\left(1 + \frac{j\xi_w}{\beta a}\right)^2 \tag{81}$$

which expands to

$$\beta^2\left(1 - j\frac{1}{Q} - \frac{1}{4Q^2}\right) - \gamma_{0n}^2 = \beta^2 - \gamma_{0n}^2\left(1 + \frac{2j\xi_w}{\beta a} - \left(\frac{\xi_w}{\beta a}\right)^2\right). \tag{82}$$

Keeping only terms of order ξ_w and $1/Q$ we obtain

$$\frac{1}{Q} = \frac{2\xi_w}{\beta a}\frac{\gamma_{0n}^2}{\beta^2} = \frac{4\xi_w}{\beta d}\frac{\gamma_{0n}^2}{\beta^2} \tag{83}$$

or

$$Q = \frac{\beta d}{4\xi_w}\frac{\beta^2}{\gamma_{0n}^2} = \frac{\beta d}{4|\xi_w|}\frac{\beta^2}{\gamma_{0n}^2}e^{-j\theta_\xi}. \tag{84}$$

This gives us an approximation to the quality factor for small losses (*i.e.* $|\xi_w| \ll 1$). Let us note that in general (84) produces a complex number.

We see that the coefficient of each eigenfunction in (78) is given by

$$c_n = \frac{2}{d}\frac{\sin\left(\frac{\pi n z_0}{d}\right)}{\beta_c^2 - \left(\frac{\pi n}{d}\right)^2} \tag{85}$$

which is the magnitude of the *n-th* spatial mode. Thus it can be seen that this magnitude is uniformly (*i.e.* independent on z) bounded by

$$|c_n| < \frac{2}{d}\left|\frac{1}{\beta^2\left(1 - j\frac{2\xi_w}{\beta d}\frac{\pi^2 n^2}{d^2\beta^2}\right)^2 - \left(\frac{\pi n}{d}\right)^2}\right| \tag{86}$$

As the mode number, n, increases, the c_n become smaller and smaller. This means that only a few modes,

for a given geometry and frequency, are excited with appreciable energy. Any mode which is close to a possible resonance will dominate. A second conclusion which can be made is that, taking into account the uniformness of the bound (86) (in the sense that it does not depend on the source position), no *significant randomization* of the modes can be achieved by moving the source location $z = z_0$. The latter could be accomplished by using either frequency variation or (equivalently) wall displacement (*i.e.* a vibrating wall). In both cases this would be equivalent to stirring the electrical length of the resonator.

3.2 Numerical simulations of the one dimensional resonator

In this section we give the results of a number of simulations which were conducted in order to better understand the effect of the wall losses on the field inside the one dimensional resonator. They are briefly described in this section. The corresponding figures are Figs. 2 to 6. In general, three methods were used: a) the one referred to as "exact" in the figures is the solution given by equations (13)-(16); b) the one referred to as "Bal. cls" refers to the closed form solution given by Balanis in [23, p. 870] which is valid only for the lossless case; and c) the method referred to as "Bal. har" refers to the harmonic lossless case expansion also given in [23, p. 871]. These are compared against the eigenfunction expansion using the Morse approximation for the lossy case given by (78) (labeled "Morse har" in the figures), and against the expansion

$$V(z) = \sum_{n=1}^{\infty} \frac{\sin\left(\frac{\pi n z_0}{d}\right)\sin\left(\frac{\pi n z}{d}\right)}{\beta^2 - \gamma_n^2} \tag{87}$$

with γ_n given by (74). This last approximation is labeled "UWO" in the figures.

3.2.1 Consistency of all solutions for the case of lossless walls

The purpose of simulating the lossless case is to show that all three methods give the same results in the case of no losses in the walls, *i.e.* when $\xi_w = 0$. A few different electrical lengths of the resonator was considered: small ($L/\lambda < 1$), intermediate ($L/\lambda \sim 1$) and large ($L/\lambda > 1$). It can be seen from Fig. 2 that all the methods are in very good agreement with each other.

3.2.2 Effects of losses on the field distribution inside 1-D resonator

In this section we investigate, using plots for various configurations, how lossy walls affect the accuracy of the different approximations we have considered so far. The results for the configurations listed in Table are plotted in Figs. 2 - 9

Table 1: List of one dimensional

Figure No.	$\xi_w = Z_w/Z_0$	L m, L/λ	location of source, z_0
3	0.05, 0.1, 0.2, 0.1+j0.1	1, 0.3	0.3
4	0.05, 0.1, 0.2, 0.1+j0.1	1, 0.8	0.3
5	0.05, 0.1, 0.2, 0.1+j0.1	1, 1.2	0.3
6	0.05, 0.1, 0.2, 0.1+j0.1	1, 6.2	0.3

It can be seen, that the Morse modification works almost as well as the complicated modification developed here and thus it can be used as the main model for two and three dimensional resonator investigations.

3.3 Summary of one dimensional resonators

We have found that the Morse modification of Green function for the case of a resonator with lossy walls produces a reasonable approximation of the exact solution. The method of approximation should extend to the case of two and three dimensional resonators. It was found that the number of modes excited which carry significant energy is very low; this is a concern since many of the statistical techniques which have been reported in the literature require that a large number of modes be present for the techniques to be valid.

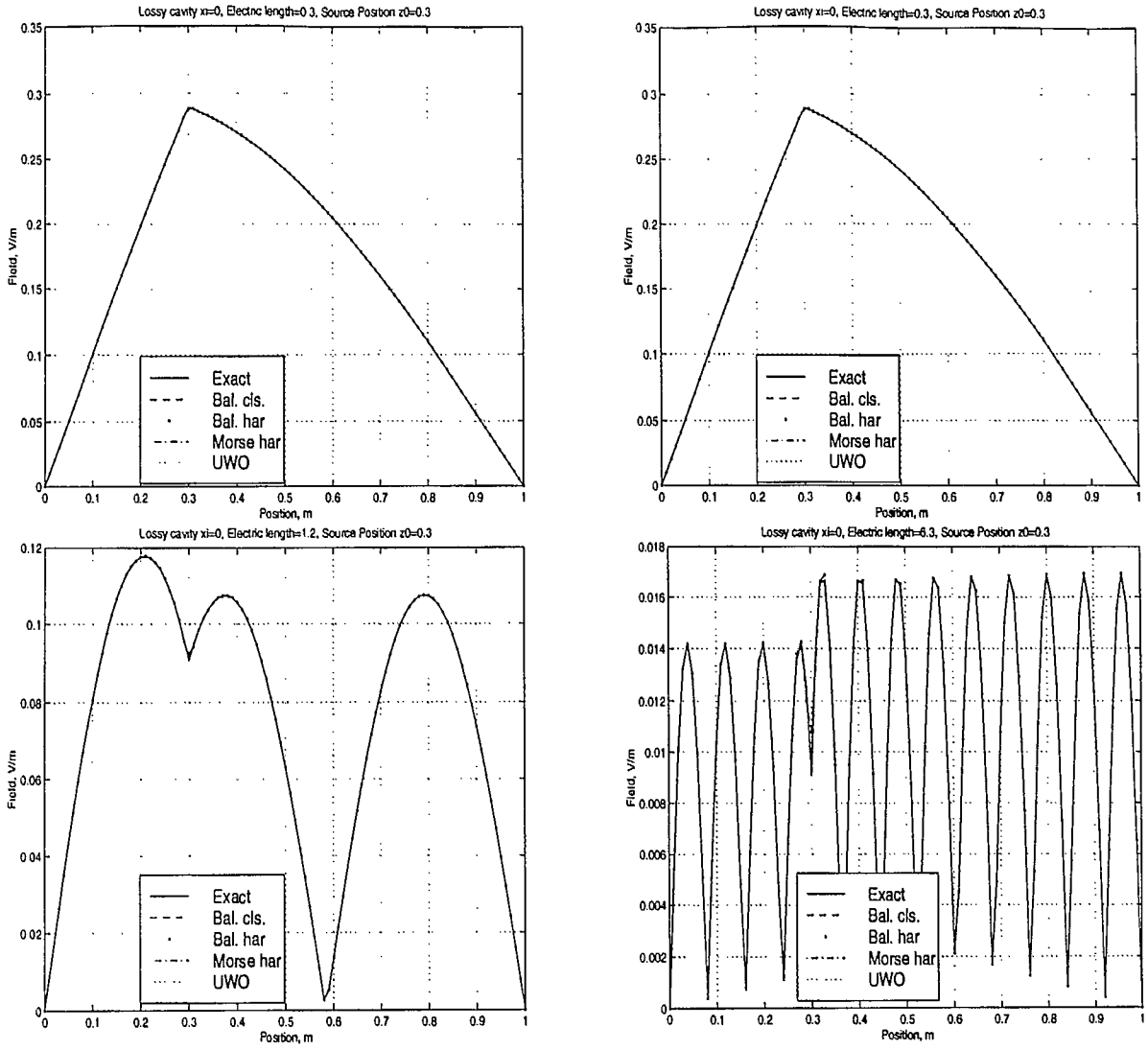

Figure 2. The case of a lossless one dimensional resonator
($\xi_w = 0$, $L/\lambda = 0.3, 0.8, 1.2, 6.3$, $L = 1$ m, source at $z_0 = 0.3$)

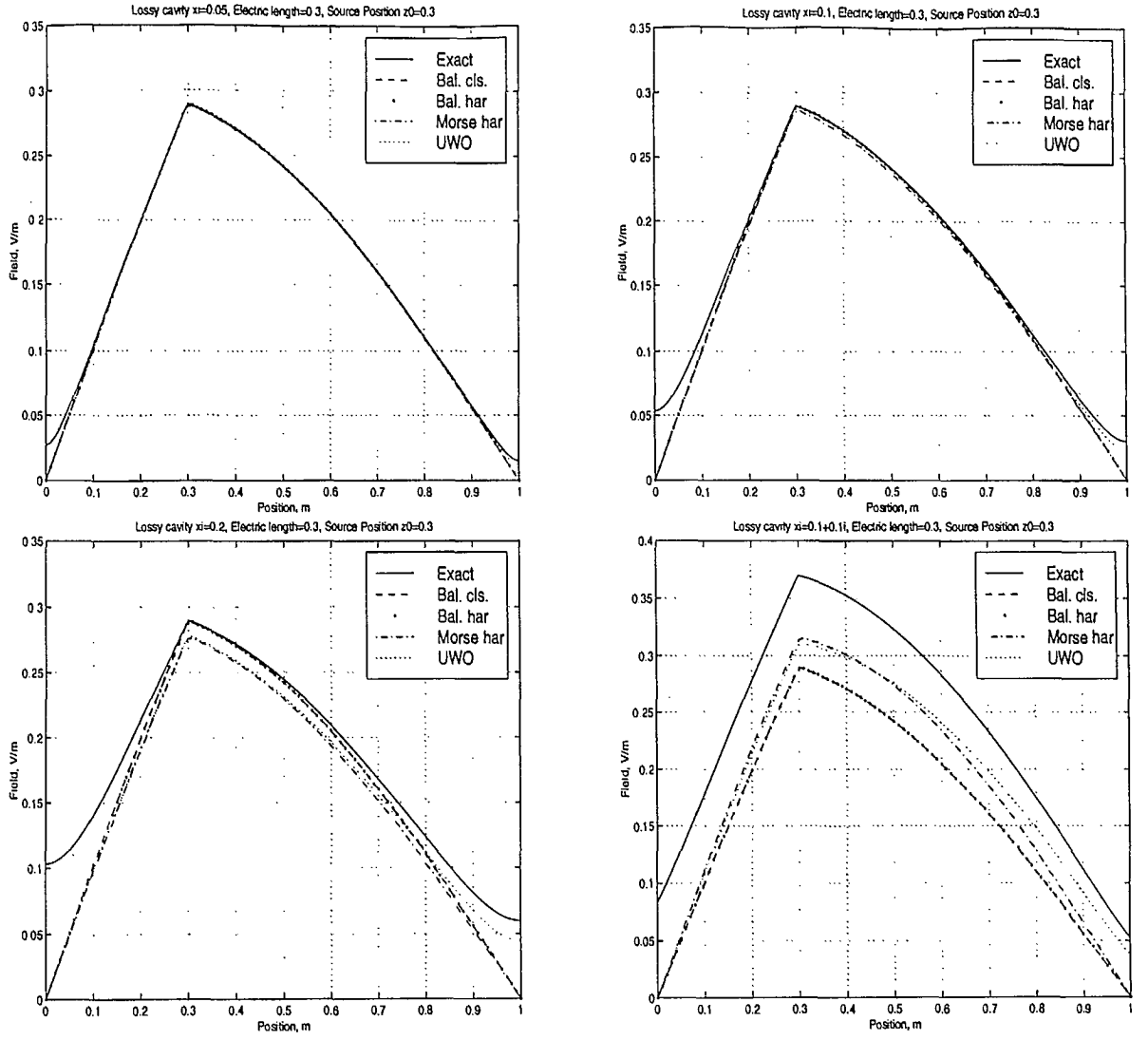

Figure 3. The case of a lossy one dimensional resonator
($\xi_w = 0.05, 0.1, 0.2, 0.1 + j0.1$, $L/\lambda = 0.3$, $L = 1$ m, source at $z_0 = 0.3$)

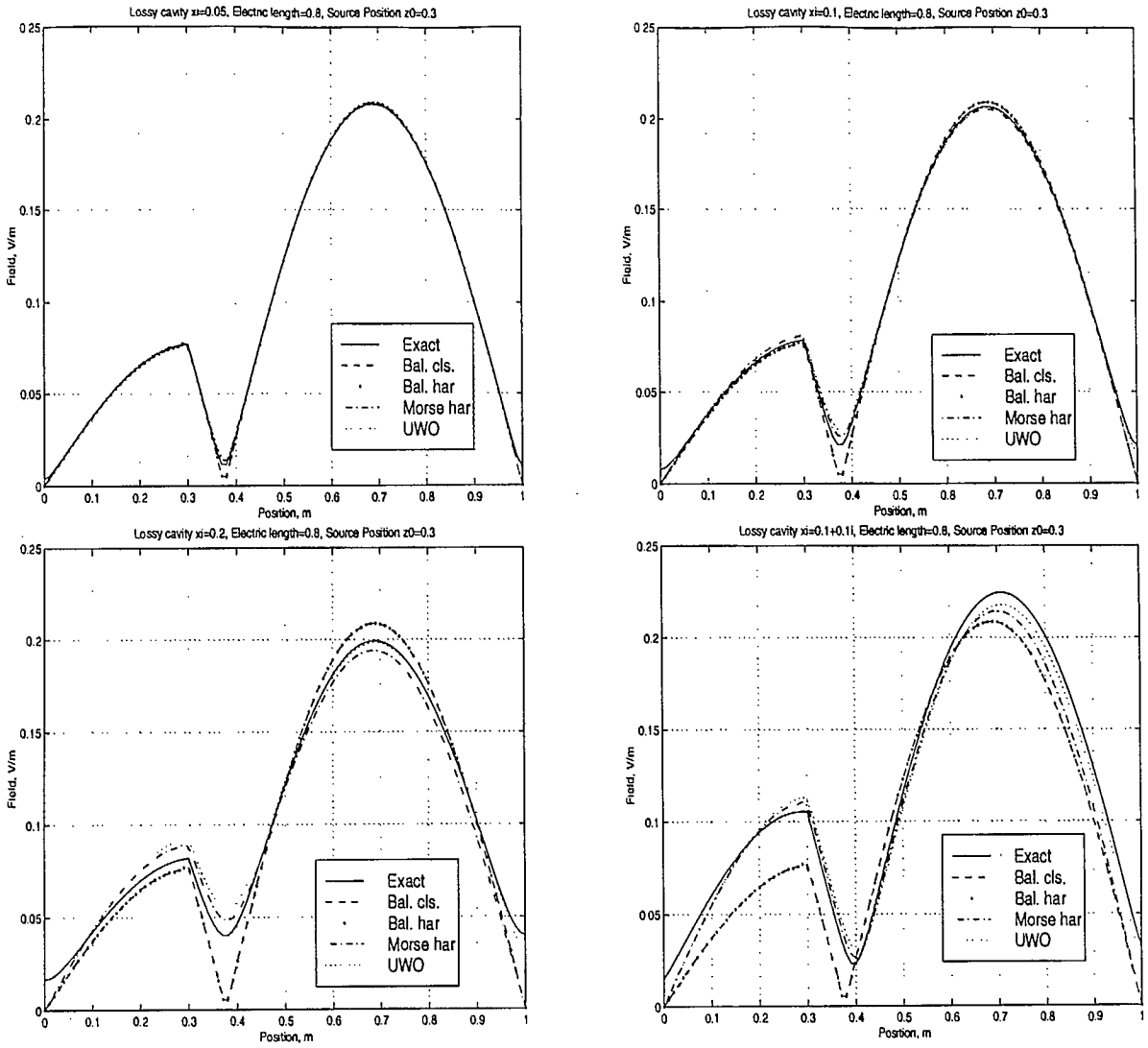

Figure 4. The case of a lossy one dimensional resonator
($\xi_w = 0.05, 0.1, 0.2, 0.1 + j0.1$, $L/\lambda = 0.8$, $L = 1$ m, source at $z_0 = 0.3$)

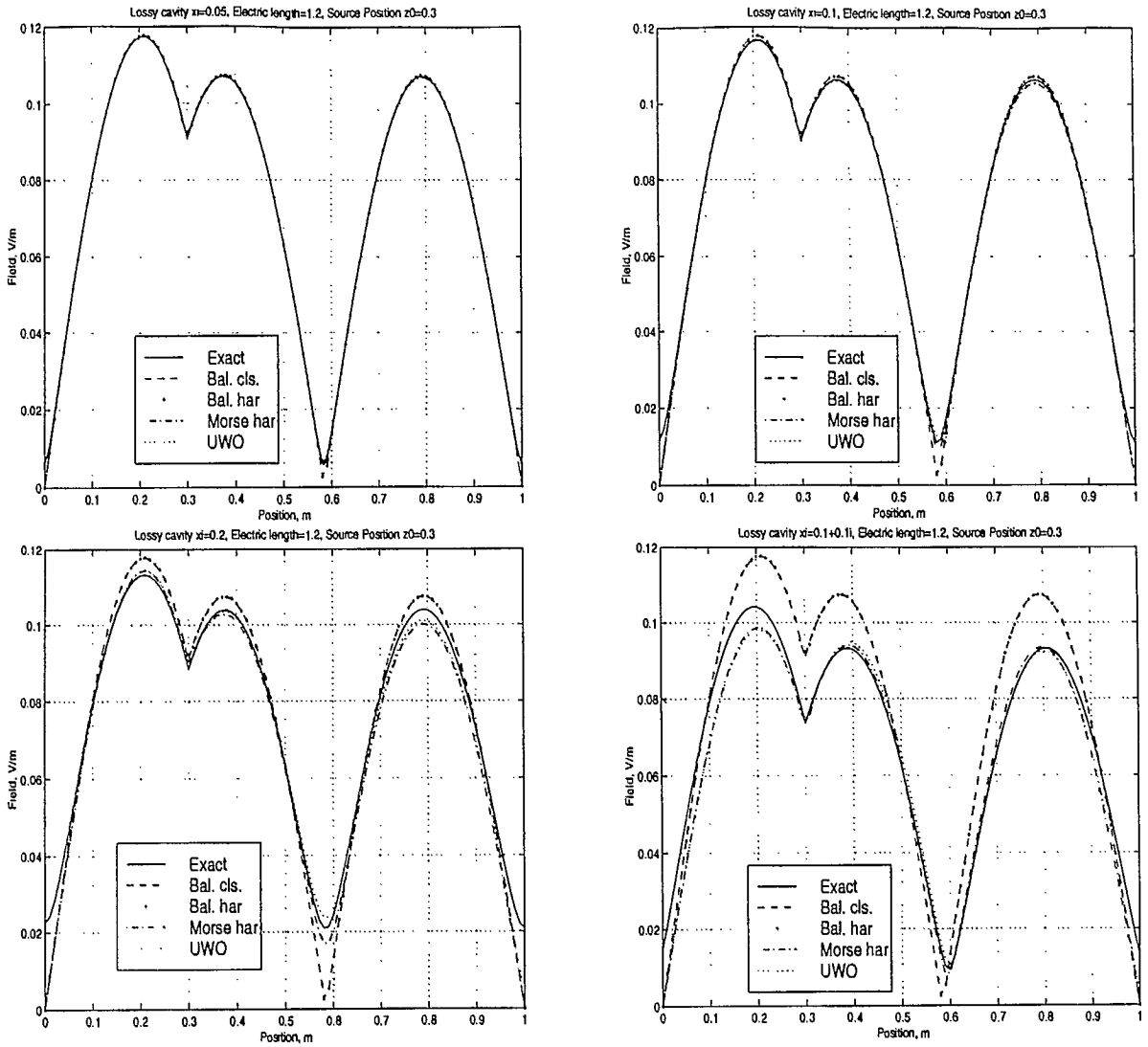

Figure 5. The case of a lossy one dimensional resonator
($\xi_w = 0.05, 0.1, 0.2, 0.1 + j0.1$, $L/\lambda = 1.2$, $L = 1$ m, source at $z_0 = 0.3$)

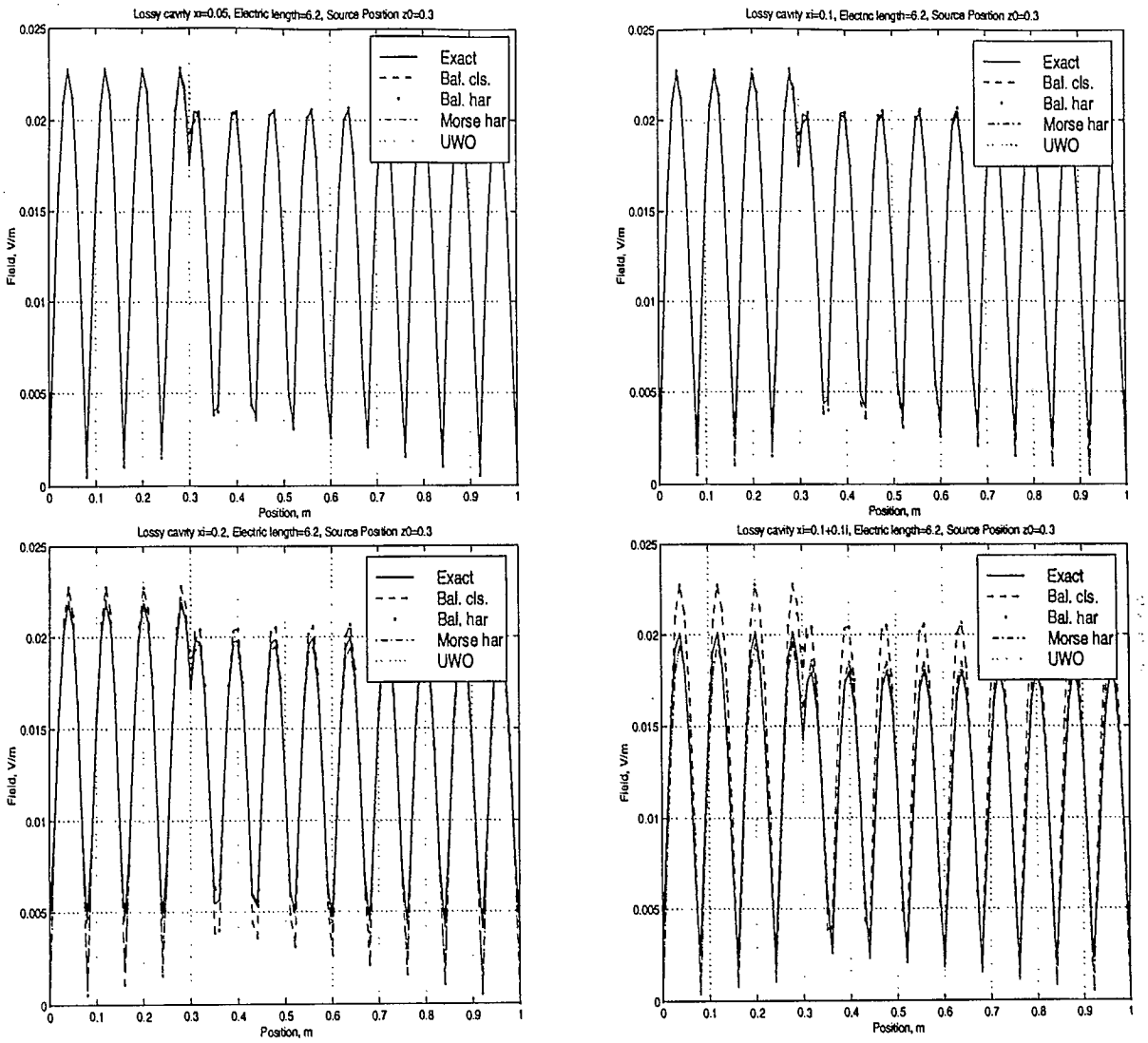

Figure 6. The case of a lossy one dimensional resonator
($\xi_w = 0.05, 0.1, 0.2, 0.1 + j0.1$, $L/\lambda = 6.2$, $L = 1$ m, source at $z_0 = 0.3$)

3.4 Fields inside a two dimensional enclosure

3.4.1 The two dimensional model

Consider a two dimensional cavity of size $a \times b$ m^2 with an infinite line source of harmonic current having a radial frequency of ω and which is located at (x_0, y_0) inside the enclosure. The corresponding geometry is shown in Fig. 7. The intensity of the source I_0 and the cavity's quality factor Q are assumed to be known.

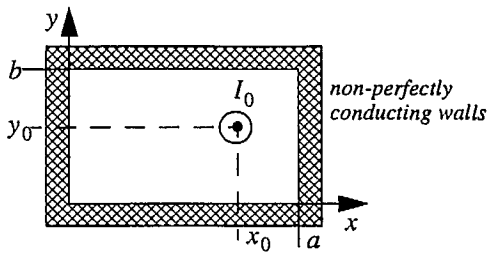

Figure 7. Geometry of the problem

3.4.2 Solution in terms of standing waves

The infinitely long current source produces a transverse magnetic field to the z-direction, TM_z. The non-zero components are E_z, H_x, and H_y. The magnetic field components can be derived from the z-directed electric component E_z as

$$H_x = \frac{1}{j\omega\mu_0}\frac{\partial E_z}{\partial y}, \; H_y = -\frac{1}{j\omega\mu_0}\frac{\partial E_z}{\partial x} \tag{88}$$

Using the standard separation of variables technique [22], the following double summation can be obtained for the electric field E_z:

$$E_z(x, y) = \frac{4j\omega\mu_0 I_0}{ab}\sum_{m=1}^{\infty}\sum_{n=1}^{\infty}\frac{\sin(m\pi x_0/a)\sin(m\pi x/a)\sin(n\pi y_0/b)\sin(n\pi y/b)}{k^2-(m\pi/a)^2-(n\pi/b)^2} \tag{89}$$

Here ε_0 and μ_0 are the permittivity and permeability of the assumed vacuum inside the enclosure, the wave vector, k, is defined as $k = \omega/v_p = \omega\sqrt{\varepsilon_0\mu_0}$ and $v_p = 1/\sqrt{\varepsilon_0\mu_0}$ is the velocity of propagation in the vacuum. It is possible to replace the second summation (based on the index n) in (89) to obtain the following alternative expression for E_z [23, pp. 870-871]

$$E_z = \frac{-2j\omega\mu_0 I_0}{a}\sum_{m=1}^{\infty}\frac{\sin(m\pi x_0/a)\sin(m\pi x/a)}{k_m\sin(k_m b)} \times \begin{cases} \sin[k_m(b-y_0)]\sin(k_m y) & y < y_0 \\ \sin(k_m y_0)\sin[k_m(b-y)] & y > y_0 \end{cases} \tag{90}$$

where k_m is defined as

$$k_m = \sqrt{k^2 - \left(\frac{m\pi}{a}\right)^2} \tag{91}$$

This second form of the solution converges much faster than (89) and thus should be used in any computations. However, in order to validate the program, we will compare the results, obtained both from (89) and (90), against each other.

It can be easily seen by inspection, that both (89) and (90) have singularities at the resonance frequencies defined by

$$\omega_{mn} = c\sqrt{\left(\frac{\pi m}{a}\right)^2 + \left(\frac{\pi n}{b}\right)^2} \tag{92}$$

This is an obvious consequence of the assumed zero losses in the cavity. If there exist some losses in the walls and/or interior of the cavity, they can be generally described through the cavity quality factor Q. As in the one dimensional case, the Morse modification [21] can also be applied for this two dimensional resonator. In this case, the wave vector k in (89) and k_m in (90) are each replaced by a modified complex wave vector given by

$$k_c = k\left(1 - \frac{j}{2Q}\right). \tag{93}$$

In this case (89) and (90) remain finite for any real frequency ω. Details about the calculation or approximation of Q itself can be found in [45, 69] and will be summarized in the last part of this chapter.

3.4.3 The uniform-field approximation

It is convenient to normalize the electric field E_z inside the cavity. One of the methods, suggested by Hill [44], uses the following idea. It is assumed that the line source radiates the same power in the lossy cavity as it does in a free-space (large cavity assumption). The free space electric field of a line source is given by

$$E_z = -\frac{\omega\mu_0 I_0}{4} H_0^{(2)}(k\rho) \tag{94}$$

where $\rho = \sqrt{x^2 + y^2}$ is the distance from an observation point to the source, and $H_0^{(2)}$ is the zero-order Hankel function of the second kind [28]. We can now use the following asymptotic expression for $H_0^{(2)}$ (see 9.2.4 on page 364 in [28]):

$$H_0^{(2)}(k\rho) = \sqrt{\frac{2}{\pi k\rho}} e^{-j\left(k\rho - \frac{\pi}{4}\right)}. \tag{95}$$

The total radiated power, P_r, is now given by

$$P_r = 2\pi\rho S_r = 2\pi\rho\frac{|E_z|^2}{\eta_0} = |I_0|^2\eta_0 k/4 \tag{96}$$

Here S_r is the radiated power density per unit arc length and $\eta_0 = \sqrt{\mu_0/\varepsilon_0}$ is the intrinsic impedance of the assumed vacuum surrounding the line source. RMS values are used for I_0 and E_z.

It is now assumed that the total radiated power P_r is uniformly spread throughout the cavity. From the definition of the quality factor Q it follows that

$$Q = \frac{\omega U}{P_r} = \frac{\omega\varepsilon_0|E_{z0}|^2 ab}{P_r} \tag{97}$$

where $U = \varepsilon_0|E_{z0}|^2 ab$ is the stored energy in the cavity (per unit length in the z direction, a and b are as in Fig. 7). Thus, solving (97) with respect to the field E_z and using (96) for radiated power, one can obtain that a "uniform" electric field E_{z0} should obey the following equation

$$|E_{z0}| = |I_0|\eta_0\sqrt{\frac{Q}{4ab}}. \tag{98}$$

Normalization of E_z by the factor $|E_{z0}|$ not only brings down the values of the field to within a small range for any frequency and any large values of Q, but may also describe the deviation of the realistic field from the "uniform" one, *i.e.* may also describe how well the cavity is stirred ($|E_z/E_{z0}| \approx 1$ for a well stirred cavity; however, normalization is meaningful only for relatively large Q values and large cavities).

3.5 Numerical simulations of the two dimensional enclosure

3.5.1 Equivalence between two methods

In order to validate both (89) and (90) some numerical examples were investigated. The same parameters as in [44] were chosen: $a = 4.57$ m, $b = 3.05$ m, and $x_0 = y_0 = 0.5$ m. The electric field, E_z, was calculated along the x-axis for $y = 1.5$ m and normalized by (98). The quality factor, Q, was chosen to be 10^5 for frequencies below 4 GHZ, and 1.5×10^5 for higher frequencies. The results for various frequencies are shown in Fig. 8, the details of which are found in Table 2. The values of the minimum number of modes with appreciable energy for each case are also shown in the table.

Table 2: Description of the parameters for plots shown in Fig. 8

f, GHz	a/λ	b/λ	$N_{min} = (2f)\max(a, b)/c$ [125]
0.05	0.76	0.5	1
0.2	3.04	2.03	6
0.8	12.2	8.1	24
2	30.5	20.3	60
4	61	41	121
6	91	61	182

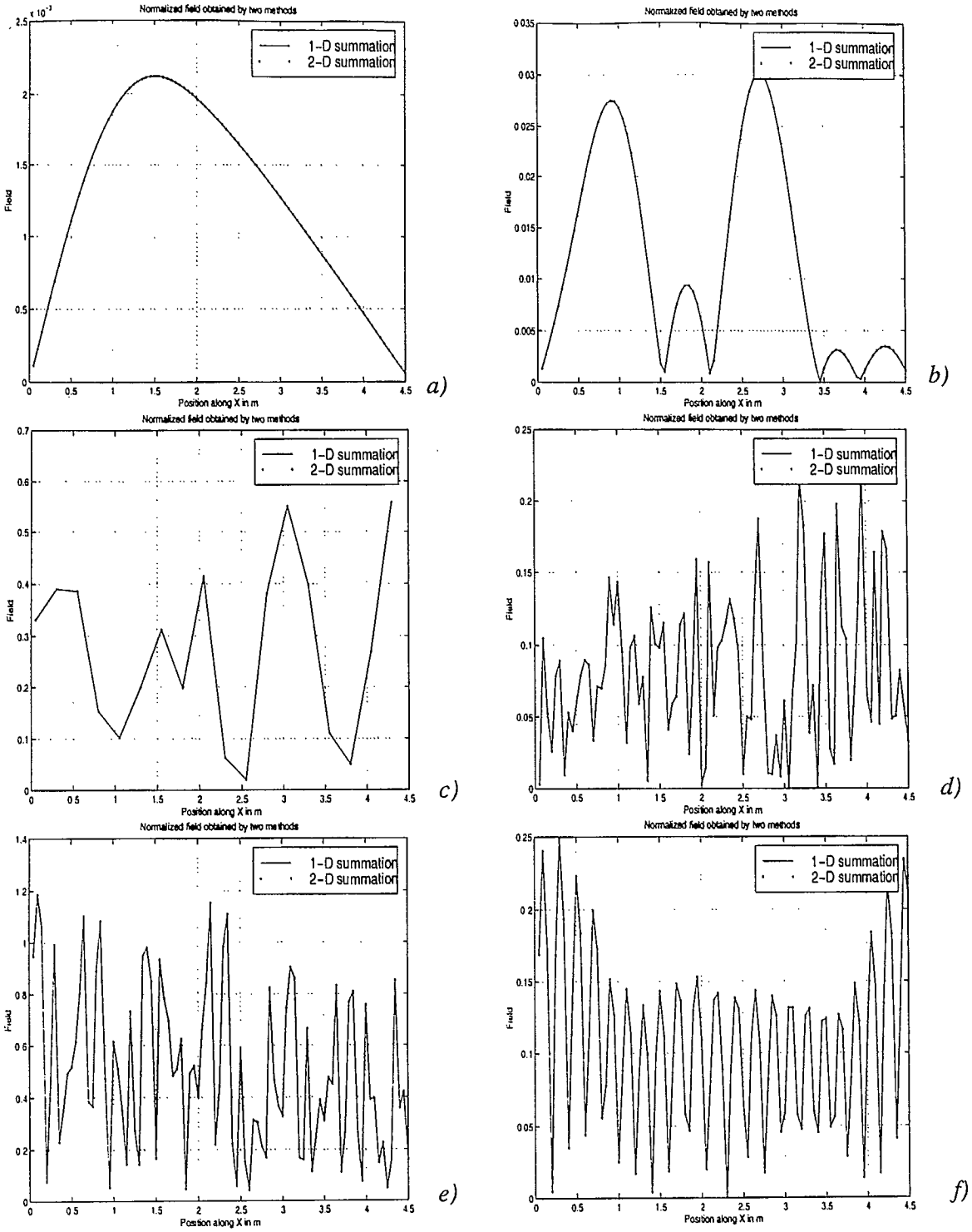

Figure 8. Comparison of the results of 1-D and 2-D summations, equations (89) and (90), normalized by using equation (98): a) $f_0 = 50MHz$, b) $f_0 = 200MHz$, c) $f_0 = 800MHz$, d) $f_0 = 2GHz$, e) $f_0 = 4GHz$, f) $f_0 = 6GHz$

3.6 Frequency Stirring

It was also shown in [44], that a homogenisation of the electric field inside a cavity can be achieved by frequency stirring of the current source. In this section we try to reproduce most of the results obtained in [44] in order to gain a better understanding of the wideband distribution of fields inside cavities.

Let the source be uniformly stirred in the frequency band BW around the central frequency f_0. As can be seen from the previously derived formulas for the field solutions (*i.e.* equations (89) and (90) and the associated supporting equations) the field at any point inside a cavity (excluding possibly the areas near the boundaries) have a strong dependence on frequency. If a relatively wideband probe (with bandwidth greater then BW) is set at a point inside the cavity, a measure of the squared current (or voltage) induced in this probe will be proportional to the squared value of the field averaged over the frequency band, that is

$$I_p^2(x) \sim \langle |E_z(f,x)|^2 \rangle = \frac{1}{BW} \int_{f_0-BW/2}^{f_0+BW/2} |E_z(f,x)|^2 df \tag{99}$$

or, normalizing the field by the magnitude of the "uniform" field previously defined

$$\tilde{I}_p^2(x) \sim \langle |\tilde{E}_z(f,x)|^2 \rangle = \frac{4ab}{Q|I_0|^2\eta_0^2 BW} \int_{f_0-BW/2}^{f_0+BW/2} |E_z(f,x)|^2 df \tag{100}$$

The results of numerical simulations of (100) for different values of parameters are shown in Fig. 9.

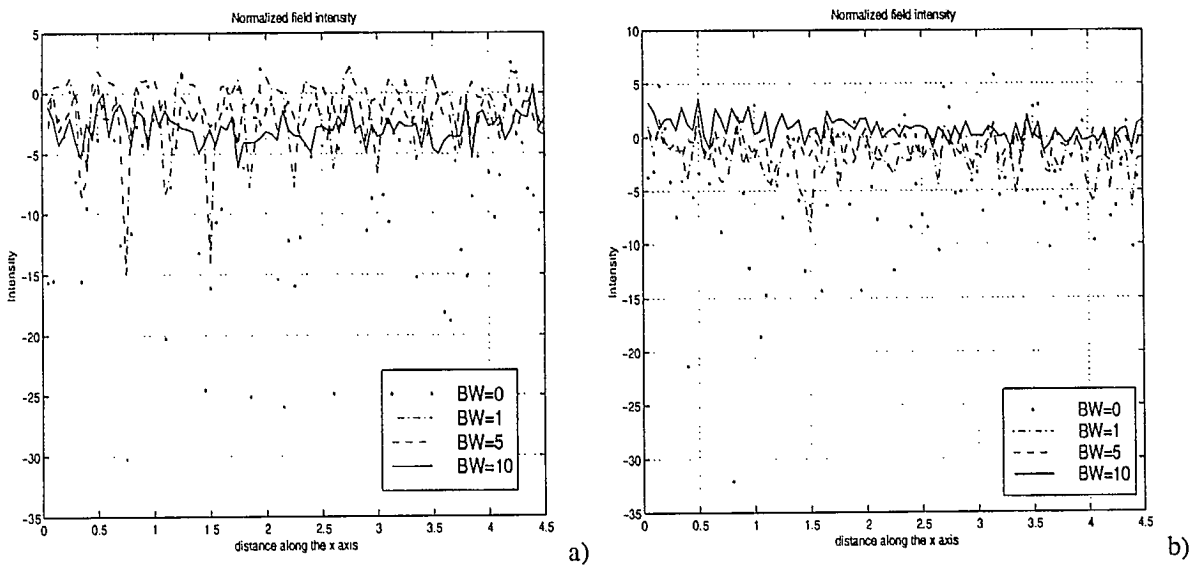

Figure 9. Frequency stirring of the cavity (Intensity is shown in dB): a) $f = 2GHz$, b) $f = 4GHz$.

3.7 Power balance

We now consider a very general technique for handling generic cavities in an approximate way. This technique, generally known by the name of power balance, allows one to make reasonable estimates about the average field inside an arbitrary enclosure. The theory was espoused by Hill and others in [45, 48, 69]. Let us consider a plane wave illuminating a cavity with an aperture as shown in Fig. 10. The cavity may contain a load inside and thus there exists the possibility for some power to be absorbed by the load. Under steady-state conditions, a power balance is achieved which means that the power P_t transmitted into the cavity is balanced by the power P_r reradiated out of the cavity plus the power P_l absorbed by the load and the power dissipated by the cavity walls [43, 45], that is

$$P_t = P_r + P_l. \tag{101}$$

The transmitted power can be calculated through the power density S_i of the incident wave and the equivalent cross-section of the aperture σ_t as

$$P_t = \sigma_t S_t. \tag{102}$$

The cross-section σ_t depends on aperture type, size, incidence angle and polarization of the excitation. Some generic formulae allowing one to estimate this parameter are considered in the next section.

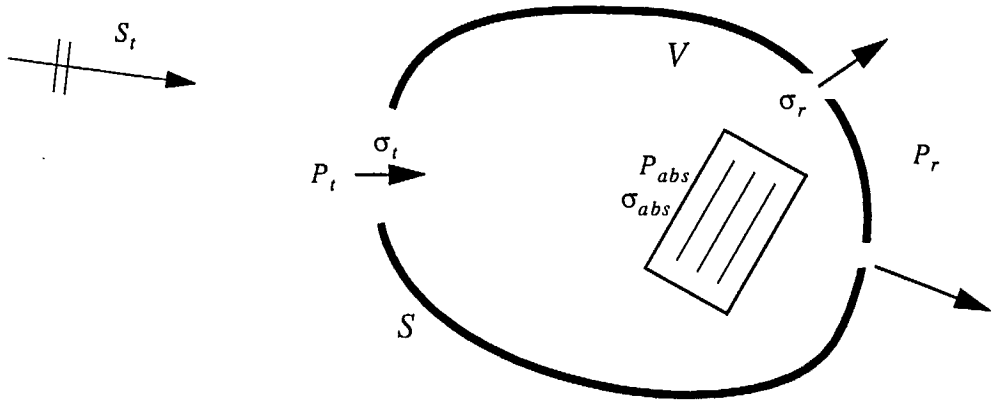

Figure 10. Geometry of the problem

Another parameter which will be useful in our investigations is the cavity quality factor, Q, which relates the energy U_s stored inside the cavity and the energy absorbed inside the cavity (including reradiated energy), that is

$$Q = \frac{\omega U_s}{P_l + P_r} = \frac{\omega U_s}{P_t} = \frac{\omega U_s}{\sigma_t S_t} \tag{103}$$

or, assuming that Q is known

$$U_s = \frac{Q\sigma_t S_t}{\omega}. \tag{104}$$

The last equation is important in determining the energy parameter of the statistical distribution of the field inside the cavity. In fact, if $p_{|E|}(|E|, m_{2E})$ describes the statistics of the magnitude of the electric field density inside the cavity, then

$$U_s = \frac{Q\sigma_t S_t}{\omega} = \varepsilon_r \varepsilon_0 V \int_0^\infty |E|^2 p_{|E|}(|E|, m_{2E}) d|E| \tag{105}$$

where V is the volume of the cavity. Usually, a certain family of distributions, which depend on one or two parameters, are chosen to describe the statistical properties of the fields. Equation (105) allows us to determine one of these unknown parameters. For the case of the Rayleigh distribution, which contains only one parameter, an estimate of the left side of equation (105) would be enough to completely determine $p_{|E|}(|E|, m_{2E})$. Extra information would need to be measured or estimated in some way if a two-parameter distribution is to be found. It is logical to use (105) to obtain an expression for the scale parameter of the distribution being considered (for example σ^2 for Rayleigh, β for Gamma, and b for K) as a function of the shape parameter (ν for K distribution, α for Gamma, *etc.*). More details are given in the next chapter.

3.8 Generic description of the Quality Factor of cavities

As is clear from the previous section, it is very important to obtain a good estimate for the quality factor Q of a cavity. Using the definition of Q as

$$\frac{1}{Q} = \frac{P_r + P_l}{\omega U_s} = \frac{P_{wall} + P_{abs} + P_r}{\omega U_s} = \frac{P_{wall}}{\omega U_s} + \frac{P_{abs}}{\omega U_s} + \frac{P_r}{\omega U_s} = \frac{1}{Q_w} + \frac{1}{Q_{abs}} + \frac{1}{Q_r} \tag{106}$$

where P_{wall} and P_{abs} are the power losses in the walls and the power absorbed by the internal loads, respectively (*e.g.* circuit boards, cables, *etc.*), and P_r is the radiation losses. Q_w, Q_{abs} and Q_r are corresponding quality factors. In the following subsections a short review of generic equations for these quantities is given.

3.8.1 Wall Losses

The wall losses can be approximated using the skin depth approximation by averaging over all incident angles, polarizations, and individual cavity modes. The result for Q_w, *i.e.* the quality factor due to the walls of the enclosure, is then given by [45]

$$Q_w = \frac{3V}{2\mu_r S\delta} \tag{107}$$

where

$$\delta = \sqrt{\frac{2}{\omega \mu_w \sigma_w}}, \ \mu_r = \frac{\mu_w}{\mu_0} \tag{108}$$

and where S is the cavity surface area, δ is the skin depth, μ_w is the wall permeability, and σ_w is the wall conductivity. This result was generalized in [48], to show that

$$Q_w = \frac{3|k_w|^2 V}{4S\mu_r Re(k_w)}, \ k_w = \omega \sqrt{\mu_w \left(\varepsilon_w - j\frac{\sigma_w}{\omega} \right)}. \tag{109}$$

Similar questions were considered in [69] for a rectangular cavity of size $a_c \times b_c \times c_c$, where the following expression was obtained for the chamber's quality factor

$$Q = \left(\frac{3V}{\mu_r S \delta_w} \right) \frac{1}{1 + (3\pi c/\omega)(1/a_c + 1/b_c + 1/c_c)}, \ V = a_c b_c c_c, \ S = 2(a_c b_c + b_c c_c + a_c c_c) \tag{110}$$

A more accurate approximation, involving a so called local analysis, was reported in [70] where it is shown that (110) should be modified to

$$Q = \frac{24\omega V^2}{\mu_r \delta_w (16\omega VS + 9\pi c S^2)}. \tag{111}$$

3.8.2 Absorption

In general the absorption cross section, σ_a, of a lossy object depends on the incident angle and polarization of the impinging plane wave. Based on the assumption that the field in the cavity is statistical, *i.e.* all directions and polarization of an incident field are present, the concept of an averaged $\langle \sigma_a \rangle$ cross-section can be introduced. Here the expectation is taken over all possible incident angles and polarizations. If M absorbers are present in the enclosure, the total absorbing cross-section is

$$\langle \sigma_a \rangle = \sum_{i=1}^{M} \langle \sigma_{ai} \rangle \tag{112}$$

where $\langle \sigma_{ai} \rangle$ is the averaged cross-section of each individual absorber. The total power density P_i coupled into each absorber is then

$$P_i = S_c \langle \sigma_{ai} \rangle \tag{113}$$

where S_c is the cavity power density. In [45] the corresponding quality factor is then given as

$$Q_{abs} = \frac{2\pi V}{\lambda \langle \sigma_{ai} \rangle}. \tag{114}$$

3.8.3 Aperture leakage

A relation, similar to (113), has been developed for power leakage through apertures:

$$P_{ap} = \frac{S_c \langle \sigma_l \rangle}{2} \tag{115}$$

Here $\langle \sigma_l \rangle$ is the transmission cross section of the aperture averaged over all possible angles and polarizations. A factor of $1/2$ is due to the fact that the energy propagates only in one direction (outside the enclosure). If a number of apertures are present, the total transmission cross-section is given as a sum of individual cross-sections $\langle \sigma_{lk} \rangle$

$$\langle \sigma_l \rangle = \sum_{k=1}^{\wedge} \langle \sigma_{lk} \rangle \tag{116}$$

As a result, a quality factor Q_{ap} corresponding to the energy leakage through the apertures is given in [45] as

$$Q_{ap} = \frac{4\pi V}{\lambda \langle \sigma_l \rangle}. \tag{117}$$

3.8.4 Receiving antenna

In order to calculate the power dissipated in the load of a receiving antenna, the concept of the averaged (over all directions and polarizations) effective area $\langle A_e \rangle$ of the antenna can be introduced. It is defined in the very same way as the averaged cross-section or transmitting cross-section. Having this, the energy absorbed by the antenna is given by [45]

$$P_{an} = S_c \langle A_e \rangle \tag{118}$$

It is accepted in [45], based on the results of [69], that

$$\langle A_e \rangle = \frac{m\lambda^2}{8\pi} \tag{119}$$

where m is an impedance mismatch factor [69]. The corresponding quality factor is

$$Q_{an} = \frac{16\pi^2 V}{m\lambda^3} \tag{120}$$

In general, a transmission line can be treated as an antenna as well. The simplest model would include a separate treatment of each trace as a monopole over a ground plane. However, we would like to investigate this in more detail using numerical techniques. Some details are given in Chapter VI.

3.9 Aperture excitation

A plane wave incident on an aperture in a perfectly conducting sheet is considered in [45] as a model for the excitation of a cavity through an aperture. For electrically large apertures, the geometrical optics approximation yields the following expression for aperture cross-section σ_t

$$\sigma_t = A\cos\theta^i \tag{121}$$

where A is the aperture area and θ^i is the incidence elevation angle. Thus σ_t is independent of frequency, polarization, and azimuth of the incidence field. For this case, the average cross-section is shown to be

$$\langle\sigma_t\rangle = \langle A\cos\theta^i\rangle = A\langle\cos\theta^i\rangle = \frac{A}{2}. \tag{122}$$

For electrically small apertures, it is stated in [45], based on polarisability theory (see [79, 80] for more details), that the transmitted fields are due to the induced electric and magnetic dipole moments. This yields a transmission cross-section that is proportional to frequency to the fourth power

$$\sigma_t = G\left(\frac{\omega}{c}\right)^4 \tag{123}$$

where the constant G depends on incidence angle and polarization, and c is the speed of light in vacuum. For the case of a circular aperture of radius a equations (122) and (123) can be reduced to

$$\langle\sigma_t\rangle = \frac{\pi a^2}{2} \tag{124}$$

$$\langle\sigma_t\rangle = \frac{16\omega^4 a^6}{9\pi c^4}. \tag{125}$$

A much more complicated situation is observed in the resonance region, *i.e.* when the wavelength is comparable to the aperture size. The only reasonable way to proceed in this case is to apply numerical techniques.

In a couple of recent publications [39, 15] the following approximate equations for the cross-sectional area were given. For a circular aperture of radius a, shown in Fig. 11

$$\sigma_t(\omega) = p(\theta,\phi)\pi a^2 \begin{cases} F_l = [\omega/\omega_r]^4 & \text{below resonance} \\ \dfrac{2F_lF_h}{F_l+F_r} & \text{near resonance} \\ F_h = 1 + [\omega_r/(\omega-\omega_0)]^2 & \text{above resonance} \end{cases} \tag{126}$$

where ω_r is the resonance frequency, given as

$$\omega_r = (0.25 \rightarrow 0.293)\frac{2\pi c}{a} \tag{127}$$

and ω_0 is an adjustable parameter to provide for the proper resonance peak of σ_t, and $k = 2\pi\omega/c$. The

function $p(\theta, \phi)$ is given as

$$p(\theta, \phi) = \left| \frac{J_1(ka\sin\theta)}{ka\sin\theta} \right|^2 (\cos^2\theta \cos^2\phi + \sin^2\phi) \tag{128}$$

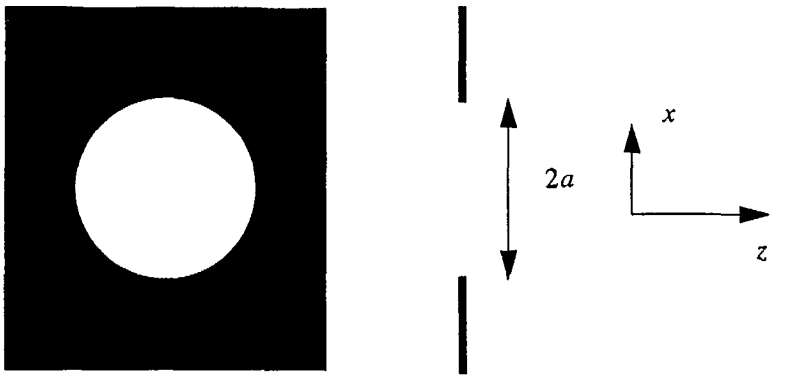

Figure 11. Circular aperture

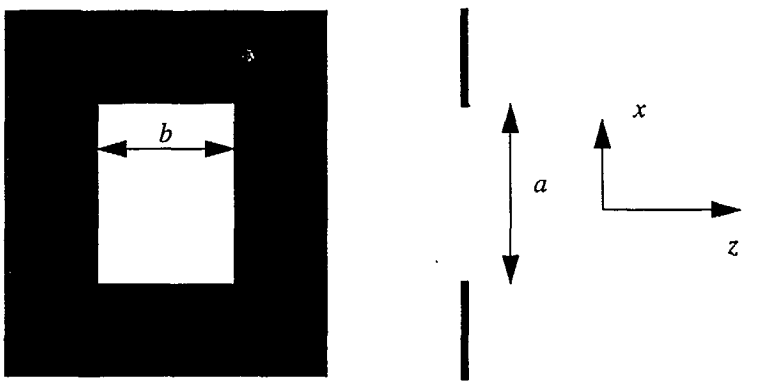

Figure 12. Rectangular aperture

A similar equation can be found for a rectangular geometry as shown in Fig. 12. In this case

$$\sigma_t(\omega) = p(\theta, \phi)ab \begin{cases} F_l = [\omega/\omega_r]^4 & \text{below resonance} \\ \dfrac{2F_lF_h}{F_l + F_r} & \text{near resonance} \\ F_h = 1 + [\omega_r/(\omega - \omega_0)]^2 & \text{above resonance} \end{cases} \tag{129}$$

$$\omega_r = \frac{c}{2\sqrt{a^2 + b^2}} \tag{130}$$

$$p(\theta, \phi) = \left| \frac{J_1(ka\sin\theta\cos\phi)}{ka\sin\theta\cos\phi} \right|^2 \left| \frac{J_1(kb\sin\theta\cos\phi)}{kb\sin\theta\cos\phi} \right|^2 (\cos^2\theta \cos^2\phi + \sin^2\phi). \tag{131}$$

IV. Field Statistics for Lossy Cavities

4.1 Motivation and Generic Model

The idea of characterizing the electromagnetic field inside of cavities statistically is of recent interest to researchers, mainly because of two factors. First of all, modern equipment is quite complicated from an electromagnetic point of view and an accurate numerical modelling is rather impossible because of the overwhelming amount of calculations and memory which would be required. The situation is further complicated by the fact that for many applications some of the parameters of the disturbing electromagnetic energy are unknown. The second factor is the continued development of reverberation chambers for testing of an equipment's response to an unknown (or partially unknown) environment. This requires, by its very definition, the creation of a statistical field. That is, one in which the field parameters fall within some range of values over the exposed area. These two problems explain the recent significant interest of the EMC community in statistical electromagnetics.

An exact analytic expression for the electromagnetic field inside a large empty cavity with lossy walls and apertures does not exist. The only closed form solutions which are known are for the case of simply shaped cavities with perfectly conducting walls. However, as was shown in the previous chapter, these expressions can be modified to produce a number of useful results for the case of lossy walls and more general shapes. One of the main goals of this study is to understand the structure of the field inside a cavity, *i.e.* understand how the electromagnetic field can be represented in terms of a small set of parameters. The power balance method described in the previous chapter is a very useful method in this regard.

A very useful way to represent the total field inside an enclosure is to decompose the field in a sum of elementary waves (or modes). These can be written generally as $a_i(\mathbf{r};t)e^{j\phi_i(r;t)}$, $i = 1, 2, \ldots, N(t)$ and assumed to be independent identically distributed complex random variables with arbitrarily distributed and arbitrarily correlated real and imaginary parts. The numbers of modes $N(t_i)$ and $N(t_j)$, measured at two different time instances, t_i and t_j, are also correlated. A way to define the process governing the fluctuations of $N(t)$ was suggested in [90] based on the so-called generalized birth and death model [91]. The classical Gaussian model is reasonable whenever the total field can be thought of as the sum of contributions from a large number of independent random variables.

It was discovered in [90] that other distributions can be attributed to the random fluctuation in the number of waves which contribute to the total field. These arise from a random walk in two dimensions where the number of terms fluctuates according to a negative bimodal distribution [91, 92]. Further generalization of this model can be found in [93] where a non-uniform phase distribution is considered and in [93] where a biased random walk is introduced. In both cases the negative-bimodal distribution for the number of steps produces a generalized K distribution for the amplitude of the total field as the mean number of steps grows to infinity.

Otherwise, the total field can be thought of as the result of a composite mechanism, wherein a complex, possibly correlated, Gaussian process with fast fluctuations is modulated by an underlying, non-negative random process (texture component) which decorrelates on a much longer scale [95, 96]. A complete statistical characterisation for this model, often referred to as compound-Gaussian, is available only in the case of infinitely slow variations of the modulating component. In this situation, the process degenerates to a spherically invariant random process (SIRP) and its multidimensional PDF can be given in terms of the first-order PDF of the modulating variable and of the covariance function of the Gaussian process [97]. A rather deep insight, highlighting the relations between compound-Gaussian and random walk models, is presented in [90].

4.2 General form of the electromagnetic field intensity PDF

4.2.1 Kluyver equation

Let us assume that any electric field component, $E(\boldsymbol{r}, t)$, inside a general cavity, is represented as a sum of N modes which are statistically independent of each other [98]:

$$E(\boldsymbol{r};t) = e^{j\omega t}\sum_{i=1}^{N} a_i(\boldsymbol{r};t)\,e^{j\phi_i(\boldsymbol{r};t)} \tag{132}$$

Note that the expansion chosen above is a complex field having a frequency ω with a slowly varying envelope.

Some additional knowledge about the statistical properties of $a_i(\boldsymbol{r};t)$ and $\phi_i(\boldsymbol{r};t)$ is needed in order to derive the statistics for the amplitude of $E(\boldsymbol{r};t)$. Independence between $a_i(\boldsymbol{r};t)$ and $\phi_i(\boldsymbol{r};t)$ can be assumed if the enclosure is large compared to the wavelength, and is well stirred or well randomized by a large number of loads inside the cavity, *i.e.* the strong dependence on deterministic boundary conditions is removed [44, 58]. The field intensity of one component, $I(\boldsymbol{r};t)$, is defined as

$$I(\boldsymbol{r};t) = |E(\boldsymbol{r};t)|^2. \tag{133}$$

The proper statistics for $I(\boldsymbol{r};t)$ have been derived in [98] and is given by

$$p_i(I;N) = \frac{1}{2}\int_{R^N} J_0(|S|\sqrt{I})|S|\prod_{i=1}^{N}\langle J_0(a_i|S|)\rangle d|S| = \frac{1}{2}\int_0^\infty J_0(U\sqrt{I})U\prod_{i=1}^{N}\langle J_0(a_iU)\rangle dU. \quad (134)$$

Here averaging brackets <•> are used to show averaging over each a_i. Note that we keep the number of modes, N, as a parameter to emphasize that only a finite number of modes are taken into account. Since we have this PDF with the mode number as a parameter, we can actually use (134) to calculate the PDF of intensity for the case of a random number of excited modes. This last equation is called the Kluyver equation and was first derived in [100]. It is impossible to calculate this integral analytically for all possible distributions of the individual scatterers. However, an exact solution can be obtained for some important cases, including the K distributions considered below.

If the statistical properties of each individual mode are assumed identical then (134) can be rewritten simply as

$$p_i(I;N) = \frac{1}{2}\int_0^\infty J_0(U\sqrt{I})U\langle J_0(a_iU)\rangle^N dU. \quad (135)$$

4.2.2 Moments of the intensity

Despite the difficulties in calculating the PDF in (134), an exact expression can be obtained for its moments. The following derivations follows that given in [101] and is based on the moment generating function $\Theta_N(\lambda)$, defined as

$$\Theta_N(\lambda) = \int_0^\infty p_i(\sigma;N)e^{-\lambda\sigma}d\sigma. \quad (136)$$

The corresponding moments m_k of a PDF $p_N(\sigma)$ can be found as [99]:

$$m_k = \left(-\frac{\partial}{\partial\lambda}\right)^k \Theta_N(\lambda)\Big|_{\lambda=0} \quad (137)$$

or, from (137), as coefficients of the Taylor series expansion of $\Theta_N(\lambda)$ around $\lambda = 0$:

$$\Theta_N(\lambda) = \sum_{k=0}^{\infty}(-1)^k\frac{m_k}{k!}\lambda^k. \quad (138)$$

After substitution of (134) into (136) one obtains

$$\Theta_N(\lambda) = \int_0^\infty \frac{1}{2}\left(\int_{-\infty}^{\infty} J_0(U\sqrt{\sigma}) U \prod_{i=1}^{N} \langle J_0(a_i U)\rangle dU \right) e^{-\lambda\sigma} d\sigma$$
$$= \int_0^\infty \frac{1}{2} U \prod_{i=1}^{N} \langle J_0(a_i U)\rangle dU \int_{-\infty}^{\infty} J_0(U\sqrt{\sigma}) e^{-\lambda\sigma} d\sigma \tag{139}$$

An analytic expression for the inner integral

$$F(U) = \int_{-\infty}^{\infty} J_0(U\sqrt{\sigma}) e^{-\lambda\sigma} d\sigma \tag{140}$$

can be found using the standard integral (6.614-1 on the page 709 in [27]):

$$\int_0^\infty e^{-\alpha x} J_\nu(\beta\sqrt{x}) dx = \frac{\beta}{4}\sqrt{\frac{\pi}{\alpha^3}} \exp\left(-\frac{\beta^2}{8\alpha}\right)\left[I_{\frac{1}{2}(\nu-1)}\left(\frac{\beta^2}{8\alpha}\right) - I_{\frac{1}{2}(\nu+1)}\left(\frac{\beta^2}{8\alpha}\right)\right] \tag{141}$$

and if the following correspondence is introduced

$$\alpha \to \lambda,\ \beta \to U,\ \nu = 0 \tag{142}$$

we can evaluate $F(U)$ as

$$F(U) = \frac{U}{4}\sqrt{\frac{\pi}{\lambda^3}} \exp\left(-\frac{U^2}{8\lambda}\right)\left[I_{-1/2}\left(\frac{U^2}{8\lambda}\right) - I_{1/2}\left(\frac{U^2}{8\lambda}\right)\right]. \tag{143}$$

This last expression can be further simplified if one observes that (10.2.13 and 10.2.14 on page 443 in [28])

$$I_{-1/2}(z) - I_{1/2}(z) = \sqrt{\frac{2}{\pi}} \frac{e^{-z}}{\sqrt{z}} \tag{144}$$

which results in

$$F(U) = \frac{U}{4}\sqrt{\frac{\pi}{\lambda^3}} \exp\left(-\frac{U^2}{8\lambda}\right) \sqrt{\frac{2}{\pi}} \frac{\exp\left(-\frac{U^2}{8\lambda}\right)}{\sqrt{\frac{U^2}{8\lambda}}} = \frac{1}{\lambda}\exp\left(-\frac{U^2}{4\lambda}\right) \tag{145}$$

and, after substitution into (139), produces

$$\Theta_N(\lambda) = \int_0^\infty \frac{1}{2} U \prod_{i=1}^{N} \langle J_0(a_i U)\rangle dU \frac{1}{\lambda}\exp\left(-\frac{U^2}{4\lambda}\right)$$
$$= \int_0^\infty \prod_{i=1}^{N} \langle J_0(\sqrt{4\lambda x} a_i)\rangle dx \exp(-x) = \left\langle \int_0^\infty \prod_{i=1}^{N} (J_0\sqrt{4\lambda x} a_i) dx \exp(-x)\right\rangle \tag{146}$$

Here, the following normalization was used:

$$x = \frac{U^2}{4\lambda} \tag{147}$$

As the next step, the Bessel function inside the integral can be expanded in terms of power of x^2, and thus, in powers of λ. In fact, the corresponding Taylor expansion can be found in [28] (9.1.10 on page 360) as

$$J_0(z) = \sum_{k=0}^{\infty} \frac{\left(-\frac{1}{4}z^2\right)^k}{k!\,k!} \tag{148}$$

and thus

$$J_0(\sqrt{4\lambda x}a_i) = \sum_{k=0}^{\infty} \frac{(-\lambda a_i^2 x)^k}{k!k!} = \sum_{k=0}^{\infty} \frac{(-1)^k a_i^{2k} x^k}{k!k!}\lambda^k \tag{149}$$

and

$$\prod_{i=1}^{N} J_0(\sqrt{4\lambda x}a_i) = \prod_{i=1}^{N}\sum_{k_i=0}^{\infty} \frac{(-1)^{k_i} a_i^{2k_i} x^{k_i}}{k_i!k_i!}\lambda^{k_i}. \tag{150}$$

It follows from the last equation that $\Theta_N(\lambda)$ is a multidimensional confluent hypergeometric function of N variables [28]

$$\Theta_N(\lambda) = \Psi_2(1;1;\ldots;1;-\lambda a_1^2;-\lambda a_2^2;\ldots;-\lambda a_N^2) \tag{151}$$

and, thus

$$m_n = (n!)^2 \sum_{k_1=0}^{\infty}\sum_{k_2=0}^{\infty}\cdots\sum_{k_N=0}^{\infty}\left[\frac{\prod_{i=1}^{N}\langle a_i^{2k_i}\rangle}{\left(\prod_{i=1}^{N} k_i!\right)^2}\right]\Bigg|_{\sum k_i = n} \tag{152}$$

where $\langle a_i^{2k}\rangle$ is the $2k$-th moment of the distribution $p_a(A)$ of a single mode, *i.e.*

$$\langle a_i^{2k}\rangle = \int_0^{\infty} A^{2k} p_{a_i}(A)dA \tag{153}$$

and the right-hand side consists of those terms of the multiple sum satisfying the condition $\sum k_i = n$. Let us for simplicity assume here that all modes are distributed alike, *i.e.* they have equal moments and drop subindex i in the future considerations. For the first four moments the following relations can be deduced

from (152) [91]:

$$m_1 = N\langle a^2\rangle \tag{154}$$

$$\frac{m_2}{m_1^2} = 2\left(1-\frac{1}{N}\right)+\frac{1}{N}\frac{\langle a^4\rangle}{\langle a^2\rangle^2} \tag{155}$$

$$\frac{m_3}{m_1^3} = 6\left(1-\frac{1}{N}\right)\left(1-\frac{2}{N}\right)+\frac{9}{N}\left(1-\frac{1}{N}\right)\frac{\langle a^4\rangle}{\langle a^2\rangle^2}+\frac{1}{N^2}\frac{\langle a^6\rangle}{\langle a^2\rangle^3} \tag{156}$$

$$\begin{aligned}\frac{m_4}{m_1^4} = {} & 24\left(1-\frac{1}{N}\right)\left(1-\frac{2}{N}\right)\left(1-\frac{3}{N}\right)+\frac{72}{N}\left(1-\frac{1}{N}\right)\left(1-\frac{2}{N}\right)\frac{\langle a^4\rangle}{\langle a^2\rangle^2}+ \\ & \frac{18}{N^2}\left(1-\frac{1}{N}\right)\frac{\langle a^4\rangle^2}{\langle a^2\rangle^4}+\frac{16}{N^2}\left(1-\frac{1}{N}\right)\frac{\langle a^6\rangle}{\langle a^2\rangle^3}+\frac{1}{N^3}\frac{\langle a^8\rangle}{\langle a^2\rangle^4}\end{aligned} \tag{157}$$

and so on.

Several important conclusions can be drawn from (152). First of all, if the number of modes approaches infinity $N\to\infty$, the normalized moments approach those of the Chi-square distribution with two degrees of freedom

$$\lim_{N\to\infty}\frac{m_n}{(m_1)^n} = n!. \tag{158}$$

independently of the original distribution of a single mode. This is in complete agreement with fundamental *The Large Number Theorem* [24, 29]. At the same time (152) allows us to demonstrate how fast this distribution converges to the Chi-square distribution. In fact if all the modes have the same constant deterministic value of amplitude, say a, then (152) approaches the Chi-square as $1/N$. However any randomness in the modes' energy will cause the second term in (155) to remain relatively big even for large N. It is convenient to define the so called "*effective number of modes*"[1] as

$$N_{eff} = N\frac{\langle a^2\rangle^2}{\langle a^4\rangle}. \tag{159}$$

For some distributions this number may be much smaller than N and this will result in a large deviation from the Chi-square distribution. In fact, if approximately $N_{eff} > 10$, then deviations from Chi-square statistics are relatively small. However, if $N_{eff} \sim 1$ distinct deviations can be found from these statistics. Finally, if $N_{eff} < 1$ then very little similarity can be found between the real statistics and those predicted by the Chi-square distribution.

Another reason for deviations from the Chi-square distribution maybe the fact that the number N of modes does not remain constant. Also, the phase of the modes cannot always be considered as uniformly distributed.

1. Effective number of scatterers in [91].

4.2.3 Two-parameter distributions

Some experimental results related to the statistical modelling of the electromagnetic field inside cavities were reported in [58, 38]. It is generally accepted there that the Chi-square distribution gives only a rough approximation of the true statistics. It was also found that the Lehman distribution, that is

$$p(x) = \frac{b^4}{8} x^3 K_2(bx), \; x \geq 0 \tag{160}$$

provides a much better fit to the experimental data. However, this distribution is still one-parameter and, in our opinion, lacks the required flexibility which would allow it to approach the Chi-square distribution in a limiting sense. We therefore suggest that the class of model distributions be expanded so as to give consideration to the various two-parameter distributions which are available. The following requirements should be satisfied for these models:

- the Chi-square distribution for the intensity (and Rayleigh for the magnitude) should correspond to a set of particular values of the parameters;
- the tail of the distribution should be heavier than that of the Chi-square distribution in order to comply with experimental results [34-48]. This is also equivalent to the requirement that the moments of the distribution should grow faster than that of the Chi square.

There are a number of families which satisfy these two major requirements. However, we would like to emphasize here that one family, the so-called K distributions, also have some additional attractive features such as

- the Lehman distribution is a particular case of the K family, (*i.e.* $\nu = 3$);
- a number of analytical results can be obtained, including an exact expressions for the distribution of the intensity, magnitude and instantaneous values; and,
- there are convenient means of generating such distributions.

The last three properties make the K family the most attractive model for investigating the statistical properties of the electromagnetic field inside leaky cavities. However, other classes of PDFs will also be considered. The next few sections contain a comprehensive description of the K distribution, including the expression for the PDF, CDF, moments, *etc.*, and also describe a few other families which were considered by different researchers as models for experimental data. We leave the important question of the numerical generation of random processes with a prescribed distribution until Chapter VI, where the equations derived here are incorporated into a software tool.

4.3 The *K* distribution as a model for the electromagnetic field inside enclosures

4.3.1 PDF and CDF

A two parameter family of K distributions is described by the following equation [91-98]:

$$p(x) = \frac{2b}{\Gamma(\nu)}\left(\frac{bx}{2}\right)^{\nu} K_{\nu-1}(bx),\ \nu > 0,\ x \geq 0 \tag{161}$$

where b and ν are scale and shape parameters and $K_{\nu-1}(\circ)$ represents the modified Bessel function of the second kind of order $\nu - 1$ [1]. The corresponding CDF can also be expressed in terms of modified Bessel functions:

$$\begin{aligned} P(x) &= \int_0^x p(t)dt = \int_0^x \frac{2b}{\Gamma(\nu)}\left(\frac{bt}{2}\right)^{\nu} K_{\nu-1}(bt)dt \\ &= \frac{1}{2^{\nu-1}\Gamma(\nu)}\int_0^{bx} y^{\nu} K_{\nu-1}(y)dy = \frac{2}{\Gamma(\nu)}\left[\left(\frac{y}{2}\right)^{\nu} K_{\nu}(y)\right]\Bigg|_{bx}^{0} = \\ &= \lim_{x\to 0}\frac{2}{\Gamma(\nu)}\left(\frac{bx}{2}\right)^{\nu} K_{\nu}(bx) - \frac{2}{\Gamma(\nu)}\left(\frac{bx}{2}\right)^{\nu} K_{\nu}(bx) = 1 - \frac{2}{\Gamma(\nu)}\left(\frac{bx}{2}\right)^{\nu} K_{\nu}(bx) \end{aligned} \tag{162}$$

where the following integral relation (11.3.27 on the page 484 in [28]) was used

$$\int_0^z t^{\nu} K_{\nu-1}(t)dt = -z^{\nu} K_{\nu}(z) + 2^{\nu-1}\Gamma(\nu). \tag{163}$$

The dependence of the PDF and the CDF on the shape parameter ν for constant mean is shown in Fig. 13.

4.3.2 Characteristic Function

The characteristic function $\Theta(s)$ of the PDF in (161) can be found as its Fourier transform, that is

$$\begin{aligned} \Theta(s) &= \int_{-\infty}^{\infty} p(x)\exp(jsx)dx = \int_0^{\infty} \frac{2b}{\Gamma(\nu)}\left(\frac{bx}{2}\right)^{\nu} K_{\nu-1}(bx)\exp(jsx)dx \\ &= \frac{b^{\nu+1}}{\Gamma(\nu)2^{\nu-1}}\int_0^{\infty} x^{\nu} K_{\nu-1}(bx)\exp(jsx)dx \\ &= \frac{\sqrt{\pi}b^{2\nu}\Gamma(2\nu)}{\Gamma(\nu)\Gamma(\nu+3/2)}\frac{1}{(b-js)^{2\nu}} F\left(2\nu, \nu-\frac{1}{2}; \nu+\frac{3}{2}, \frac{js+b}{js-b}\right) \end{aligned} \tag{164}$$

1. This function is also known as MacDonald's function [27, 28].

Here, the following standard integral (6.621-3 on the page 712 in [27]) was used:

$$\int_0^\infty x^{\mu-1}e^{-\alpha x}K_\gamma(\beta x)dx = \frac{\sqrt{\pi}(2\beta)^\gamma}{(\alpha+\beta)^{\mu+\gamma}}\frac{\Gamma(\mu+\gamma)\Gamma(\mu-\gamma)}{\Gamma(\mu+1/2)}F\left(\mu+\gamma,\gamma+\frac{1}{2};\mu+\frac{1}{2},\frac{\alpha-\beta}{\alpha+\beta}\right) \tag{165}$$

with $\mu = \nu+1$, $\gamma = \nu-1$, $\beta = b$, $\alpha = -js$ and F is the hypergeometric function [28].

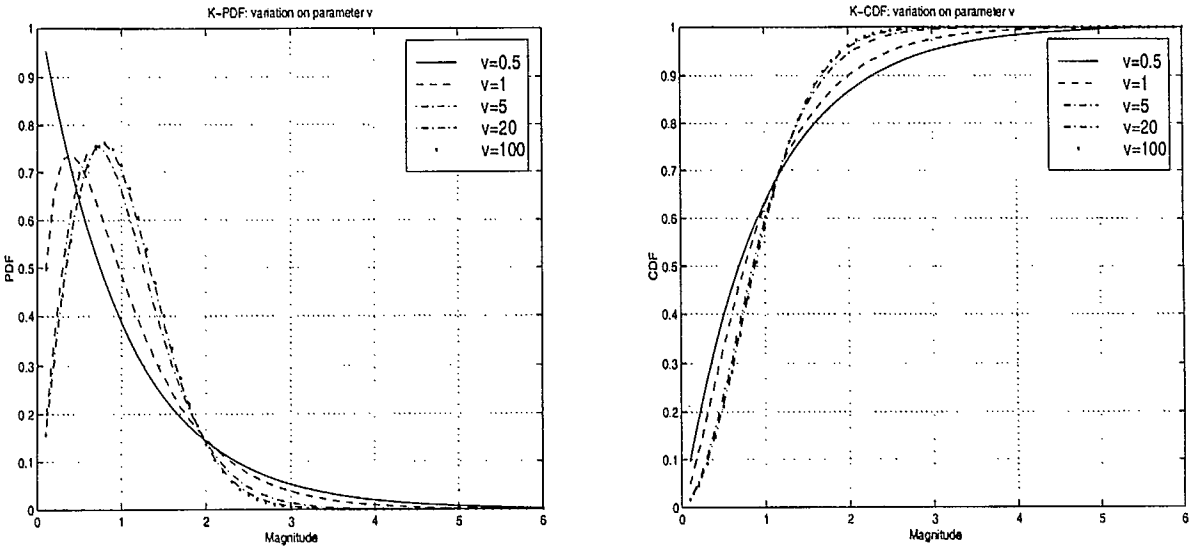

Figure 13. Dependence of the PDF (left) and CDF (right) on parameter ν with constant mean value. The case $\nu = 100$ is almost identical to the Rayleigh distribution with the same mean value.

4.3.3 Moments

The moments m_k of this distribution can be found by integrating (161) with appropriate weight x^k:

$$\begin{aligned} m_k &= \int_0^\infty x^k p(x)dx = \int_0^\infty x^k \frac{2b}{\Gamma(\nu)}\left(\frac{bx}{2}\right)^\nu K_{\nu-1}(bx)dx \\ &= \frac{1}{2^{\nu-1}b^k\Gamma(\nu)}\int_0^\infty (bx)^{\nu+k}K_{\nu-1}(bx)d(bx) \\ &= \frac{1}{2^{\nu-1}b^k\Gamma(\nu)}\int_0^\infty t^{\nu+k}K_{\nu-1}(t)dt = \left(\frac{2}{b}\right)^k\frac{\Gamma\left(\nu+\frac{k}{2}\right)\Gamma\left(1+\frac{k}{2}\right)}{\Gamma(\nu)} \end{aligned} \tag{166}$$

Here standard integral (6.561.16 on page 684 in [27]):

$$\int_0^\infty x^\mu K_w(ax)dx = 2^{\mu-1}a^{-(\mu+1)}\Gamma\left(\frac{1+\mu+w}{2}\right)\Gamma\left(\frac{1+\mu-w}{2}\right) \tag{167}$$

was used with $\mu = \nu + k$, $w = \nu - 1$ and $a = 1$. In particular, (166) gives the following expressions for the mean and the second moment:

$$m_1 = \frac{2}{b}\frac{\Gamma\left(\nu+\frac{1}{2}\right)\Gamma\left(\frac{3}{2}\right)}{\Gamma(\nu)} = \frac{\sqrt{\pi}}{b}\frac{\Gamma\left(\nu+\frac{1}{2}\right)}{\Gamma(\nu)} \tag{168}$$

$$m_2 = \left(\frac{2}{b}\right)^2\frac{\Gamma(\nu+1)\Gamma(2)}{\Gamma(\nu)} = \left(\frac{2}{b}\right)^2\frac{\nu\Gamma(\nu)1!}{\Gamma(\nu)} = \left(\frac{2}{b}\right)^2\nu \tag{169}$$

The normalized moments of the distribution in (161) are given by

$$\frac{m_k}{m_1^k} = \frac{\left(\frac{2}{b}\right)^k\frac{\Gamma\left(\nu+\frac{k}{2}\right)\Gamma\left(1+\frac{k}{2}\right)}{\Gamma(\nu)}}{\left[\left(\frac{2}{b}\right)\frac{\Gamma\left(\nu+\frac{1}{2}\right)\Gamma\left(\frac{3}{2}\right)}{\Gamma(\nu)}\right]^k} = \frac{\Gamma\left(1+\frac{k}{2}\right)}{\Gamma^k\left(\frac{3}{2}\right)}\frac{\Gamma\left(\nu+\frac{k}{2}\right)\Gamma^{k-1}(\nu)}{\Gamma^k\left(\nu+\frac{1}{2}\right)} \tag{170}$$

4.3.4 Intensity distribution

If the magnitude distribution is given by a family of K distributions, *i.e.* by (161), then the distribution of its square $I = x^2$ is the intensity distribution, $p_i(I)$, related to (161) by a simple transformation [99]:

$$p_i(I) = \frac{p(\sqrt{I})}{2\sqrt{I}} = \frac{\frac{b}{\Gamma(\nu)}\left(\frac{b\sqrt{I}}{2}\right)^\nu K_{\nu-1}(b\sqrt{I})}{\sqrt{I}} = \frac{b^2}{2\Gamma(\nu)}\left(\frac{b\sqrt{I}}{2}\right)^{\nu-1}K_{\nu-1}(b\sqrt{I}) \tag{171}$$

The dependence of the PDF and the CDF on the shape parameter ν for a constant mean is shown in Fig. 14.

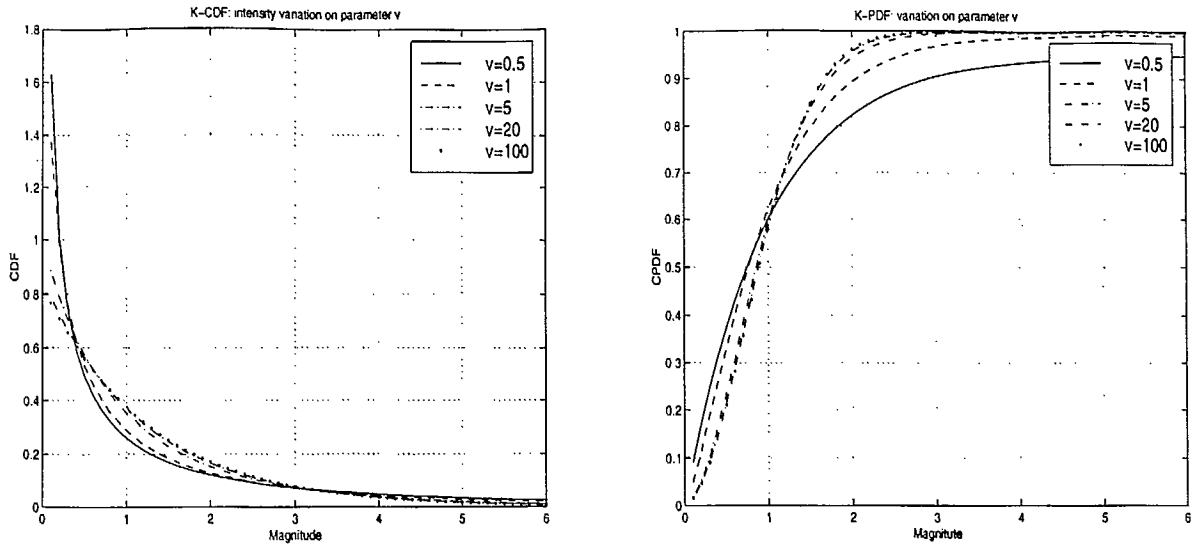

Figure 14. Dependence of the PDF (left) and the CDF (right) of intensity of the K-distribution on parameter ν with constant mean value. The case $\nu = 100$ is almost identical to Chi-square distribution with the same mean value.

The moments of this intensity distribution can be related to the moments of the distribution in (161) by

$$\begin{aligned} m_{ki} &= \int_0^\infty I^k p_i(I)dI = \int_0^\infty I^k \frac{b^2}{2\Gamma(\nu)}\left(\frac{b\sqrt{I}}{2}\right)^{\nu-1} K_{\nu-1}(b\sqrt{I})dI \\ &= \int_0^\infty x^{2k}\frac{b^2}{2\Gamma(\nu)}\left(\frac{bx}{2}\right)^{\nu-1} K_{\nu-1}(bx)2xdx \\ &= 2\int_0^\infty x^{2k}\frac{b}{2\Gamma(\nu)}\left(\frac{bx}{2}\right)^{\nu} K_{\nu-1}(bx)dx \\ &= m_{2k} = \left(\frac{2}{b}\right)^{2k}\frac{\Gamma(\nu+k)k!}{\Gamma(\nu)} \end{aligned} \tag{172}$$

and thus, the average value of the intensity is

$$m_{1i} = \left(\frac{2}{b}\right)^2\frac{\Gamma(\nu+1)\Gamma(2)}{2\Gamma(\nu)} = \frac{4\nu}{b^2} \tag{173}$$

Equation (173) also allows us to obtain an expression for the normalized moments of the intensity:

$$f_{nK} = \frac{m_{ni}}{(m_{1i})^n} = \frac{\left(\frac{2}{b}\right)^{2n}\frac{\Gamma(\nu+n)n!}{\Gamma(\nu)}}{\left(\left(\frac{2}{b}\right)^2\nu\right)^n} = n!\frac{\Gamma(\nu+n)}{\Gamma(\nu)\nu^n} = n!\frac{(\nu+1)(\nu+2)\ldots(\nu+n-1)}{\nu^{n-1}}$$
$$= n!\left(1+\frac{1}{\nu}\right)\left(1+\frac{2}{\nu}\right)\ldots\left(1+\frac{n-1}{\nu}\right) = f_{n\chi}\left(1+\frac{1}{\nu}\right)\left(1+\frac{2}{\nu}\right)\ldots\left(1+\frac{n-1}{\nu}\right) \tag{174}$$

using the fact that $f_{n\chi} = n!$ for the Chi-square distribution [90]. This last equation means that if the shape parameter ν approaches infinity, then the PDF (161) approaches the Chi-square PDF. At the same time, the normalized moments of the K distribution are always greater than those of the Chi-square, that is

$$f_{nK} > f_{n\chi} \tag{175}$$

4.3.5 Distribution of instantaneous values [32]

The PDF of instantaneous values $p_x(x)$ and the PDF of magnitude $p_A(A)$ are related by the Blanc-Lapierre transformation [99][1], if the corresponding phase is uniformly distributed on the interval $[0, 2\pi]$ and is statistically independent of the magnitude. This transformation is given by

$$p_x(x) = \frac{1}{2\pi}\int_{-\infty}^{\infty}\exp[-jsx]ds\int_0^{\infty}p_A(A)J_0(sA)dA\,. \tag{176}$$

Let us first find the characteristic function of the PDF in equation (176) using the Bessel transform [99]

$$\theta_x(s) = \int_0^{\infty}p_A(A)J_0(sA)dA = \frac{b^{\nu+1}}{2^{\nu-1}\Gamma(\nu)}\int_0^{\infty}A^{\nu}K_{\nu-1}(bA)J_0(sA)dA\,. \tag{177}$$

It can be calculated using standard integral (6.576-7 on the page 694 in [27])

$$\int_0^{\infty}x^{\eta+\mu+1}J_{\mu}(ax)K_{\eta}(bx)dx = 2^{\mu+\eta}a^{\mu}b^{\eta}\frac{\Gamma(\mu+\eta+1)}{(a^2+b^2)^{\mu+\eta+1}} \tag{178}$$

where the following transformation of variables should be used:

$$\mu = 0,\ a = s,\ x = A,\ \eta = \nu-1\,. \tag{179}$$

This yields

$$\theta_x(s) = \frac{b^{\nu+1}}{2^{\nu-1}\Gamma(\nu)}2^{\nu-1}b^{\nu-1}\frac{\Gamma(\nu)}{(a^2+b^2)^{\nu}} = \frac{b^{2\nu}}{(s^2+b^2)^{\nu}}. \tag{180}$$

The PDF $p_x(x)$ can be found using an inverse Fourier transform of its characteristic function, given in (180) [99]:

1. This is a particular case of (146) for $N = 1$

$$p_x(x) = \frac{1}{2\pi}\int_{-\infty}^{\infty}\theta_x(s)\exp(-isx)ds = \frac{b^{2\nu}}{2\pi}\int_{-\infty}^{\infty}\frac{\exp(-isx)}{(s^2+b^2)^{\nu}}ds = \int_{-\infty}^{\infty}\frac{\exp(-isx)}{(is+b)^{\nu}(-is+b)^{\nu}}ds$$
$$= \frac{b^{2\nu}}{2\pi}\int_{-\infty}^{\infty}(is+b)^{-2\frac{\nu}{2}}(-is+b)^{-2\frac{\nu}{2}}\exp(-isx)ds \tag{181}$$

The last integral is a tabulated integral (3.384-9 on the page 321 in [27]):

$$\int_{-\infty}^{\infty}(\beta+jx)^{-2\mu}(\beta-jx)^{-2\mu}e^{-jpx}dx = 2\pi(2\beta)^{-2\mu}\frac{|p|^{2\mu-1}}{\Gamma(2\mu)}W_{0,\frac{1}{2}-2\mu}(2\beta|p|), \tag{182}$$

thus, setting

$$\mu = \frac{\nu}{2},\ \beta = b,\ p\to x,\ x\to s \tag{183}$$

the expression for the PDF becomes

$$p_x(x) = \frac{b^{2\nu}}{2\pi}2\pi(2b)^{-\nu}\frac{|x|^{\nu-1}}{\Gamma(\nu)}W_{0,\frac{1}{2}-\nu}(2b|x|) = \frac{2^{-2\nu+1}b}{\Gamma(\nu)}(2b|x|)^{\nu-1}W_{0,\frac{1}{2}-\nu}(2b|x|). \tag{184}$$

This equation can be further simplified using the following expression for the Whittaker function $W_{0,1/2-\nu}(\circ)$, first in terms of the Kummer function $U(a, b, z)$ (equation 13.1-33 on page 505) and then in terms of the modified Bessel function K of the second kind (equation 13.6.21 on page 510 in [28]):

$$W_{0,\frac{1}{2}-\nu}(z) = \exp\left(-\frac{z}{2}\right)z^{1-\nu}U(1-\nu, 2-2\nu, z) = \frac{z^{1/2}}{\sqrt{\pi}}K_{\nu-\frac{1}{2}}\left(\frac{z}{2}\right),\ z = 2b|x| \tag{185}$$

and thus

$$p_x(x) = \frac{2^{-\nu+1/2}b}{\Gamma(\nu)\sqrt{\pi}}(b|x|)^{\nu-\frac{1}{2}}K_{\nu-\frac{1}{2}}(b|x|) \tag{186}$$

Thus, the distribution of instantaneous values, corresponding to the K distribution of magnitude is again expressed in terms of the modified Bessel function K. The dependence of the PDF and CDF on the shape parameter ν for a constant mean are shown in Fig. 15.

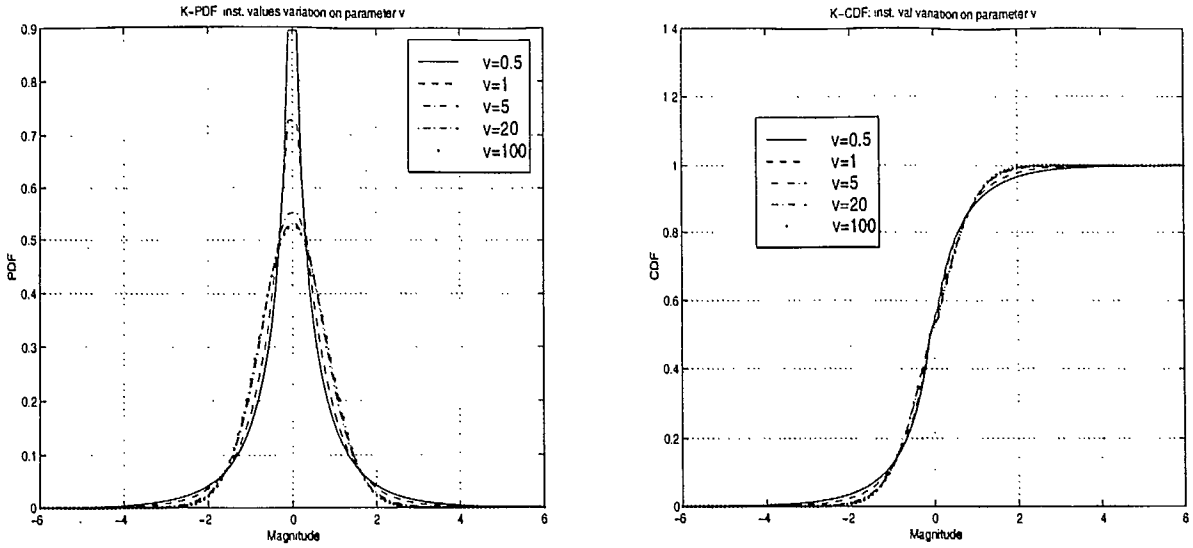

Figure 15. Dependence of the PDF (left) and the CDF (right) on parameter ν with a constant mean value. The case $\nu = 100$ is almost identical to the Rayleigh distribution with the same mean value.

4.4 Other candidates

4.4.1 The generalized Gamma distribution

The Generalized Gamma distribution, described by the PDF

$$p_{Gi}(I) = \frac{1}{\beta^{\alpha}\Gamma(\alpha)} I^{\alpha-1} e^{-I/\beta} \tag{187}$$

is a straightforward generalization of the exponential distribution (*i.e.* it coincides with the Chi-square distribution with $n \geq 2$ degrees of freedom if $\alpha = n/2$, and with the Porter-Thomas distribution with $\alpha = 1/2$). The Gamma distribution gives rise to generalized Laguerre polynomials and the Gram-Charlier expansion, widely used in statistics and communications theory [99]. It is easy to find (see [102]) that the moments of the PDF (187) are given by

$$m_{Gin} = \frac{\Gamma(\alpha+n)}{\Gamma(\alpha)}\beta^n \tag{188}$$

and thus

$$f_{Gn} = \frac{m_{Gin}}{(m_{Gi1})^n} = \frac{\frac{\Gamma(\alpha+n)}{\Gamma(\alpha)}\beta^n}{\left(\frac{\Gamma(\alpha+1)}{\Gamma(\alpha)}\beta\right)^n} = \frac{\Gamma(\alpha+n)}{\Gamma(\alpha)\alpha^n} \tag{189}$$

4.4.2 The log-normal distribution

The general form of the PDF for the log-normal distribution is given by the following equation [102]:

$$p_{Li}(I) = \frac{1}{I\sigma\sqrt{2\pi}}\exp\left[-\frac{(\ln I - a)^2}{2\sigma^2}\right]. \tag{190}$$

Despite its complicated appearance, the expression for its moments is rather simple [102]:

$$m_{Lin} = e^{an + \frac{n^2\sigma^2}{2}}. \tag{191}$$

This results in the following expression for normalized moments

$$f_{Ln} = \frac{m_{Lin}}{(m_{Li1})^n} = \frac{e^{an + \frac{n^2\sigma^2}{2}}}{e^{an + \frac{n\sigma^2}{2}}} = e^{\frac{(n^2-n)\sigma^2}{2}}. \tag{192}$$

We see that the normalized moments of the log-normal distribution grow exponentially. This explains the very heavy tail of this distribution. The log-normal distribution is usually used in combination with the normal distribution to obtain stronger tails than that for the Gaussian [39].

4.4.3 The Weibull distribution

Yet another generalization of the Chi-square distribution is the so-called Weibull distribution, which is frequently used to describe processes with a rapidly decaying probability of large values. Its PDF is given by

$$p_{Wi}(I) = \frac{\alpha}{\beta} I^{\alpha-1} e^{-I^\alpha/\beta} \tag{193}$$

with corresponding moments

$$m_{Win} = \beta^{n/\alpha}\Gamma(1 + \frac{n}{\alpha}) \tag{194}$$

This can be recast in terms of normalized moments as

$$f_{nW} = \frac{\beta^{n/\alpha}\Gamma(1 + \frac{n}{\alpha})}{\left(\beta^{1/\alpha}\Gamma(1 + \frac{1}{\alpha})\right)^n} = \frac{\Gamma(1 + \frac{n}{\alpha})}{\Gamma^n(1 + \frac{1}{\alpha})} \tag{195}$$

4.4.4 Comparison of the statistical moments for various intensity distributions

Let us compare consecutive normalized moments for the various distributions considered above, that is, let us consider the ratio

$$g_n = \frac{f_{n+1}}{f_n} = \frac{m_{i(n+1)}/m_{i1}^{(n+1)}}{m_{in}/m_{i1}^n} \tag{196}$$

For the K distribution, it follows from (174) that this ratio is

$$g_{nK} = \frac{(n+1)!\dfrac{\Gamma(\nu+n+1)}{\Gamma(\nu)\nu^{n+1}}}{n!\dfrac{\Gamma(\nu+n)}{\Gamma(\nu)\nu^{n}}} = (n+1)(1-n+nf_{2K}/2) \tag{197}$$

It follows from (197), and the fact that $f_{2\chi} = 2$ for the Chi-square distribution, that

$$g_{n\chi} = (n+1) \tag{198}$$

Based on (192) and the non-negativity of ε, equation (196) for the case of the log-normal distribution can be rewritten as

$$g_{nL} = f_{2L}^{n} \tag{199}$$

For any of these distributions $f_{2(\bullet)} \geq 2$, and thus it can be represented as

$$f_{2(\bullet)} = 2(1+\varepsilon) \tag{200}$$

where the parameter ε is a non-negative number. Consequently, the following estimates can be given:

$$g_{nK} = (n+1)(1+n\varepsilon) > n+1 = g_{n\chi}, \tag{201}$$

$$g_{nL} = 2^{n}(1+\varepsilon)^{n} \geq (n+1)(1+n\varepsilon) = g_{nK}. \tag{202}$$

This last inequality is based on the facts that $2^{n} > n+1$ for $n > 1$, and $(1+\varepsilon)^{n} > 1+n\varepsilon$. The last estimate follows from the Newton binomial expansion

$$(1+\varepsilon)^{n} = 1+n\varepsilon+\ldots+\varepsilon^{n} \geq 1+n\varepsilon \tag{203}$$

The first estimate can be proven as follows. Let us consider the function

$$h(t) = 2^{t}-t-1 \tag{204}$$

Its derivative is

$$\frac{d}{dt}h(t) = 2^{t}\ln 2 - 1 \tag{205}$$

which is a positive number for $t > 1$, and, thus

$$h(t) > h(1) = 2^{1}-1-1 = 0. \tag{206}$$

This is equivalent to $2^{t} > t+1$ which completes the proof.

The consecutive normalized moments of the generalized Gamma distribution are also between those of the Chi-square and those of log-normal which can be seen from the following simple calculations:

$$g_{nG} = \frac{f_{G(n+1)}}{f_{Gn}} = \frac{\dfrac{\Gamma(\alpha+n+1)}{\Gamma(\alpha)\alpha^{n+1}}}{\dfrac{\Gamma(\alpha+n)}{\Gamma(\alpha)\alpha^{n}}} = \frac{\Gamma(\alpha+n+1)}{\Gamma(\alpha+n)\alpha} = \frac{\alpha+n}{\alpha} = 1+n(f_{2}-1) = 1+n+2\varepsilon n \tag{207}$$

However, they are still less than the corresponding moments of the K distribution:

$$g_{nG}-g_{nK} = 1+n+2\varepsilon n-(n+1)(1+n\varepsilon) = (1-n)n\varepsilon < 0 \tag{208}$$

A similar calculation can be performed for the Weibull distribution. In fact, using the equation for normalized moments (195), one can obtain that

$$g_{nW} = \frac{\Gamma(1+\frac{n+1}{\alpha})}{\Gamma^{(n+1)}(1+\frac{1}{\alpha})} \cdot \frac{\Gamma(1+\frac{n}{\alpha})}{\Gamma^{n}(1+\frac{1}{\alpha})} = \frac{1}{\Gamma(1+\frac{1}{\alpha})} \frac{\Gamma(1+\frac{n+1}{\alpha})}{\Gamma(1+\frac{n}{\alpha})} \tag{209}$$

which grows slower than for the Chi-square.

Thus, the moments of the K distribution always lie between those of the generalized Gamma distribution (including Chi-squared) and those of the log-normal distribution having the same mean and variance.

4.5 Conclusions

The following conclusions can be drawn from the above considerations. A family of K distributions is an attractive model for describing a random field inside cavities. It coincides with the Chi-square distribution for $\nu = \infty$ and it also contains the Lehman distribution for $\nu = 3$. A smooth transition between these two classes can be achieved by varying the parameter ν. From another point of view, it was shown that the moments of the intensity of the random field described by a K distribution are always bounded by those of log-normal (upper bound) and those of the generalized Gamma distribution (lower bound). This also gives an additional degree of freedom for modelling purposes. Yet another useful property is the invariance of a K distributed random field under a linear transformation. This may be extremely useful when the effect of the external coupling into transmission lines is considered. The models considered here have been implemented in the *UWO StEm Tool* which is described in more details in Chapter VI.

V. FDTD Simulation of a Computer Box

In this chapter a full-field time domain analysis of a plane wave impinging on a computer case, using the finite difference time domain technique (FDTD), is conducted in order to estimate the statistics of the electromagnetic field inside the case. The impinging plane wave is a transient Gaussian pulse containing frequencies up to about 3 GHz. The Fourier transform is used to obtain frequency domain information and this allows us to investigate the internal field at various practical frequencies of interest. Details of the FDTD technique will not be discussed as this is a very well known technique and information on its merits is widely available.

5.1 Geometry of the problem

Consider a standard computer box of size $0.35m \times 0.45m \times 0.17m$. We treat this as a rectangular cavity which is open on one side, as shown in Fig. 16. The opening may represent a dielectric (plastic) panel at the front of the computer or just a model for a side which has many apertures.

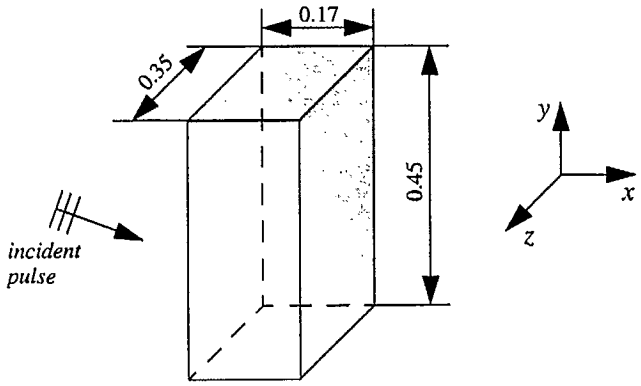

Figure 16. Geometry of the problem

The impinging plane electromagnetic wave has a Gaussian time variation given by

$$E^{inc}(t) = E_0^{inc} \exp\left[-\frac{(t-t_0)^2}{2\beta^2}\right] \tag{210}$$

where $t = t_0$ represents the time location of the field maximum and β describes the width of the Gaussian pulse [122]. The incident electric field was polarized in the $\hat{a}_x$ direction and the incidence plane was $y-z$ plane. A typical input file for the UWO FDTD program is shown in Fig. 17. The total side of the grid in

cells was 73 X 110 X 110, or 883,300 cells and the simulation was run for 1024 time steps (allowing the use of the Fast Fourier Transform in obtaining frequency domain data). The cells were cubical having a size of 5 mm and the time step was set to the Courant limit, that is $\Delta t = 9.6$ ps for a total simulation time of about 10 ns. First order Mur boundary conditions was used.

```
**************************************************************************
* Input data file for HPM pulse hitting an empty PC box
**************************************************************************
.formulation
scattering
.Problem size: lower_x, upper_x, lower_y, upper_y, lower_z, upper_z
0 73 0 110 0 110
.Number of time steps and output frequency of the data
1024 8
.Space increment: delta_x, delta_y, delta_z
1
0 73  0.005
1
0 110  0.005
1
0 110  0.005
.Directory to which output the files
/home/faculty/primak/FDTD/WORKS/PC/T1/
.Boundary conditions: specify with characters ('e' or 'a')
aaeaaa
.Mur
1
.Animator output of Ex, Ey, Ez at x=38 plane
total 1 38 7 X38
.Animator output of Ex, Ey, Ez at y=55 plane
total 2 55 7 Y55
.Animator output of Ex, Ey, Ez at z=45 plane
total 3 45 7 Z45
.Test point
incident  38 55 45 1 Inc
.Test point
incident  38 55 45 2 Inc
.Test point
incident  38 55 45 2 Inc
.Object: Wall 1
20 53 20 21 0 90 1 1 999
.Object: Wall 2
20 21 20 90 0 90 1 1 999
.Object: Wall 3
20 53 89 90 0 90 1 1 999
.Object: Wall 4
52 53 20 90 0 90 1 1 999
.Field IC's
gaussian
0 0 1 0 -100 32
```

Figure 17. Typical UWO FDTD input file

Simulations were conducted for four incidence angles of incoming electromagnetic plane wave: $\theta_1 = 0°$, $\theta_2 = 10°$, $\theta_3 = 20°$, and $\theta_4 = 30°$ for a constant angle of $\phi = 90°$. For each angle, time domain data for the E_x component of the field were recorded at all the points of the FDTD grid corresponding to the planes: $x = 25$, $x = 30$, $x = 35$, $x = 40$ and $x = 45$ cells respectively. At every point the FFT of the time domain data was performed and the magnitude and phase of the field at two frequencies $f_1 = 0.8\ GHz$ and $f_1 = 1.9\ GHz$ was found. The results were used to produce histograms of the field characteristics throughout the corresponding planes. The "experimental" histograms are compared against the Rayleigh distribution having the same first moment and the K distribution with the same first and second moments. Details of the parameter estimation procedure can be found in [130].

5.2 Simulation results

The following Figures 18-19 reflect results obtained by means of numerical simulation described in the section above. It can be clearly seen that for frequency $f = 1.9\ GHz$ the K distribution provides a very good fit to the numerical data. However, it is worth noting that the phase distribution is far from being uniform and should be modelled as a weighted sum of Tikchonov distributions. The detailed investigation of these questions will be conducted in the next project.

It can also be seen that the approximation is worsening as the frequency decreases to $f = 0.8\ GHz$. This can be explained by the fact that for the lower frequencies the number of modes allowed and excited is smaller. In fact, only few modes may exist in our experiment. However, the K distribution still provides the best fit. A similar picture can be observed when frequency stirring of a closed high Q cavity is investigated [44]. Some numerical results are shown below in Fig. 20.

5.3 Conclusions

The following conclusions can be drawn from these numerical experiments.

1) The applicability of the FDTD simulations to derive the appropriate statistics of the electromagnetic field inside enclosures is proven.
2) The K distribution provides a better fit to the numerical data than the Chi-square distribution at least for a cavity whose size is larger than the wavelength of the incident field. However more work is required to investigate the case when the frequency of the excitation is close to the cut-off frequency of the box.
3) It is shown that even a "weak randomization" (*i.e.* averaging over only a few incidence angles) of the incidence field allows one to obtain results close to those predicted by statistical theory.
4) As it can be seen from Fig. 18, the phase distribution is not uniform, and can be modelled as a mixture of Tikhonov distributions.

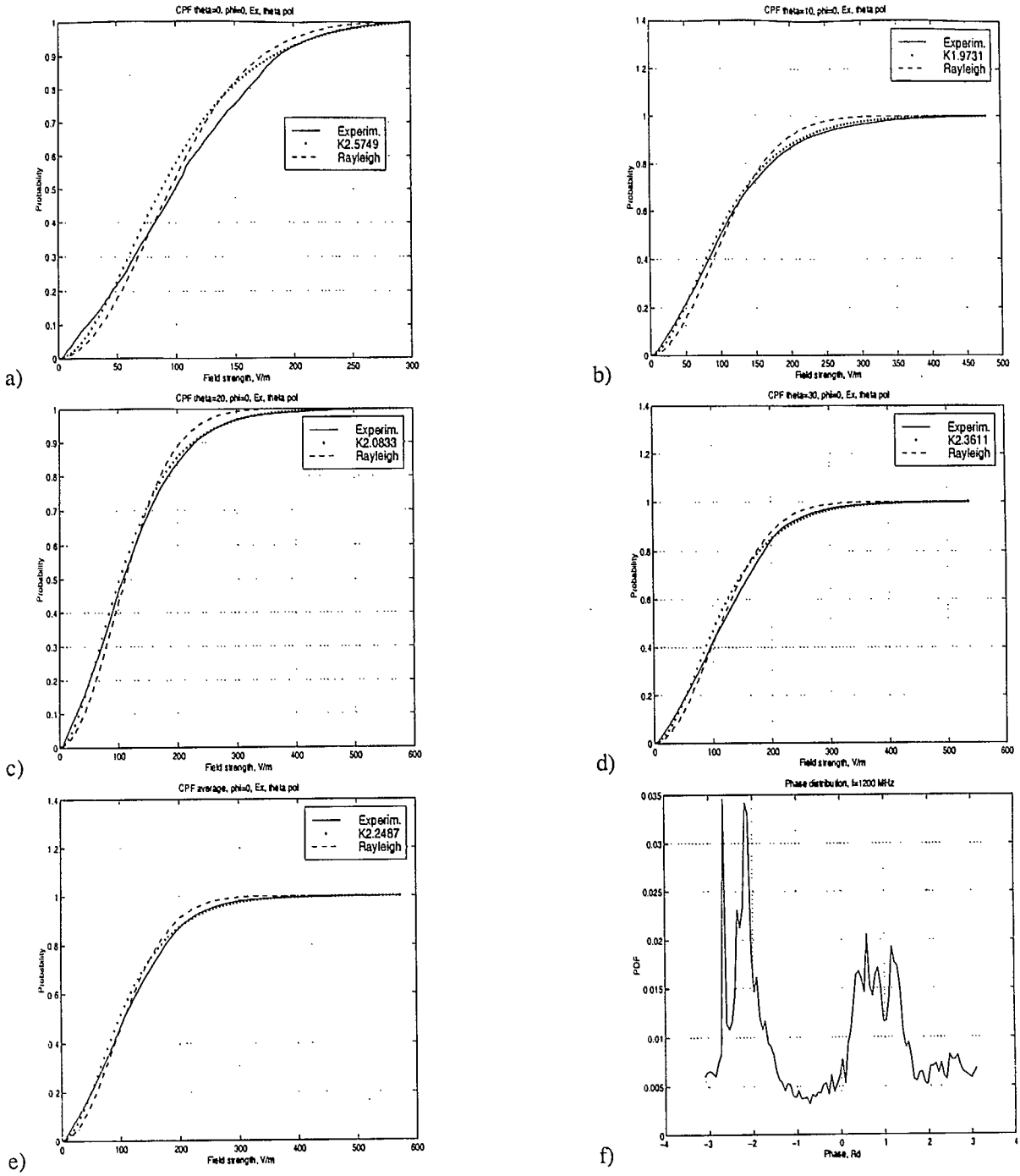

Figure 18. Results of simulating an open computer box at frequency $f = 1.9\ GHz$:
a) incidence angle $\theta = 0°$, $\nu = 2.6$, b) incidence angle $\theta = 10°$, $\nu = 1.9$,
c) incidence angle $\theta = 20°$, $\nu = 2.0$, d) incidence angle $\theta = 30°$, $\nu = 2.4$,
e) averaged over the four angles, $\nu = 2.25$, f) typical phase distribution,

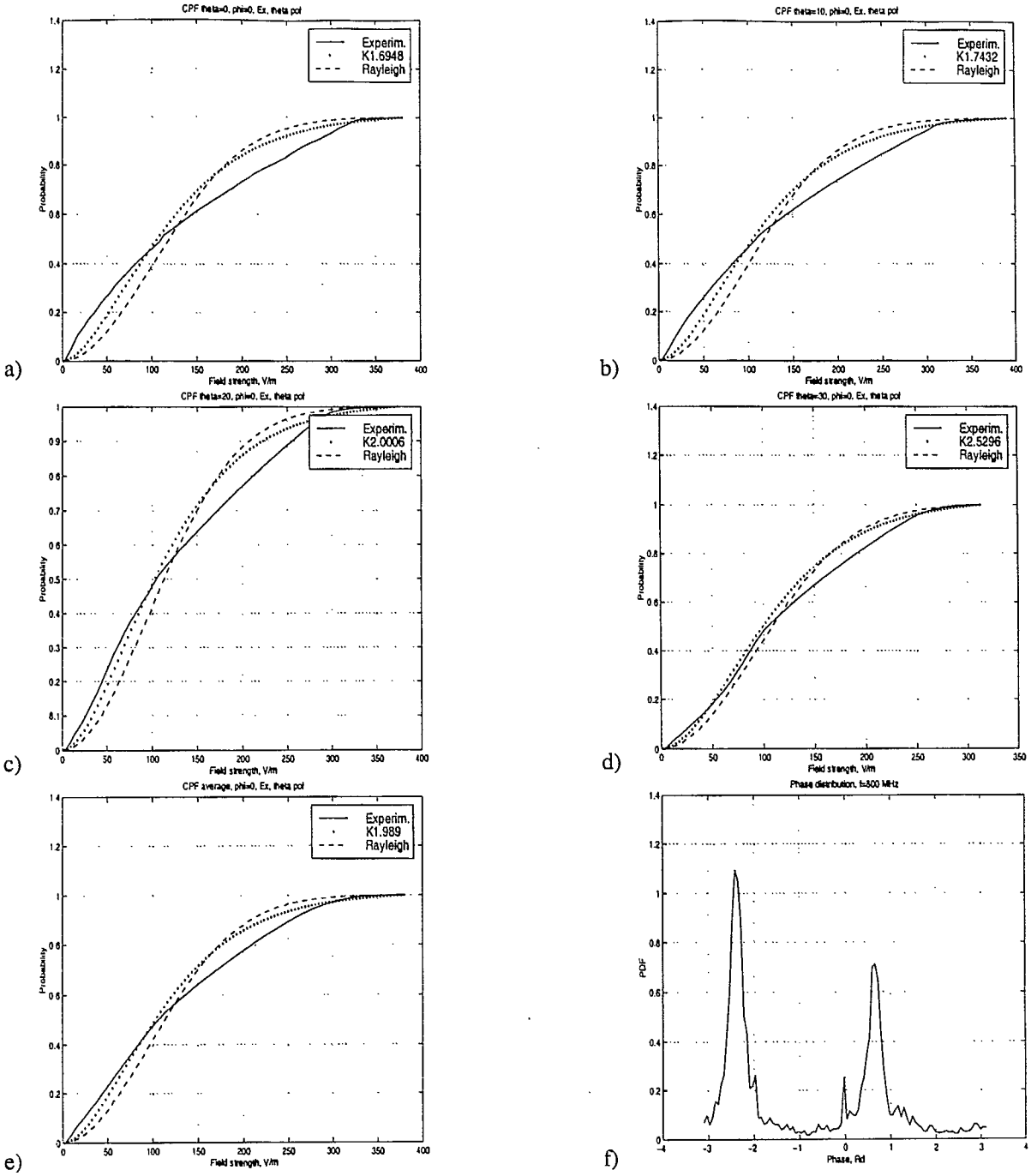

Figure 19. Results of simulating a open computer box at frequency $f = 0.8\ GHz$:
a) incidence angle $\theta = 0°$, $\nu = 1.7$, b) incidence angle $\theta = 10°$, $\nu = 1.7$,
c) incidence angle $\theta = 20°$, $\nu = 2.0$, d) incidence angle $\theta = 30°$, $\nu = 2.5$,
e) averaged over the four angles, $\nu = 2.0$, f) typical phase distribution,

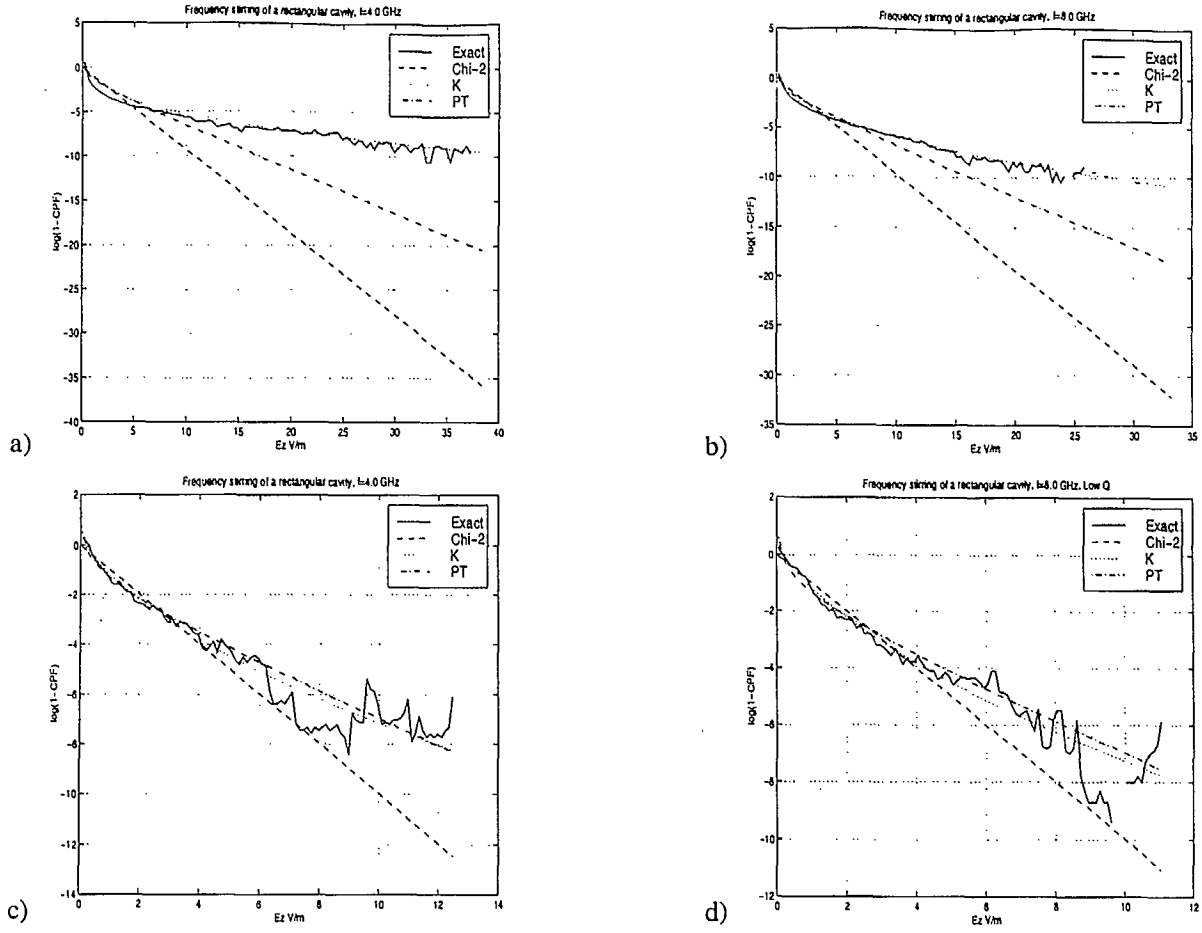

Figure 20. Results of simulating a closed two dimensional cavity of size 3.54×4.05 m excited by a line source, located at $x_0 = y_0 = 0.5m$:

a) $f = 4\ GHz$, $Q = 10^5$, $\nu = 0.5$, b) $f = 8\ GHz$, $Q = 10^5$, $\nu = 0.8$,

c) $f = 4\ GHz$, $Q = 100$, $\nu = 0.9$, d) $f = 8\ GHz$, $Q = 100$, $\nu = 1.2$.

The bandwidth of the excitation is $\Delta f = 10\ MHz$ for all cases.

VI. The Coupling of Statistical Fields to Transmission Lines

In this chapter we consider the simulation of a randomly distributed field which couples to a transmission line. In previous chapters, an attempt was made to describe the statistics of the electromagnetic field inside an enclosure. Here, we take such a field and assume that it couples to a transmission line which is present inside the enclosure. The main choice one has to make about how to model the physics of this problem is whether to use a full-wave model or to use an approximate quasi-TEM transmission line based model. The latter, although less accurate, requires much less computer resources. On the other hand, since the purpose of the simulations is to generate data which can be used to generate statistical distributions governing the load voltages at the terminals of the transmission line, it is hoped that the small inaccuracies will not affect the statistics of these load voltages. In future research, the differences between the two models, with respect to the generation of such Monte Carlo type data, will be investigated further.

In transmission line type modelling, the effect of the coupling field is taken into account via distributed source voltages and currents along the transmission line length. Thus, the second choice to be made is to incorporate the statistical properties of the field by: a) assuming a plane wave coupling and randomizing its parameters (*i.e.* incidence angle, polarization, frequency, phase, amplitude); or b) generating a random field with a given distribution and spatial correlation and injecting this directly into the transmission line. The problem with the first choice is that, although some of the statistics have been derived assuming a multiple plane wave model, the structure of the field inside an enclosure has more complicated features than those of a plane wave in general (*i.e.* the wave impedance is not equal to the intrinsic impedance and E is not necessary orthogonal to H). Thus, we choose to generate a statistical field with a desired distribution and spatial correlation and to inject this field directly into the source terms of the transmission line equations.

One advantage of this procedure is that, if it is successful, it effectively decouples the enclosure problem from the transmission line coupling problem. This is necessary if the topological formulation discussed in the introduction is to be used in the future along with statistical characterizations. The success of this method cannot fully be ascertained until an experimental investigation is conducted. This will be

one of the goals of future research. For now, in this chapter, we outline how these calculations are carried out.

6.1 Solution of the inhomogeneous transmission line equations

Consider a section of transmission line having a length d, per-unit-length parameters: L,C, R, and G, and terminated at $x = 0$ and $x = d$ with lumped Thevenin sources having voltage sources denoted as V_{T1} and V_{T2} and impedances Z_1 and Z_2 respectively (see Fig. 22 for voltage and current directions). The characteristic impedance is given by

$$Z_0 = \sqrt{\frac{R + j\omega L}{G + j\omega C}} \tag{211}$$

and the system of ordinary differential equations which must be solved for the time-harmonic voltage and current along the line is given by

$$\begin{cases} \dfrac{dV}{dx} + ZI = V^s(x) \\ \dfrac{dI}{dx} + YV = I^s(x) \end{cases}, \quad 0 < x < d. \tag{212}$$

where $V^s(x)$, and $I^s(x)$ are distributed per-unit-length voltage and current sources along the line which model an electromagnetic field coupling to the line. Boundary conditions are imposed such that Kirchhoff's voltage and current laws are satisfied at the terminations, that is

$$\begin{cases} V(0) + Z_1 I(0) = V_{T1} \\ V(d) - Z_2 I(d) = V_{T2} \end{cases}. \tag{213}$$

We can solve this system by using a finite difference method. The line is discretized using N equal intervals of length Δx such that $d = N\Delta x$. The $2N + 1$ discretized voltages and currents are interlaced along the line and defined as

$$\begin{cases} V_{j+1/2} = V((j + 1/2)\Delta x), & j = 0 \ldots N-1 \\ I_j = I(j\Delta x), & j = 0 \ldots N \end{cases}. \tag{214}$$

Using centred differences, the differential equations in (212) become the $2N - 1$ algebraic equations

$$\begin{cases} V_{j+1/2} - V_{j-1/2} + \Delta x Z I_j = \Delta x V_j^s & j = 1 \ldots N-1 \\ I_j - I_{j-1} + \Delta x Y V_{j-1/2} = \Delta x I_{j-1/2}^s & j = 1 \ldots N \end{cases} \tag{215}$$

and at the boundaries we have two equations

$$\begin{cases} V_{1/2} - V_0 + \left(\frac{\Delta x}{2} Z\right) I_0 = \frac{\Delta x}{2} V_0^s \\ V_N - V_{N-1/2} + \left(\frac{\Delta x}{2} Z\right) I_N = \frac{\Delta x}{2} V_N^s \end{cases} \tag{216}$$

Note that we have used $\Delta x/2$ since the discretization at the boundaries is only over half a cell. Now since V_0 and V_N do not exist, we can use the boundary conditions given by (213) and substitute

$$\begin{cases} V_0 = V_{T1} - Z_1 I_0 \\ V_N = V_{T2} + Z_2 I_N \end{cases} \tag{217}$$

into (216) to get

$$\begin{cases} V_{1/2} + \left(Z_1 + \frac{\Delta x}{2} Z\right) I_0 = \frac{\Delta x}{2} V_0^s + V_{T1} \\ -V_{N-1/2} + \left(Z_2 + \frac{\Delta x}{2} Z\right) I_N = \frac{\Delta x}{2} V_N^s - V_{T2} \end{cases} \tag{218}$$

The discretized system can be written in matrix form as

$$\boldsymbol{A}\boldsymbol{x} = \boldsymbol{b} \tag{219}$$

where

$$\boldsymbol{x} = \begin{bmatrix} I_0 \\ V_{1/2} \\ I_1 \\ \cdots \\ \cdots \\ I_{N-1} \\ V_{N-1/2} \\ I_N \end{bmatrix}, \boldsymbol{b} = \Delta x \begin{bmatrix} \frac{V_0^s}{2} + \frac{V_{T1}}{\Delta x} \\ I_{1/2}^s \\ V_1^s \\ \cdots \\ \cdots \\ V_{N-1}^s \\ I_{N-1/2}^s \\ \frac{V_N^s}{2} - \frac{V_{T2}}{\Delta x} \end{bmatrix} \tag{220}$$

$$A = \begin{bmatrix} Z_1 + \frac{\Delta x}{2}Z & 1 & 0 & 0\,0 \ldots & 0 & 0 & 0 & 0 \\ -1 & \Delta x Y & 1 & 0\,0 \ldots & 0 & 0 & 0 & 0 \\ 0 & -1 & \Delta x Z & 1\,0 \ldots & 0 & 0 & 0 & 0 \\ : & : & : & : : : & : & : & : & : \\ 0 & 0 & 0 & 0\,0 \ldots & -1 & \Delta x Z & 1 & 0 \\ & & & & & -1 & \Delta x Y & 1 \\ & & & & & & -1 & Z_2 + \frac{\Delta x}{2}Z \end{bmatrix}. \tag{221}$$

These equations allow us to model the coupling of the external field into the transmission line. The effect of the statistical field shows up only on the right hand side vector $\boldsymbol{b}$. Thus, once the inverse of A is found, that is A^{-1}, the response $\boldsymbol{x}$ to any random field $\boldsymbol{b}$ is obtained by a simple matrix multiplication:

$$\boldsymbol{x} = A^{-1}\boldsymbol{b}. \tag{222}$$

Thus we see that it is very simple to generate Monte Carlo data for this model assuming that we have a method of generating the random fields, $\boldsymbol{b}$, with a prescribed distribution and spatial correlation. This part is taken up in the next section.

6.2 Random field generation

6.2.1 An exponentially correlated Markov chain

In this section we consider the discrete time scheme which arises from the approximation of a continuous time continuous Markov process using Markov chains. Following [32], we represent the random process $x(t)$ as the finite Markov chain y_m with N states:

$$\gamma_1 < \gamma_2 < \ldots < \gamma_N. \tag{223}$$

If the stationary random process $x(t)$ is described by the marginal PDF $p_x(x)$ or its cumulative distribution function (CDF)

$$P_x(x) = \int_{-\infty}^{x} p_x(z)dz \tag{224}$$

then the probability q_i of the i-th state γ_i of the approximating chain can be expressed as

$$q_1 = \int_{-\infty}^{\frac{(\gamma_1+\gamma_2)}{2}} p_x(z)dz = P_x\left(\frac{\gamma_1+\gamma_2}{2}\right), \tag{225}$$

$$q_i = \int_{\frac{(\gamma_{i-1}+\gamma_i)}{2}}^{\frac{(\gamma_i+\gamma_{i+1})}{2}} p_x(z)dz = P_x\left(\frac{\gamma_i+\gamma_{i+1}}{2}\right) - P_x\left(\frac{\gamma_{i-1}+\gamma_i}{2}\right),\ i = 2, \ldots, N-1 \tag{226}$$

$$q_N = \int_{\frac{\gamma_{N-1}+\gamma_N}{2}}^{\infty} p_x(z)dz = 1 - P_x\left(\frac{\gamma_{N-1}+\gamma_N}{2}\right), \tag{227}$$

We denote the transition probability matrix by $\boldsymbol{T} = [T_{k,l}]$ where

$$T_{k,l} = \text{Prob}\{y_m = \gamma_k | y_{m-1} = \gamma_l\},\ k, l = 1, 2, \ldots, N, \tag{228}$$

which is the probability of the event $y_m = \gamma_k$ when $y_{m-1} = \gamma_l$ and fits the conditions

$$T_{k,l} \geq 0,\ \sum_{k=1}^{N} T_{k,l} = 1,\ k = 1, 2, \ldots, N. \tag{229}$$

It is well known that the stationary probabilities q_k are obtained as the eigenvectors of the transition probability matrix $\boldsymbol{T}$ corresponding to the eigenvalue $\lambda = 1$

$$\sum_{i=1}^{N} T_{k,i} q_i = q_k,\ k = 1, 2, \ldots, N. \tag{230}$$

The transition matrix $\boldsymbol{T}$ determines the mathematical properties of the Markov chain [99]. The same matrix defines the power spectrum in the stationary case. However we consider the inverse problem, having defined only the stationary probabilities of the states. For a case where the correlation function is an exponential one the solution was obtained in [32]. We follow this procedure here to obtain the chain approximation with a finite number of states.

To achieve the first goal, we define the following matrix $\boldsymbol{Q}$ in terms of the probabilities of the states

$$\boldsymbol{Q} = \begin{bmatrix} q_1 & q_1 & \cdots & q_1 \\ q_2 & q_2 & \cdots & q_2 \\ \cdots & \cdots & \cdots & \cdots \\ q_N & q_N & \cdots & q_N \end{bmatrix}. \tag{231}$$

It is easy to check that

$$\boldsymbol{Q}^2 = \boldsymbol{Q}, \tag{232}$$

and [32]

$$\det[\boldsymbol{Q} - \lambda \boldsymbol{I}] = (1-\lambda)(-\lambda)^{N-1}. \tag{233}$$

In terms of the matrix $\boldsymbol{Q}$, the transition matrix $\boldsymbol{T}$ can be defined as [32]

$$\boldsymbol{T} = \boldsymbol{Q} + d(\boldsymbol{I} - \boldsymbol{Q}), \tag{234}$$

where $0 \le d < 1$ will define the correlation properties (described below) and $\boldsymbol{I}$ is the unit matrix. At the same time $\boldsymbol{T}$ fits condition (230).

For any integer m we obtain the following expression from (234) and (232)

$$\boldsymbol{T}^m = \boldsymbol{Q} + d^m(\boldsymbol{I} - \boldsymbol{Q}). \tag{235}$$

Since d is a positive number less than 1, we obtain

$$\lim_{m \to \infty} \boldsymbol{T}^m = \boldsymbol{Q}, \tag{236}$$

which means that the Markov chain described by (234) becomes ergodic [99] and has the stationary probability given by q_k.

Next, we consider the correlation function R_m of the Markov chain y_m. In terms of the stationary probability q_k, we obtain the average and the square average as

$$\langle y_m \rangle = \sum_{i=1}^{N} \gamma_k q_k, \tag{237}$$

$$\langle y_m^2 \rangle = \sum_{i=1}^{N} \gamma_k^2 q_k. \tag{238}$$

To calculate the correlation function, we consider the two-dimensional probability which may be obtained from (235) as

$$Q^{(m)}(k, l) = Prob\{y_m = \gamma_k, y_0 = \gamma_l\} = \{q_k + d^m(\delta_{k,l} - q_k)\}q_l, \tag{239}$$

where $m > 0$ and $Q^{(m)}(k, l)$ stands for m steps transitional probability. It is easy to find that (239) fits the consistency relation

$$\sum_{k=1}^{N} Q^{(m)}(k, l) = \sum_{k=1}^{N} Q^{(m)}(l, k) = q_l. \tag{240}$$

The correlation function R_m is an even function of m defined as

$$R_m = R_{-m} = \langle y_m y_0 \rangle - \langle y_m \rangle^2 \tag{241}$$

Substitution of equations (237) to (240) into equation (241) produces

$$R_m = R_{-m} = \langle y_m y_0 \rangle - \langle y_m \rangle^2 = \sum_{k,l=1} \gamma_k \gamma_l Prob\{y_m = \gamma_k, y_0 = \gamma_l\} - \langle y_m \rangle^2 =$$

$$\sum_{k,l=1}^{N} \gamma_k \gamma_l \{q_k + d^m(\delta_{k,l} - q_k)\} q_l - \langle y_m \rangle^2 = \sum_{k,l=1}^{N} \gamma_k \gamma_l q_k q_l + d^m \sum_{k,l=1}^{N} \gamma_k \gamma_l (\delta_{k,l} - q_k) q_l - \langle y_m \rangle^2 = \tag{242}$$

$$\langle \nu_m \rangle^2 + d^{|m|}(\langle \nu_m^2 \rangle - \langle \nu_m \rangle^2) - \langle \nu_m \rangle^2 = d^{|m|}(\langle \nu_m^2 \rangle - \langle \nu_m \rangle^2)$$

which is the exponential function with a correlation length defined as

$$N_{corr} = (-1)/\ln d. \tag{243}$$

The sequence corresponding to the transition matrix $\boldsymbol{T} = [T_{k,l}]$ can be generated by the following recurrent equation [32]:

$$y_m = F(y_{m-1}, \zeta_m), \; m = 0, \pm 1, \pm 2, \ldots, \tag{244}$$

where ζ_m is an independent random number uniformly distributed over the interval [0,1], and $F(y_{m-1}, \zeta_m)$ is a discontinuous function of ζ_m, defined as

$$F(\gamma_l, \zeta) = \begin{cases} \gamma_1 & 0 < \varsigma \le T_{1,l} \\ \gamma_2 & T_{1,l} < \varsigma \le T_{1,l} + T_{2,l} \\ \gamma_3 & T_{1,l} + T_{2,l} < \varsigma \le T_{1,l} + T_{2,l} + T_{3,l} \\ \ldots & \ldots \\ \gamma_N & 1 - T_{N,l} < \varsigma \le 1 \end{cases} . \tag{245}$$

Solving (244) numerically, we obtain a sample of Markov chain with the exponential correlation and given probabilities of the states.

6.2.2 Program description

Two MATLAB programs have been written in order to implement the algorithm described in the previous section: `rnd.m` and `rnd_field.m`. The function `rnd.m` is a direct implementation of equations (231), (234), (244) and (245) and is used to generate a given number of samples, assuming that the probabilities q_i of the states of Markov chain are given and a certain correlation coefficient d is expected. This function is called from `rnd_field.m`.

The function `rnd_field.m` is a function where the required probabilities of states q_i and the correlation coefficient d are effectively calculated. As the output this function produces a normalized, complex valued, electric (or magnetic) field. The average value of the magnitude of this field is

$$\langle |E| \rangle = 1 \frac{V}{m}, \; \langle |H| \rangle = 1 \frac{A}{m} \tag{246}$$

The required intensity can be achieved by scaling these fields by a constant.

Currently, the following distributions are implemented in this program:

- the K-distribution [123] (set *Type* = *'K'*) (for magnitude)

$$p(x) = \frac{2b}{\Gamma(\nu)}\left(\frac{bx}{2}\right)^{\nu} K_{\nu-1}(bx),\ \nu > 0,\ x \geq 0 \tag{247}$$

- the Rayleigh distribution [123] (set *Type* = *'Rayleigh'*) (for magnitude)

$$p(x) = \frac{x}{\sigma^2}\exp\left[-\frac{x^2}{2\sigma^2}\right],\ \sigma > 0,\ x \geq 0 \tag{248}$$

- the Gamma distribution [123] (set *Type* = *'Gamma'*) (for intensity) (the case $\alpha = 0.5$ corresponds to the Porter-Thomas distribution)

$$p(x) = \frac{1}{\beta^{\alpha}\Gamma(\alpha)} x^{\alpha-1} e^{-x/\beta} \tag{249}$$

- the log-normal distribution [123] (set *Type* = *'Log-Normal'*) (for intensity)

$$p(x) = \frac{1}{x\sigma\sqrt{2\pi}}\exp\left[-\frac{(\ln x - \ln m)^2}{2\sigma^2}\right] \tag{250}$$

and

- the Weibull distribution[123] (set *Type* = *'Weibull'*) (for intensity)

$$p(x) = \frac{\alpha}{\beta} x^{\alpha-1} e^{-x^{\alpha}/\beta} \tag{251}$$

Once the average value of the generated field is fixed by (246), only one "shape" parameter (*i.e.* ν for K, α for Gamma and Weibull, σ for log-normal and none for Rayleigh) should be specified in the field *ParA*. The number of states approximating the continuous distribution is specified by the parameter *NBins*.

The phase is assumed to be distributed according to the Tikhonov distribution [99]

$$p(\phi) = \frac{1}{2\pi I_0(D)} e^{D\cos\phi} \tag{252}$$

where I_o is the modified Bessel function [28]. For small values of the parameter D, which should be specified in the field *ParP*, $p(\phi)$ in equation (252) becomes the uniform distribution of phase

$$p(\phi) = \frac{1}{2\pi}. \tag{253}$$

Another limiting case, $D = \infty$, corresponds to a fixed (deterministic) phase, *i.e.* $p(\phi) = \delta(\phi)$. The shape of the distribution for different values of D is shown in Fig. 21.

The corresponding spatial correlation is calculated using the discretization interval Δx (*i.e.* parameter *Dx*) and interval of spatial correlation x_{corr} (*i.e.* parameter *Xcorr*) as

$$x_{corr} = N_{cor}\Delta x. \tag{254}$$

6.3 Numerical Results

The following example is considered. It is assumed that field inside a cavity is distributed according to the Lehman distribution, i.e. according to the K distribution with parameter $\nu = 3$ [123]. The correlation interval for the magnitude is chosen to be $x_{corr} = \lambda/6$ and the phase is assumed to be uniformly distributed on the interval $[0, 2\pi]$. Frequency of the excitation is chosen to be $f = 0.8\ GHz$. This corresponds to the free space wavelength of $\lambda = 37.5\ cm$. We assume that the typical transmission line of the PC mother board has a length of $5\ cm$, which results into the electrical length of 0.133. The transmission line is assumed to have a characteristic impedance of 50Ω and to be terminated by matched impedances. Fig. 21 shows the results of the simulation and the corresponding report can be found in Section 6.3.2. It can easily be seen that the distribution of voltage and current on both terminals greatly deviates from the Gaussian one.

6.3.1 Default Input Parameters

The following parameters are used as default in UWO STEM Ver. 1.0 Tool. All values are referred to variables shown in Fig. 22.

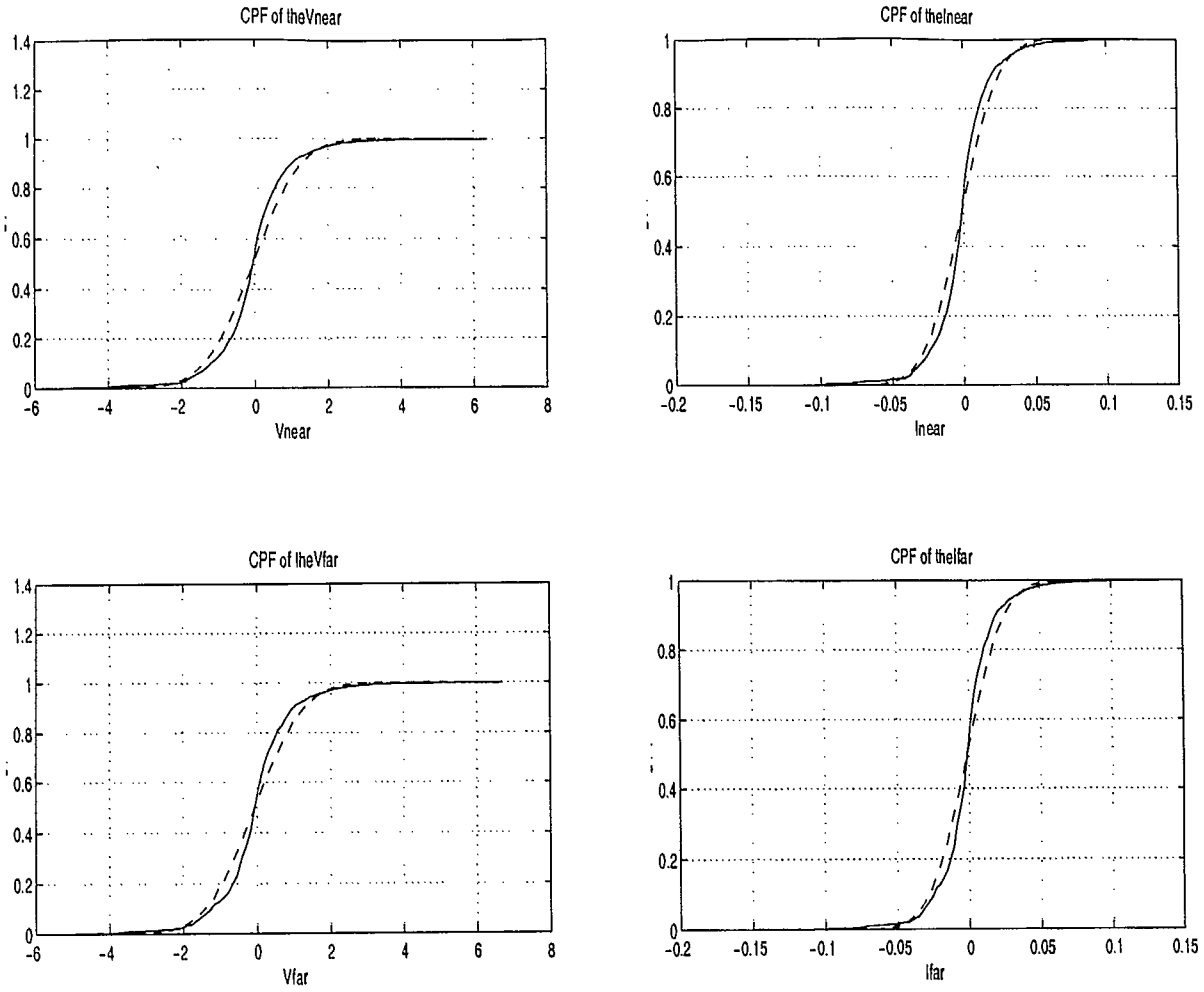

Figure 21. Results of numerical simulation of the random field coupled to a transmission line. The top two pictures refer to the near-field voltage and current, and the lower two pictures refer to far-end voltage and current. Distribution of instantaneous values are considered.

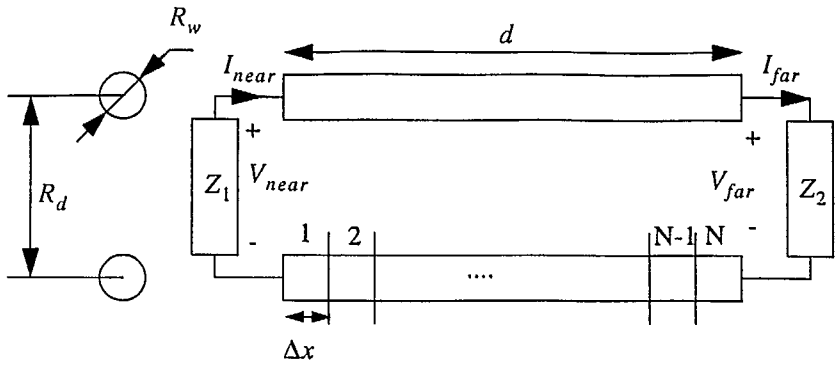

Figure 22. Transmission line geometry

Table 3:

No.	Parameter	Default value	Variable designation	Comments
	Electric Length, L/λ	1	TL.ElectricLength	unitless
	Length, L	1	TL.Length	meters
	Char. Impedance Z_0	50	TL.Z0	Ω
	Near end load Z_{near}	50	TL.Znear	Ω
	Far end load Z_{far}	50	TL.Zfar	Ω
	Near end voltage source V_{near}	0	TL.Vnear	V
	Far end voltage source V_{near}	0	TL.Vfar	V
	Frequency, f	300	Field.Frequency	MHz, calculated through L and L/λ
	Correlation interval X_{corr} for magnitude	1/6	Field.Xcorr	λ
	Correlation interval X_{corr} for phase	1/6	Field.Pcorr	λ
	Distribution of the magnitude	Rayleigh	Field.DistType	
	Parameters of the magnitude distribution	0	Field.pA	Does not matter for the Rayleigh distribution

Table 3:

No.	Parameter	Default value	Variable designation	Comments
	Parameter for the phase distribution, D	0	Field.pPh	Corresponds to uniform phase
	Average value of E field magnitude, $\|E_{m0}\|$	1	Field.Em0	V/m
	Average value of H field magnitude, $\|H_{m0}\|$	1	Field.Hm0	A/m
	Discretization parameter N	50	Numbers.N	Number of points per wavelength
	Number of bins in histo-gram	100	Numbers.Nbins	Shows home many bins will be considered when histogram is built
	Number of trials	1000	Numbers.Ntrials	Number of trials in Monte-Carlo simulation

6.3.2 Example of the generated report

This report is created on 01-Mar-1999 at 12:00:00 AM

by UWO STEM Tool Ver 0.3

TL parameters

Electric length: 0.133

Characteristic impedance: 50.000 + j 0.000

Far end load: 50.000 + j 0.000

Near end load: 50.000 + j 0.000

External field parameters

Frequency, MHz: 800.000

Normalized Em field: 1.000

Normalized Hm field: 0.003

Corr. interval for magnitude: 0.167

Corr. interval for phase: 0.001

Distribution type: K

Parameter pA: 3.000

Parameter D: 0.000

6.4 Conclusions

A prototype of the UWO StEm Tool 1.0, which allows a user to investigate the coupling of random electromagnetic fields to a transmission line, has been developed and described in this chapter. Despite the fact that a very specific configuration has been implemented, this tool allows us to capture quite a few statistical tendencies. Mainly, it is shown that deviations from the Chi-square distribution for the statistics of the intensity of the coupling field lead to similar deviations in the statistics for the instantaneous values of the induced voltages and currents at the ends of the transmission line. This effect disappears when the length of the transmission line approaches several wavelengths. However, this situation is impossible as far as PCB traces are concerned if the dimensions of the cavity itself are of the order of only a few wavelengths. In turn, non-Chi-square distributions of the terminal currents and voltages may lead to heavier tails of the corresponding PDF, thus resulting in more probable overvoltages. The specific effects of these overvoltages should be studied separately and this will depend on the application.

Yet another important feature, easily found by conducting numerical experiments, is that highly resonant behaviour of a cavity leads to a non-uniform phase distribution, and this causes significant deviations from the Chi-square distribution for the statistics of the intensity of the coupling field. We recommend that a detailed investigation of this phenomenon be considered in a future project.

We also confirmed that it is important to consider the spatial correlation properties of the external field. In fact, a completely decorrelated excitation results in an almost Chi-square behaviour of the terminal voltages and currents even for relatively short (less then 0.25λ) transmission lines, while highly correlated non-Chi-square external fields result in highly irregular terminal voltage behaviour, *i.e.* deviations from the Chi-square statistics is significant even for relatively long transmission lines.

As was mentioned above, the StEm Tool implements only the simplest mathematical models of external field coupling to a transmission line. We suggest that more work be done on the validation of the applicability of such models for the case of random excitation. Another direction which should be explored is to extend the capability of the software tool to include the treatment of multiconductor transmission lines. This will require some more research on numerical techniques that allow the generation of non-Gaussian random fields.

VII. Conclusions and Recommendations

7.1 Overview and conclusions

In this preliminary study, we have attempted to review the relevant material on the use of statistical techniques for characterizing electromagnetic interactions in electronic systems. There have been many studies in the past, but no systematic method of applying such techniques exists as of yet. It is safe to say that most studies have been undertaken on simplified systems, such as the single interaction path shown in Figure 23. Here, even though there are many physical ways in which energy can enter the interior volume, the interaction path between exterior volume and interior volume is conceptually a single path. These types of single path systems are what have been mostly studied in the literature.

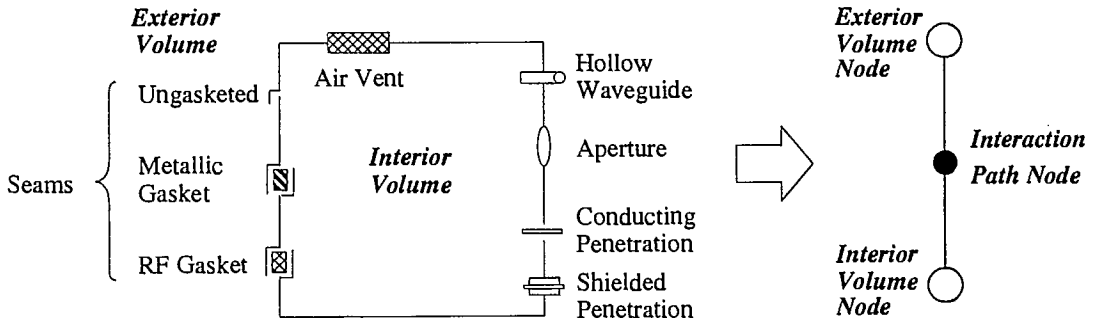

Figure 23. Penetration through an enclosure as a *node-edge-node* link.

One interesting outcome of these studies is that the statistical characterization of the electromagnetic fields inside the interior volume is mostly independent of the method of penetration. The total energy which enters the enclosure is important, but, at least for over-moded cavities, the entry path is unimportant. This fact may change when we consider enclosures which are close to or below the cut-off frequency. We plan to study such enclosures in the next phase of the study.

We have proposed the K distribution as a better way of characterizing the statistics of fields inside an enclosure. This distribution is a two-parameter distribution which will allow us more flexibility in characterizing the fields. The advantages and disadvantages of using this family of distributions were discussed and its relationship to other commonly used distributions such as the Lehman and the Chi-square distributions were described.

A preliminary investigation of two problems which are of great interest in the electromagnetic compatibility community was undertaken. These are: a) the coupling of randomly oriented plane waves into enclosures with an aperture (Chapter V); and b) the coupling of statistically described fields to a single transmission line (Chapter VI). The finite difference time domain technique was used to perform the simulations. Results of the first investigation showed that the K distribution is useful for describing the statistics of the fields inside an enclosure. It was also shown that even a "weak randomization" of the incident field allows one to obtain results close to those predicted by statistical theory. The phase distribution inside an enclosure is shown to be non-uniform and can be modelled as a mixture of Tikhonov distributions.

A computer program was written for performing the calculations of the transmission line problem in which the quasi-TEM approximation was made and the coupling was modelled as distributed voltages and currents along the line. It was shown that deviations of the coupling field statistics from Chi-square lead to similar deviations in the statistics of the induced voltages and currents at the ends of the transmission line but that this effect disappears when the length of the transmission line approaches several wavelengths. A completely decorrelated excitation along the line results in an almost Chi-square behaviour of the terminal voltages and currents even for relatively short transmission lines, whereas for highly correlated non-Chi-square external fields, a highly irregular terminal voltage behaviour is observed.

All these conclusions and observations allow us to assume that a number of meaningful results can be obtained during the next stage of this project. In particular, the effect of different apertures and the "filling" of the box should be investigated in more detail.

7.2 Recommendations for future work

The following is a list of recommended steps which should be followed for future work:

1) The StEm software package should be expanded to contain more features. This would include the ability to describe a cavity in generic terms such as an area, a volume, a number of apertures, and the conductivity of the enclosure walls, *etc.*;
2) More full-wave simulations of complex cavities such as computer boxes with apertures and transmission lines should be conducted in order to obtain a larger set of data on which to validate the statistical methods;
3) The collected data should be analysed in order to identify the important degrees of freedom, and some probabilistic models of interaction between an external field and muticonductor transmissions line should be created. Special attention should be paid to the investigation of the correlation properties of the electromagnetic field components;
4) A further investigation and clarification of the term "complex cavity" should be undertaken. An analysis of the relationship between the statistical distribution parameters and the parameters of arbitrary cavities should be developed further and validated using the simulation data;

5) An investigation of complex cavity behaviour at frequencies close to or below the cut-off frequency should be made. Statistics of the mixture of standing and travelling waves should be conducted.
6) More general structures of MTL networks should be considered. Each MTL should be described by a simplified probabilistic model. Dependence of the induced terminal voltages and currents on the cavity parameters and the transmission line parameters should be investigated.
7) Requirements for the possible experimental validation of all the statistical approaches which are developed should be specified.

Although this list of recommendations is quite lengthy we believe that the time frame of one year of intense research should be enough to cover most, if not all, of these topics. Of course, during the course of these investigations, it is always possible that future results may lead us into a different direction.

VIII. Appendix: Review of Some Basics on Statistics and Stochastic Processes

In this short appendix, some basic statistical definitions, facts, and methods are reviewed. The purpose is to briefly overview the relevant statistical background which is used in this report and to define the notation which is used. The reader is referred to the standard texts on statistics and probability theory for more in-depth accounts of the material.

8.1 Basic definitions

An *experiment* is a set of rules governing an operation which is performed. An *outcome* is a result realized after performing the experiment once. An *event* is a combination of outcomes. An event which is equal to an outcome is also called an *elementary event.* As an example, which is pertinent to the EMC problem, an experiment may be an electromagnetic measurement which is made on a system. Such a measurement may be the value of the electric field inside an enclosure given some rules of making the measurement (*e.g.* probes to use, locations to probe inside the enclosure, description of the environment surrounding the enclosure, *etc.*). The results of a single measurement would be an elementary event while a measurement being one out of a set of outcomes would define an event.

The *probability of an event* is defined as follows. If an event A happens n_A times when an experiment is performed N times, then the probability of the event A is defined as

$$Pr\{A\} \stackrel{\Delta}{=} \lim_{N \to \infty} \left[\frac{n_A}{N} \right] \tag{255}$$

the probability of an event A or event B happening is given as

$$Pr\{A \text{ or } B\} = \lim_{N \to \infty} \left[\frac{n_A + n_B}{N} \right] = Pr\{A\} + Pr\{B\} \tag{256}$$

where it has been assumed that events A and B are *disjoint* (*i.e.* they cannot possibly occur at the same time). All elementary events are by definition disjoint. From a knowledge of the probability of all the elementary events in an experiment, the probability of any event can be determined.

Outcomes, and thus events, may not be numerical entities. For example, the outcome of an election can

be assigned a probability but the outcome itself is not mathematical in nature. A mapping, or function, which assigns a number to each outcome in an experiment is called a *random variable*. A random variable can be discrete, when the mapping is to the integers (a finite or infinite set), or it can be continuous, when the mapping is to the real numbers (a finite or infinite interval). Once a random variable is defined, say X, then a *distribution function*, $F(x)$ or $P(x)$, can be defined as

$$F(x_0) = Pr\{X \leq x_0\} \tag{257}$$

where the set of values, $\{X \leq x_0\}$, defines an event. (Note that the distribution function is sometimes called the *cumulative distribution function*, *CDF* or just *distribution*.) Two important properties of any distribution function are:

$$F(-\infty) = 0 \text{ and } F(\infty) = 1. \tag{258}$$

It is also easy to see that a distribution function is a monotonically increasing function of its argument.

Another important function is the *probability density function*, $p_X(x)$ [1], (or just density function) which is defined as the derivative of the distribution:

$$p_X(x) \stackrel{\Delta}{=} \frac{d}{dx}F(x). \tag{259}$$

Therefore, the inverse operation holds:

$$F(x_0) = \int_{-\infty}^{x_0} p_X(x)dx. \tag{260}$$

We also have the important property, that

$$Pr\{x_1 \leq X \leq x_2\} = \int_{x_1}^{x_2} p_X(x)dx. \tag{261}$$

It is easy to see that the probability density function can never be negative, and the integral of the PDF from $-\infty$ to ∞ must be unity.

The *characteristic function*, $\Theta_X(j\omega)$, corresponding to a probability density function, say $p_X(x)$, of a random variable X is just the conjugate of the Fourier transform of the PDF, that is

$$\Theta_X(j\omega) = \int_{-\infty}^{\infty} p_X(x)\exp(j\omega x)dx \tag{262}$$

where we are using a negative exponential in the definition of the Fourier transform, as is usual.

If we are interested in the probability of two events happening, we can define two random variables, X

1. Here the subscript X indicates which random variable is considered while x is the independent continuous variable.

and Y say, and ask what is the probability that X takes on the values $x_1 < X \leq x_2$ (an event) while Y takes on the values $y_1 < Y \leq y_2$ (another event). We would then require a two dimensional or *joint probability density function*, $p_{XY}(x, y)$, such that

$$Pr\{x_1 < X \leq x_2 \text{ and } y_1 < Y \leq y_2\} = \int_{y_1}^{y_2}\int_{x_1}^{x_2} p_{XY}(x, y)dxdy \tag{263}$$

The effect of one random variable on another is measured by the *conditional probability*. The probability of an event A given that event B has occurred is defined by the conditional probability $Pr\{A/B\}$, and can be calculated as

$$Pr\{A/B\} \stackrel{\Delta}{=} \frac{Pr\{A \text{ and } B\}}{Pr\{B\}}. \tag{264}$$

Two events are *independent* if

$$Pr\{A/B\} = Pr\{A\}. \tag{265}$$

Thus, by the definition of conditional probability, if two events are independent of each other, then the probability that they both occur is just the product of the two probabilities for the two events, that is

$$Pr\{A \text{ and } B\} = Pr\{A\}Pr\{B\}. \tag{266}$$

In terms of the probability density functions, independence of two random variables implies that

$$p_{XY}(x, y) = p_X(x)p_Y(y), \tag{267}$$

that is, the joint probability density function is the product of the individual densities.

8.2 The Gaussian, uniform, Rayleigh, and Chi-square density functions

The most common PDF is the *Gaussian density function* which is defined as

$$p_X(x) = \frac{1}{\sqrt{2\pi}\sigma}\exp\left[-\frac{(x-m)^2}{2\sigma^2}\right] \tag{268}$$

where the given parameters, m and σ^2, are known as the *average* or *mean* and *variance* of the PDF. A sketch of this PDF is shown in Fig. 24. The average value m determines the centre of the so-called bell-shaped curve and the variance σ^2 determines the spread (*i.e.* a larger variance means a larger spread).

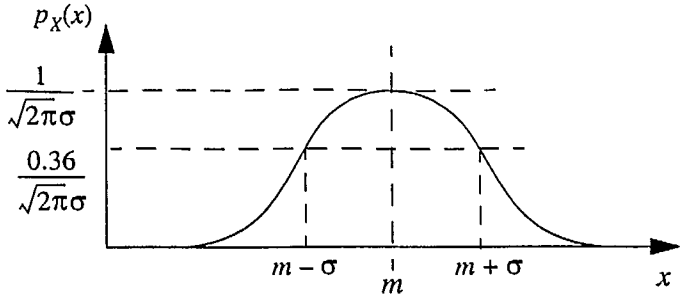

Figure 24. Sketch of the Gaussian density function

The integral of the Gaussian function is given by the so-called *Error function* defined as

$$\text{erf}\,(x) = \frac{1}{\sqrt{2\pi}} \int_{-\infty}^{x} e^{-y^2/2} dy\,. \tag{269}$$

Another commonly occurring density function is the *uniform density function* which is defined as

$$p_X(x) = \begin{cases} 0 & x < 0 \\ 1/x_0 & 0 \le x \le x_0 \\ 0 & x > x_0 \end{cases} \tag{270}$$

and is sketched in Fig. 25. (Note: x_0 is a given parameter.)

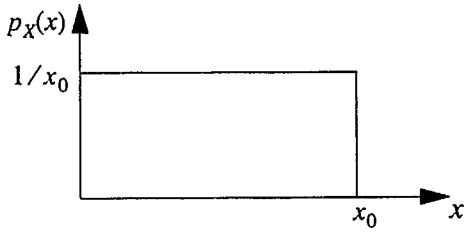

Figure 25. Sketch of the uniform density function

Given two random variables, X and Y, which are Gaussian distributed, the square-root of the sum of the squares of the two random variables (assuming that the two random variables are independent of each other, have zero mean and an equal variance, as defined below) will have a *Rayleigh density function* which is defined as

$$p_R(r) = \begin{cases} \frac{r}{\sigma^2} \exp\left[\frac{-r^2}{2\sigma^2}\right] & r > 0 \\ 0 & r < 0 \end{cases} \tag{271}$$

where

$$r = \sqrt{x^2 + y^2}\,. \tag{272}$$

A sketch of the Rayleigh distribution is shown in Fig. 26.

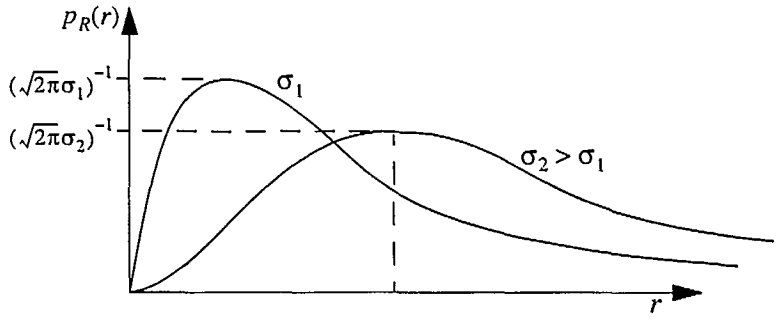

Figure 26. Sketch of the Rayleigh density function

If we were interested in r^2 instead of r we would find that r^2 was *Chi-square* distributed with 2 degrees of freedom. If we take the sum of the squares of n variables, that is

$$z = x_1^2 + x_2^2 + x_3^2 + \ldots + x_n^2 \tag{273}$$

then we get a Chi-square distribution with n degrees of freedom. The mathematical form of this probability density function is given by

$$p_Z(z) = \begin{cases} \dfrac{z^{n/2-1}}{2^{n/2}(n/2-1)!}\exp\left(\dfrac{-z}{2}\right) & z > 0 \\ 0 & z < 0 \end{cases} \tag{274}$$

where the symbol "!" denotes factorial.

8.3 Functions of a random variable

Consider a random variable, X, having a PDF of $p_X(x)$. Now consider another random variable, Y, which is a deterministic function of X. This can be denoted as $y = g(x)$ and the event $\{x_1 < X \le x_2\}$ corresponds to the event $\{y_1 < Y \le y_2\}$ where $y_1 = g(x_1)$ and $y_2 = g(x_2)$ and it is assumed that $y_1 < y_2$ if $x_1 < x_2$. The events are identical and therefore share the same probability, that is

$$Pr\{x_1 < X \le x_2\} = Pr\{y_1 < Y \le y_2\} \tag{275}$$

and

$$\int_{x_1}^{x_2} p_X(x)dx = \int_{y_1}^{y_2} p_Y(y)dy \tag{276}$$

from which, letting $x_2 \to x_1$, we get

$$p_X(x_1)dx = p_Y(y_1)dy \Rightarrow p_Y(y_1) = \frac{p_X(x_1)}{dy/dx}. \tag{277}$$

If we had $y_1 > y_2$ we would then get

$$p_Y(y_1) = -\frac{p_X(x_1)}{dy/dx}. \tag{278}$$

Thus in general, we have

$$p_Y(y_1) = \frac{p_X(x_1)}{|dy/dx|} \text{ and } p_Y(y) = \frac{p_X(g^{-1}(y))}{|dy/dx|}. \tag{279}$$

Care must be taken when the function $g(x)$ is not monotone since then more than one interval in x will correspond to a single interval in y. (Consider $g(x) = x^2$ for instance where the interval $0 < y \leq 1$ corresponds to the two intervals $0 < x \leq 1$ or $-1 > x \geq 0$.)

8.3.1 The sum of two random variables

Consider two statistically independent random variables, X and Y, and take the random variable Z to be the sum of the two. That is, $z = x + y$. The probability distribution is given by the double integral

$$F_Z(z_0) = \int_{-\infty}^{\infty}\int_{-\infty}^{z_0 - y} p_{XY}(x, y)dxdy = \int_{-\infty}^{\infty}\int_{-\infty}^{z_0 - y} p_X(x)p_Y(y)dxdy \tag{280}$$

and therefore the PDF is given by

$$p_Z(z_0) = \frac{\partial}{\partial z_0}F_Z(z_0) = \int_{-\infty}^{\infty} p_Y(y)p_X(z_0 - y)dy = p_Y(z) * p_X(z) \tag{281}$$

where $f(z) * g(z)$ represents convolution between the functions $f(z)$ and $g(z)$. That is, the probability density function of the sum of two independent random variables is the convolution of the two individual PDF's. This implies that in terms of the characteristic functions, $\Theta_X(j\omega)$ and $\Theta_Y(j\omega)$, we have

$$\Theta_Z(j\omega) = \Theta_X(j\omega)\Theta_Y(j\omega). \tag{282}$$

8.3.2 Expected values: mean, moments, and variance

The probability of a random variable X being in the interval $\{k\Delta x - \Delta x/2 < X \leq k\Delta x + \Delta x/2\}$ is given by

$$\int_{k\Delta x - \Delta x/2}^{k\Delta x + \Delta x/2} p_X(x)dx \tag{283}$$

which for $\Delta x \to 0$ can be written as $p_X(k\Delta x)\Delta x$. The average value of the random variable can be written as

$$\sum_{k=-\infty}^{\infty} k\Delta x\{p_X(k\Delta x)\Delta x\} \cong X_{avg} \tag{284}$$

which as $\Delta x \to 0$ becomes the integral

$$X_{avg} = m_x = \int_{-\infty}^{\infty} x\, p_X(x)dx. \tag{285}$$

The average value is also called the *mean* or *expected value* and is given the symbol m_x as above. This notation refers to the fact that the mean is the *first moment* of the PDF (or the moment with respect to x).

We can, in general take the moment with respect to any function of x, that is we can form the integral

$$m_{g(x)} = \int_{-\infty}^{\infty} g(x)\, p_X(x)dx \tag{286}$$

which, if we have a random variable Y which is a function of X, $y = g(x)$ say, then the above integral becomes

$$m_{g(x)} = \int_{-\infty}^{\infty} g(x)\, p_X(x)dx = \int_{-\infty}^{\infty} y p_X(g^{-1}(y))\frac{dy}{|dy/dx|} = \int_{-\infty}^{\infty} y\, p_Y(y)dy = Y_{avg} = [g(x)]_{avg}. \tag{287}$$

Some other notations which are used are

$$[g(x)]_{avg} = \overline{g(x)} = E\{g(x)\} \tag{288}$$

where the latter means the "expected value" of $g(x)$. The expected value of $g(x) = x^2$ is called the *second moment* and is explicitly defined as

$$m_{x^2} = \int_{-\infty}^{\infty} x^2 p_X(x)dx. \tag{289}$$

For a Gaussian distributed random variable having mean m and variance σ, that is

$$p_X(x) = \frac{1}{\sqrt{2\pi}\sigma}\exp\left[-\frac{(x-m)^2}{2\sigma^2}\right] \tag{290}$$

it can be shown that

$$E\{x\} = m_x = m, \tag{291}$$

$$E\{(x-m)^2\} = \sigma^2. \tag{292}$$

In fact, $E\{(x-m_x)^2\}$ is defined as the *variance* of any random variable. The positive square root of the variance is called the *standard deviation* (*i.e.* σ in our notation). A useful relationship between the variance and the second moment is given by

$$\sigma_x^2 = E\{x^2\} - (E\{x\})^2. \tag{293}$$

8.4 Review of stochastic processes

A *stochastic process* is an ensemble of random functions of either a discrete or continuous variable, like time, along with the associated statistical properties. If $x(t)$ represents a stochastic process then for every specific value of t, say $t = t_0$, $x_0 = x(t_0)$ is a random variable which can be described by a one dimensional probability density function $p(x_0)$ (where we've dropped the subscript for notational convenience). The random variables associated with N specific values of t, say $t = \{t_1, t_2, \ldots, t_N\}$ can be completely described by the N-dimensional PDF $p(x_1, x_2, \ldots, x_N)$. In order to describe the complete stochastic process we would require an infinite dimensional PDF. Since this is impossible, it is common to resort to a description of the stochastic process through its moments, that is

$$m(t) \stackrel{\Delta}{=} E\{x(t)\} = \int_{-\infty}^{\infty} x(t)\, p_X(x(t))\, dx \tag{294}$$

the first moment, is the time-varying mean of the ensemble. The second moments are given by

$$R_{XX}(t_1, t_2) \stackrel{\Delta}{=} E\{x(t_1)x(t_2)\} = \int_{-\infty}^{\infty}\int_{-\infty}^{\infty} x_1 x_2 p(x_1, x_2) dx_1 dx_2 \tag{295}$$

for any t_1 and t_2 where $x_1 = x(t_1)$ and $x_2 = x(t_2)$. This is referred to as the correlation between the two random variables.

If a stochastic process is such that the overall statistics are independent of the time reference we call it a stationary *process*. Thus for a stationary process, $x(t)$, the time translated process, $x(t-T)$, will have the same statistics for any value of T. Therefore the mean will be independent of t and the correlation will depend only of the distance separating t_1 and t_2. That is

$$R_{xx}(t_1, t_2) = R_{xx}(t_2 - t_1) = R_{xx}(\tau) \tag{296}$$

where $\tau = t_2 - t_1$. The function $R_{xx}(\tau)$ is called the *autocorrelation* of the stationary process, $x(t)$. For τ sufficiently larger than the correlation interval τ_{corr}, such that $x(t_1)$ and $x(t_2)$ are independent random variables, the autocorrelation simplifies to the square of the mean, that is

$$R_{xx}(t_2 - t_1) = E\{x(t_1)x(t_2)\} = E\{x(t_1)\}E\{x(t_2)\} = m^2. \tag{297}$$

We say that the process is uncorrelated for values of τ greater than τ_{corr}.

A stochastic process is called *ergodic* if any single sample function of the process contains all the information about the statistics of the process. This allows one to find the mean by measuring only one function in the process and averaging, that is

$$m_x = E\{x(t)\} = \lim_{T\to\infty} \frac{1}{T}\int_{-T/2}^{T/2} x_i(t) dt \tag{298}$$

where $x_i(t)$ denotes a particular sample function. An ergodic process must be stationary since the mean does not vary as a function of time but it is not true to say that all stationary processes are ergodic since our stochastic process may contain a sample function which is exceptional to the rest and whose statistics measured on the t axis are different than the ensemble statistics. (The ensemble statistics in this latter situation may still be independent of t, *i.e.* stationary.) For an ergodic process the autocorrelation is found from any sample function by

$$R_{xx}(\tau) = E\{x(t)x(t+\tau)\} = \lim_{T\to\infty}\frac{1}{T}\int_{-T/2}^{T/2} x_i(t)x_i(t+\tau)dt. \tag{299}$$

Note that in (298) and (299), under the assumption of ergodicity, the mean and autocorrelation can be found without knowledge of the probability density functions. This is the great advantage in analysing ergodic stochastic processes and this assumption is made whenever feasible.

IX. Additional Comments and Clarifications

9.1 Comments on Chapter III

9.1.1 Complex Q

It appears in the text that a correction factor Q in the Morse's approximation (79) is a complex quantity if ξ_w is a complex number

$$Q = \frac{\beta d}{4\xi_w}\frac{\beta^2}{\gamma_{0n}^2} = \frac{\beta d}{4|\xi_w|}\frac{\beta^2}{\gamma_{0n}^2}e^{-j\theta_\xi}. \tag{300}$$

However, for any real normalized impedance ξ_w, this value can be interpreted as a conventional quality factor defined in a way similar to (97)

$$\frac{1}{Q} = \frac{P_r}{\omega U} \tag{301}$$

where $U = \varepsilon_0|E_{z0}|^2 ab$ is the stored energy in the cavity and P_r is the active loss in the walls. We suggest that the "complex" Q_z can be defined as follows:

$$\frac{1}{Q_z} = \frac{P_r + jX_w}{\omega U + X_w} \approx \frac{P_r + jX_w}{\omega U} = \frac{1}{Q} + j\frac{X_w}{\omega U} = \frac{1}{Q} + j\frac{1}{Q_w} \tag{302}$$

Here, X_w represents the reactive power stored in the walls. Thus, the real part of the complex $1/Q_z$ is just the inverse of the conventional Q while its imaginary part can be considered as a ratio of the reactive power stored in the walls with respect to the reactive power stored in the cavity.

9.1.2 How small ξ_w should be?

Our approximation produces better results when the correction factor is smaller, *i.e.*

$$Q = \frac{\beta d}{4\xi_w}\frac{\beta^2}{\gamma_{0n}^2} = \frac{\beta d}{4|\xi_w|}\frac{\beta^2}{\gamma_{0n}^2}e^{-j\theta_\xi} \to \infty \tag{303}$$

However, this expression approaches infinity at the rate

$$r = \frac{d}{|\xi_w|} \tag{304}$$

assuming that all other parameters are fixed. This explains why our approximation produces better results for lager cavities.

X. References

10.1 Electromagnetic compatibility, electromagnetic topology, and bounds

[1] C.E. Baum, "On the Use of Electromagnetic Topology for the Decomposition of Scattering Matrices for Complex Physical Structures," *Interaction Note 454*, July 1985.

[2] F.M. Tesche, "Topological Concepts for Internal EMP Interaction," *IEEE Transactions on Antennas and Propagation*, Vol. , No. , Jan. 1978, pp. 60-64.

[3] A.K. Agrawal and C.E. Baum, "Bounding of Signal Levels of Terminations of a Multiconductor Transmission-line Network," *Interaction Note 419*, April 1983.

[4] F.C. Yang and C.E. Baum, "Use of Matrix Norms of Interaction Supermatrix Blocks for Specifying Electromagnetic Performance of Subshields," *Interaction Note 427*, April 1983.

[5] C.E. Baum, "Black Box Bounds," *Interaction Note 429*, May 1983, and *Proceedings of the EMC Symposium, Zurich*, March 1985, pp. 381-386.

[6] C.E. Baum, "Bounds on norms of scattering matrices," *Interaction Note 432*, June 1983.

[7] C.E. Baum, "Some bounds concerning the response of linear systems with a nonlinear element," *Interaction Note 438*, June 1984.

[8] J. LoVetri, and G.I. Costache, "An Electromagnetic Interaction Modelling Advisor," *IEEE Transactions on Electromagnetic Compatibility*, Vol. 33, No. 3, Aug. 1991, pp 241-251.

[9] J. LoVetri, W.H. Henneker, "Fuzzy Logic Implementation of an Electromagnetic Interactions Modelling Tool," *1992 IEEE Int. Symp. on EMC Symposium Record*, Anaheim, California, August 17-21, pp. 127-130.

[10] S.L. Primak, J. LoVetri, "Modal Estimates to Describe the Topological Attributes of Multidimensional Systems," *1994 IEEE International Symposium on Electromagnetic Compatibility*, Chicago, Aug. 22-26, 1994, pp. 89-94.

[11] Lapohos, T., and LoVetri, J., *Coupling of Complex Electromagnetic Waves into Uniform Multiconductor Transmission Line Networks*, Final Report under CRC contract U6800-7-1522, February, 1998.

[12] T. Lapohos, J. LoVetri, J. Seregelyi, and N. Simons "Experimental validation of numerical models for packaged MTL networks in non-plane wave external fields," *1998 IEEE International Symposium on Electromagnetic Compatibility*, Denver, Colorado, August 23-28, 1998.

[13] C.L. Gardner and A. Louie, *Use of Energy Bounds to Estimate Fields and Coupling Inside a Cavity with Apertures*, Defence Research Establishment Ottawa (DREO), Ottawa, Ontario, Report #1261, March 1995, 41 pages.

[14] C.L. Gardner and A. Louie, "Bounds on Aperture Coupling from Radar and Other EM Pulses", *IEEE Transaction on EMC*, vol. 37, no. 4, 1995; pp. 543-547.

[15] C.L. Gardner and P.A. Hrubik, "An Experimental and Analytical Study of the Use of Bounds to Estimate the Coupling to a Monopole Inside a Cavity with an Aperture", *IEEE Transactions on EMC*, Sept. 1997.

[16] Kelvin S.H. Lee and Fang-Chou Yang, "Trends and Bounds in RF Coupling to a Wire Inside a Slotted Cavity", *IEEE Transactions on EMC*, vol. 34, no. 3, pp. 154-161, 1992.

[17] L.K. Warne and K.C. Chen, "A Bound on EMP Coupling", *IEEE Transactions on EMC*, vol. 32, pp. 217, 1990.

[18] L.K. Warne and K.C. Chen, "A Bound on Aperture Coupling from Realistic EMP", *IEEE Transactions on EMC*, vol. 36, pp. 149, 1994.

[19] Mats G. Backstom and Jorgen Loren, "Microwave Coupling into a Slotted Cavity", *Proceedings of Joint 3rd International Conference on Electromagnetics in Aerospace Applications and 7th European Electromagnetic Structures Conference*, Politecnico di Torino, Italy, Sept-14-17, 1993.

[20] J. LoVetri, A.T.M. Wilbers, A.P. Zwamborn, "Microwave Interaction with a Personal Computer: Experiment and Modelling," presented at *Zurich EMC'99*.

10.2 Books on probability theory, stochastic processes, EM theory and integration

[21] P.M. Morse and K.U. Ingard, *Theoretical Acoustics*, New York:McGraw Hill, 1968.

[22] P.M. Morse and H. Feshback, *Methods of Theoretical Physics*, Vol. I and II, New York:McGraw Hill, 19.****

[23] C. Balanis, *Advanced Engineering Electromagnetics*, New York: John Wiley, 1989.

[24] A. Papoulis, *Probability, Random Variables, and Stochastic Processes*, McGraw-Hill, New York, 1984.

[25] R.E. Walpole and R.H. Myers, *Probability and Statistics for Engineers and Scientists*, 2nd edition, MacMillan Publishing Co., Inc, New York, 1978.

[26] R.N. McDonough and A.D. Whalen, *Detection of Signals in Noise*, 2nd Edition, Academic Press, Inc., San Diego, California, 1995.

[27] I.S. Gradshteyn, I.M. Ryzhik, *Table of Integrals, Series, and Products*, New York: Academic Press, 1980.

[28] M. Abramowitz, and I. Stegun, *Handbook of Mathematical Functions*, New York: Dover, 1970.

[29] A. Zayezdny, D. Tabak, and D. Wulich, *Engineering Applications of Stochastic Processes*, New York: John Wiley and Sons, 1989.

[30] V.I. Tikhonov, *Statisticheskaya Radiotekhnika (Statistical Radio Communication)*, Moscow: Radio i Svyaz, 1966, (In Russian).

[31] V.I. Tikhonov, V.N. Harisov, *Statisticheskii Analiz i Sintez Radiotechnicheskih Ustroistv i Sistem* (StatisticalAnalysis and Synthsis of Radiocommunication Systems), Moscow: Radio i Svyaz, 1991.

[32] S.L. Primak, *Modelling, Synthesis and Numerical Simulation of non-Gaussian Random Processes with Application to Communications*, Ph.D. Thesis, Beer-Sheva, 1997, Israel.

10.3 Statistical approach to EM coupling

[33] T.H. Lehman, "A Statistical Theory of Electromagnetic Fields in Complex Cavities", *Interaction Note 494*, May, 1993.

[34] R. Holland, and R. St. John, "Statistical Coupling of EM fields to Cables in an Overmode Cavity," *Proc. ACES*, March, 1996, pp. 877-887.

[35] R. Holland, and R. St. John, "Statistical Description of Cable Current Response Inside a Leaky Enclosure," *Proc. ACES*, March, 1997.

[36] R. Holland, and R. St. John, "Statistical Response of EM-Driven Cables Inside an Overmoded Enclosure," Accepted for *IEEE Transactions on EMC.*

[37] R. St. John, "Approximate Field Component Statistics of the Lehman, Overmoded Cavity Distribution," *Internet.*

[38] R. Holland, and R. St. John, "Statistical Response of Enclosed Systems to HPM Environment," *Proc. ACE*, March, 1994, pp. 554-568.

[39] R. Holland, and R. St. John, *Statistical Electromagnetics*, Philadelphia: Taylor and Francis Scientific Publishers, in press.

[40] T.H. Lehman, G.J. Freyer, M.O. Hatfield, J.M. Ladbury, and G.H. Koepke, "Verification of Fields Applied to an EUT in a Reverberation Chamber Using Numerical Modeling," *Proceedings of IEEE EMC Symposium*, Denver, Colorado, August, 1998, pp. 28-33.

[41] T.H. Lehman, G.J. Freyer, M.O. Hatfield, J.M. Ladbury, and G.H. Koepke, "Verification of Fields Applied to an EUT in a Reverberation Chamber Using Statistical Theory," *Proceedings of IEEE EMC Symposium*, Denver, Colorado, August, 1998, pp. 34-38.

[42] T.H. Lehman, and G.J. Freyer, "Characterization of the Maximum Test Level in a Reverberation Chamber," *Proceedings of IEEE EMC Symposium*, Austin, Texas, August, 1997, pp. 44-47.

[43] D. Hill, M.L. Crawford, M. Kanda, and D.I. Wu, "Aperture Coupling to a Coaxial Air Line: Theory and Experiment," *IEEE Transactions on EMC*, Vol. 35, No. 1, February, 1993, pp. 69-74.

[44] D.A. Hill, "Electronic Mode Stirring for Reverberation Chambers," *IEEE Transactions on EMC*, Vol. 36, No. 4, November, 1994, pp. 294-299.

[45] D.A. Hill, M.T. Ma. A.R. Ondreijka, B. Riddle, M.L. Crawford, and R.T. Johnk, "Aperture Excitation of Electrically Large, Lossy Cavities," *IEEE Transactions on EMC*, Vol. 36, No. 4, November, 1994, pp. 169-177.

[46] D.A. Hill, "Spatial Correlation Function for Fields in a Reverberation Chamber," *IEEE Transactions on EMC*, Vol. 37, No. 1, February, 1995, p.138.

[47] J.G. Kostas, and B. Boverie, "Statistical Model for a Mode-Stirred Chamber," *IEEE Transactions on EMC*, Vol. 33, No. 4, November, 1991, pp.366-370.

[48] D.A. Hill, "A Reflection Coefficient Derivation for the Q of a Reverberation Chamber," *IEEE Transactions on EMC*, Vol. 38, No. 4, November, 1996, pp. 591-592.

[49] J.S. Daba, and M.R. Bell, "Statistics of Scattering Cross-Section of a Small Number of Random Scatterers," *IEEE Transactions on Antennas and Propagation*, Vol. 43, No. 8, August, 1995, pp. 773-783.

[50] J.-G. Yook, V. Chandramouli, L.P.B. Katehi, K.A. Sakallah, T.R. Arabi, and T.A. Schreyer, "Computation of Switching Noise in Printed Circuit Boards," *IEEE Transactions on Components, Packaging, and Manufacturing Technology*, Part A, Vol. 20, No. 1, March, 1997, pp. 64-74.

[51] S. Shiran, B. Reiser, and H. Cory, "A Probabilistic Model for the Evaluation of Coupling Between Transmission Lines," *IEEE Transactions on Electromagnetic Compatibility*, Vol. 35, No. 3, August, 1993, pp. 387-392.

[52] S.H. Lin, "Statistical Bahavior of Multipair Crosstalk", *The Bell System Technical Journa*l, Vol. 59, No. 6, July-August, 1980, pp. 955-974.

[53] T. Mikazuki, and N. Matsui, "Statistical Design Techniques for High-Speed Circuit Board with Correlated Structure Distributions," *IEEE Transactions on Components, Hybridsg, and Manufacturing Technology*, Part A, Vol. 14, No. 31, September, 19917, pp.512-517.

[54] C. Chrysanthou, "Statistical Models for Differential-Mode Conversion of Common-Mode Impulse Voltage Measured on Telecommunication Pairs," *IEEE Transactions on Electromagnetic Compatibility*, Vol. 38, No. 3, August, 1996, pp. 489-495.

[55] J.L. Pinto de Sa, " The Stochastic Modeling of Fault Induced Transients," *IEEE Transactions on Power Delivery*, Vol. 7, No. 3, July, 1992, pp. 1156-1166.

[56] J.F. Hall, and A.K. Deb, " Prediction of Overhead Transmission Line Ampacity by Stochastic and Deterministic Models," *IEEE Transactions on Power Delivery*, Vol. 3, No.2, April, 1988, pp. 789-800.

[57] S. Koike, "High-Speed Signal Transmission at the Front of a Bookshelf Packaging System," *IEEE Transactions on Components, Packaging, and Manufacturing Technology*, Part A, Vol. 20, No. 4, November, 1997, pp. 353-359.

[58] R.H. Price, H.T. Davis, and E.P. Wenaas, "Determination of the Statistical Distribution of Electromagnetic-Field Amplitudes in Complex Cavities," *Physical Review E*, Vol. 48, No. 6, 1993, pp. 4716-4729.

[59] N. Ben-Yosef, B. Rahat, and G. Feigin, "Simulation of IR images of Natural Backgrounds," *Applied Optics*, Vol. 22, No. 1, January, 1983, pp. 190-193.

[60] P. Corona, G. Latmiral, E. Paolini, and L. Piccioli, "Use of a Reverberating Enclosure for Measurements of Radiated Power in the Microwave Range," *IEEE Transactions on EMC*, Vol. 18, No. 2, February, 1976, pp.54-59.

[61] L. Capetta, M. Feo, V. Fiumara, V. Pierro, and I.M. Pinto, "Electromagnetic Chaos in Mode-Stirred Reverberation Enclosure," *IEEE Transactions on EMC*, Vol. 40, No. 3, August, 1998, pp.185-192.

[62] P. Jennings, and C.-M. Ting, "System EMC Assessment Using Transmission Line Theory," *Proceedings of IEEE EMC Symposium*, Denver, Colorado, August, 1998, pp. 596-601.

[63] V.Ya. Kontorovich, and R. Linares, "EMC Analysis of Communication Systems Under Influence of Multipoint Interference," *Proceedings of IEEE EMC Symposium*, Denver, Colorado, August, 1998, pp. 842-846.

[64] A.K. Mitra, and T.F. Trost, "Power Transfer Chracteristics of a Microwave Reverberation Chamber," *IEEE Transactions on EMC*, Vol. 38, No. 2, May, 1996, pp. 197-200.

[65] J.M. Ladbury, G.H. Koepke, and D.G. Camell, "Improvements in the CW Evaluation of Mode-Stirred Chambers," *Proceedings of IEEE EMC Symposium*, Austin, Texas, August, 1997, pp. 48-53.

[66] A.K. Mitra, and T.F. Trost, "Statistical Simulations and Measurements Inside a Microwave Reverberation Chamber," *Proceedings of IEEE EMC Symposium*, Austin, Texas, August, 1997, pp. 48-53.

[67] C.L. Holloway, P.McKenna, and D.A. Steffen, "Finite-Difference Time-Domain Modelling for Field Prediction Inside Rooms," *Proceedings of IEEE EMC Symposium*, Austin, Texas,. August, 1997, pp. 60-65.

[68] M.O. Hatfield, G.J. Freyer, and M. Slocum, "Reverberation Characteristics of a Large Welded Steel Shielded Enclosure," *Proceedings of IEEE EMC Symposium*, Austin, Texas, August, 1997, pp. 38-43.

[69] B.H. Liu, D.C. Chang, and M.T. Ma, "Eigenmodes and the Composite Quality Factor of a Reverberation Chamber," *NBS Technichal Notes*, No. 1066, August, 1983.

[70] J.M. Dunn, "Local, High-Frequency Analysis of the Fields in a Mode-Stirred Chamber," *IEEE Transactions on EMC*, Vol. 32, No. 2, February, 1990, pp. 53-58.

[71] M. Petirsch, I. Sotriffer, A. Schwab, "Mode-Stirred Chamber as Test Facility for Electrmognatic Susceptibility measurements," *Proceedings of Zurich EMC Symposium*, Zurich, March, 1999, pp. 679-684.

[72] A.P. Duffy, A.J.M. Williams, "Optimizing Mode Stirred Chamber," *Proceedings of Zurich EMC Symposium*, Zurich, March, 1999, pp. 685-688.

[73] P. Corona, G. Ferrara, M. Migliaccio, "A Stochastic Approach for Determining the Reverberating Chamber Quality Factor," *Proceedings of Zurich EMC Symposium*, Zurich, March, 1999, pp. 689-692.

[74] S. Salio, F. Canavero, J. Lefebvre, W. Tabbara, "Statistical Description of Signal Propagation on Random Bundles of Wires," *Proceedings of Zurich EMC Symposium*, Zurich, March, 1999, pp. 499-504.

[75] B. Audone, and A. Lamprati, "The Use of Statistical Signal Processing in EMC," *Proceedings of Zurich EMC Symposium*, Zurich, March, 1999, pp. 511-514.

10.4 Other related publications

[76] M. Rangaswamy, D. Weiner, and A. Ozturk, "Computer generation of Correlated Non-Gaussian Radar Clutter," *IEEE Transactions on Aerospace and Electronic Systems*, Vol. 31, No. 1, January, 1995, pp. 106-116.

[77] C.T. Tai, "On the Definition of Effective Aperture of Antennas," *IEEE Transactions on Antennas and Propagation*, Vol. 9, No. 2, February, 1961, pp. 224-225.

[78] D.A. Hill, and M.H. Francis, "Out-of-Band Response of Antenna Arrays," *IEEE Transactions on EMC*, Vol. 29, pp. 282-288.

[79] H.A. Bethe, "Theory of Diffraction by Small Holes," *Phys. Review*, Vol. 66, pp. 163-182, 1944.

[80] C.M. Butler, Y. Rahmat-Samii, and R. Mittra, "Electromagnetic Penetration through Apertures in Conducting Surfaces," *IEEE Transactions on Antennas and Propagation*, Vol. 26, No. , pp. 82-93, 1978.

[81] R. Pnini, and B. Shapiro, "Intensity Fluctuations in Closed and Open Systems," *Physical Review E*, Vol. 54, August, 1996, pp. R1032-R1035.

[82] B. Shapiro, "Large Intensity Fluctuations for Wave Propagation in Random Media," *Physical Review Letters*, Vol. 57, No. 17, October, 1986, pp. 2168-2171.

[83] E. Kogan, M. Kaveh, R. Baumgartner, and R. Berkovits, "Statistics of Waves Propagating in a Random Medium," *Physical Review B*, Vol. 48, No. 13, October, 1993, pp. 9404-9410.

[84] M.V. Berry, "Focusing and Twinkling: Critical Exponents from Catastrophes in non-Gaussian Randon Short Waves," *J. Phys.*, Vol. 10, No. 12, 1977, pp. 2061-2081.

[85] K.B. Efedotov, and V.N. Prigodin, "NMR in a System of Small Metallic Particles: a Novel Mesoscopic Phenomenon," *Modern Physics Letters B*, Vol. 7, 1993, pp. 981-990.

[86] Y.V. Fyodorov, and A.D. Mirlin, "Statistical Properties of Eigenfuctions in a Disordered Metallic Sample," *JETP Letters*, Vol. 60, 1994, pp. 790-801.

[87] S. Ramo, J.R. Whinnery, and T. van Duzer, *Fields and Waves in Communication Electronics*, 3-rd Ed., New York: John Wiley, 1994.

[88] A.A. Andronov, A.A. Vitt, and S.E. Khaikin, *Theory of Oscillators*, New York: Dover, 1966.

[89] S.L. Sobolev, *Partial Differential Equations of Mathematical Physics*, New York: Dover, 1964.

[90] M. Di Bisceglie, and C. Galdi, "Backcatterer from the Sea Surface," *IEE Proc.-Radar, Sonar and Navigation*, Vol. 145, No. 4, August 1998, pp. 216-225.

[91] E. Jakeman, "On the Statistic of *K*-distributed Noise," *J. Phys., A: Math.Gen.*, Vol. 13, 1980, pp. 31-48.

[92] E. Jakeman, and R.J.A. Tough, "Non-Gaussian Models for Statistics of Scattered Waves," *Adv. Phys.*, Vol. 37, No. 5, 1988, pp. 471-529.

[93] R. Barakat, "Weak-Scatterer generatlization of the K-density Function with Application to Laser Scattering in Atmospheric Turbulence," *J. Opt. Soc. Am.*, A, Vol. 3, No. 4, 1986, pp. 401-409.

[94] E. Jakeman, and R.J.A. Tough, "Generalized K-distribution: a Statistical Model for Weak Scattering," *J. Opt. Soc. Am. A*, Vol. 4, No. 9, September, 1987, pp. 1764-1772.

[95] K.D. Ward, C.J. Baker, and S. Watts, "Maritime Surveillance Radar; Part 1: Radar Scattering from the Ocean Surface," *IEE Proc. F*, Vol. 137, 1990, pp. 51-62.

[96] E. Conte, G. Galati, and M. Longo, "Exogenous Modelling of Non-Gaussian Clutter," *J. IR*E, Vol. 57, No. 4, July/August, 1991, pp. 151-155.

[97] E. Conte, and M. Longo, "Characterization of Nnon-Gaussian Spherically Invariant Random Process," *IEE Proc. F.*, Vol. 134, No. 2, 1987, pp. 191-197.

[98] E. Jakeman, and P.N. Pusey, "A Model for Non-Rayleigh Sea Echo," *IEEE Tran. Antennas and Propagation*, Vol. 26, No. 6, November, 1976, pp. 806-814.

[99] S.M. Rytov, Yu. A. Kravtsov, and V.I. Tatarskii, *Principles of statistical radiophysics*, New York : Springer-Verlag, 1987-1989.

[100] J.C. Kluyver, "A Local Probability Problem," *Proc. Royal Acad. Sci.*, Amsterdam, Vol. 8, pp. 341-350, 1905.

[101] P.N. Pusey, D.W. Schaefer, and D.E. Koppel, "Single-interval Statistics of Light Scattered by Identical Independent Scatterers," *J. Phys. A: Math., Nucl. Gen.*, Vol. 7, No. 4, 1974, pp. 530-540.

[102] N.L. Johnson, S. Kotz, and N. Balakrishnan, *Continuous Univariate Distributions*, John Wiley: New York, 1995.

10.5 Random field generation

[103] T. Daggett, I.R. Greenshields, "A Cluster Computer System for the Analysis and Classification of Massively Large Biomedical Image Data," *Computers in Biology and Medicine*, Vol.28, No.1, Jan. 1998, p.47-60.

[104] L.P. Ue, "Generating cosmological Gaussian random fields," *Astrophysical Journal, Letters*, Vol. 490, No.2, Pt.2, 1 December, 1997, pp. L127-L130.

[105] D.E. Kreithen, W.W. Irving, S.M. Crooks, "Generating Correlated Gamma Random Fields with Application to Synthesis of Simulated SAR Imagery," *ICASSP 91: 1991 International Conference on Acoustics, Speech and Signal Processing*, IEEE, New York, NY, USA, 1991, pp. 2601-2604.

[106] C.O. Acuna, "Texture Modeling Using Gibbs Distributions," *CVGIP: Graphical Models and Image Processing*, Vol. 54, No.3, May 1992, pp. 210-222.

[107] Y. Hoffman, E. Ribak, "Constrained Realizations of Gaussian Fields: a Simple Algorithm," *Astrophysical Journal, Letters*, Vol. 380, No. 1, Pt. 2, 10 October, 1991, pp.L5-L8.

[108] S.E. Silliman, A.L. Wright, "Generation of Random Fields Characterized by Discrete Regions of Constant Values," *Applied Mathematics and Computation*, Vol. 45, No. 3, October, 1991, pp. 293-311.

[109] L. Onural, "Generating Connected Textured Fractal Patterns Using Markov Random Fields," *IEEE Transactions on Pattern Analysis and Machine Intelligence*, Vol. 13, No. 8, August, 1991, pp. 819-825.

[110] W. Czarnecki, "Modelling of a 2-D Discrete Stationary Random Signal Having Specified Probabilistic Properties," *Signal Processing V. Theories and Applications*, Proceedings of EUSIPCO-90, Fifth European Signal Processing Conference, Elsevier, Amsterdam, Netherlands, 1990, pp. 493-496.

[111] M.I. Gurelli, L. Onural, "A Parallel Algorithm for the Generation of Markov Random Field Textures," *Communication, Control and Signal Processing. Proceedings of the 1990 Bilkent International Conference on New Trends in Communication*, Control and Signal Processing, Elsevier, Amsterdam, Netherlands, 1990, pp. 1330-1336.

[112] M.O. Vlad, M.C. Mackey, J. Ross, "Generating Functional Approach to Space and Time-Dependent Colored Noise," *Physical Review E (Statistical Physics, Plasmas, Fluids, and Related Interdisciplinary Topics)*, Vol. 50, No. 2, Pt. A, August, 1994, pp.798-821.

[113] N. Takahashi, T. Tanaka, H. Ogura, "Synthesis of Narrow-Band Random Moving Image via Computer," *Electronics and Communications in Japan, Part 3 (Fundamental Electronic Science)*, Vol. 77, No. 1, January, 1994, pp. 53-63.

[114] V. Rouillard, G.T. Lleonart, "A Spectral Feedback Compensation Technique for the Generation of Random Wave Fields," *Proceedings of the Institution of Mechanical Engineers, Part C (Journal of Mechanical Engineering Science)*, Vol. 208, No. C2, 1994, pp.105-112.

[115] L. Bingcheng, D.M. Song, "A Pyramid AR Model To Generate Fractal Brownian Random (FBR) Field," *Proc. of the SPIE*, Vol. 2094, Pt.3, 1993, pp. 1094-1102.

[116] F.W. Elliott, A.J. Majda, D.J. Horntrop, R.M. McLaughlin, "Hierarchical Monte Carlo Methods for Fractal Random Fields," *Journal of Statistical Physics*, Vol. 81, No. 3-4, November, 1995, pp. 717-736.

[117] A. Brandenburg, "Flux Tubes and Scaling in MHD Dynamo Simulations," *Chaos, Solitons and Fractals*, Vol. 5, No. 10, October, 1995, pp. 2023-2045.

[118] M. Glasner, D. Yevick, "A Numerical Procedure for Soliton Generation," *Optical and Quantum Electronics*, Vol. 27, No. 9, September, 1995, pp. 799-803.

[119] M.D. Wheeler, K. Ikeuchi, "Sensor Modeling, Probabilistic Hypothesis Generation, and Robust Localization for Object Recognition," *IEEE Transactions on Pattern Analysis and Machine Intelligence*, Vol. 17, No. 3, March, 1995, pp. 252-265.

[120] C. Baillard, O. Dissard, O. Jamet, H. Maitre, "Detection of Above-Ground in Urban Areas: Application to DTM Generation," *Proceedings of the SPIE*, Vol. 2955, 1996, pp. 129-140.

[121] Dias-JMB; Silva-TAM; Leitao-JMN, "Adaptive restoration of speckled SAR images," *IGARSS '98. Sensing and Managing the Environment.* IEEE, New York, NY, USA; 1998; p.19-23 vol.1.

[122] D. Mardare, R. Siushansian, and J.LoVetri, *3-D Dispersive EMFDTD Version 1.3*, User's Manual, The University of Western Ontario, December 1995.

10.6 UWO internal notes

[123] S. Primak, and J. LoVetri, "On Properties of K-Distributions," *UWO Internal Note 1.*

[124] S. Primak, and J. LoVetri, "1-D Resonator with Lossy Walls," *UWO Internal Note 2.*

[125] S. Primak, and J. LoVetri, '2-D Resonator with Lossy Walls Excited by a Line Current Source," *UWO Internal Note 3.*

[126] S. Primak, and J. LoVetri, "Statistics of the EM Field Inside 1-D Lossy Resonator with Stirring," *UWO Internal Note 4.*

[127] S. Primak, and J. LoVetri, "On Simplified Models of Coupling Into a Cavity," *UWO Internal Note 5.*

[128] S. Primak, and J. LoVetri, "On Statistical Description of a Sum of Random Harmonic Waveforms," *UWO Internal Note 6.*

[129] S. Primak, and J. LoVetri, "Effect of Standing Wave Ration on Field Statistics," *UWO Internal Note 7.*

[130] S. Primak, and J. LoVetri, "On Statistical Curve Fitting Tests," *UWO Internal Note 8.*

[131] S. Primak, and J. LoVetri, "A Markov Chain Approximation and Generation of Exponentially Correlated Random Process," *UWO Internal Note 9.*

[132] S. Primak, and J. LoVetri, "Solution of the Inhomogeneous Transmission Line Equations with Random Force Function: UWO STEM1.0 Simulation Tool," *UWO Internal Note 10.*

[133] S. Primak, and J. LoVetri, "On Statistics of Electromagnetic Field Inside A Computer Box", *Internal UWO Internal Note 11.*

A
autocorrelation 96
C
characteristic function 90
complex cavity 10
complex enclosures 21
conditional probability 91
convolution 94
cumulative distribution function 90
D
disjoint events 89
distribution 90
distribution function 90
E
electromagnetic compatibility 3
electromagnetic interference 3
elementary event 89
EMC 3
EMI 3
ergodic 96
Error function 92
event 89
expected valu 95
Expected values 94
    mean 94
    moments 94
    variance 94
experiment 89
F
first moment 95
functions of a random variable 93
I
independent events 91
J
joint probability density function 91
K
Kluyver equation 51
L
Large Number Theorem 54
M
mean 95
O
outcome 89
P
PDF's
    Chi-square density function 93

Gaussian density function 91
Rayleigh density function 92
uniform density function 92
probability density function 90
probability of an event 89
process 96
R
random variable 90
S
second moment 95
standard deviation 95
stationary process 96
STEM 8
stochastic process 96
sum of two random variables 94
V
variance 95

CRC Publication Approval and Record Form

This form is to be completed for the approval of all CRC publications and presentations. The level of approval varies with the category of the publication. For details of publication procedures, see the document: Publication Policy and Procedures. For items sponsored by DND, the DREO yellow and green sheets must also be prepared and submitted separately.

Category A: CRC Reports & CRC Technical Notes. **Category B:** Journal & conference papers. **Category C:** Contributions to outside documents such as TTCP, ITU, AGARD, standards, etc. **Category D:** Abstracts **Category E:** Documents with non-CRC employee as main author.

Title: The Search for a Statistical Approach Capable of Predicting the Coupling Strength from an External Electromagnetic Field to Electronic Equipment

Author(s): Serguei Primak Ph.D and Joe LoVetri, Ph.D, P.Eng

Branch and Directorate VPRS/REMC **Document category:** E

Web Address (for CRC Reports & Technical Notes): _____

Details of Publication or Presentation: (e.g. report type & number; name & sponsor of journal; technical body (ex. TTCP), or conference; date & place of publication or presentation; etc.)
University Of Western Ontario Contract report, March 1999

CRC Contract No.U6800-9-0696

Security Classification: Unclassified

Releasability: Releasable (X) Non releasable ( ) Conditionally releasable ( )
If limitations apply, describe the conditions: _____

Intellectual Property: May require IP protection. Copy sent to DMKT ( ) or Does not require IP protection ( ). Explain: _____

_____

Certifications

All Categories:

Author and date: _____

Manager and date: _____

For Categories A and B:

Reviewer and date: _____

Editor and date: _____

VP and date: _____

For Category D:

VP and date: _____